NISTIR 7352

NIST Liquid Hydrogen Cold Source

P. Kopetka
R. E. Williams
J. M. Rowe

National Institute of Standards and Technology
Technology Administration, U.S. Department of Commerce

NISTIR 7352

NIST Liquid Hydrogen Cold Source

P. Kopetka
R. E. Williams
J. M. Rowe
Materials Science and Engineering Laboratory
National Institute of Standards and Technology
Gaithersburg, MD 20899-8560

September 2006

U.S. Department of Commerce
Carlos M. Gutierrez, Secretary

Technology Administration
Robert Cresanti, Under Secretary of Commerce for Technology

National Institute of Standards and Technology
William Jeffrey, Director

Disclaimer

Certain commercial entities, equipment, or materials may be identified in this document in order to describe an experimental procedure or concept adequately. Such identification is not intended to imply recommendation or endorsement by the National Institute of Standards and Technology (NIST), nor is it intended to imply that the entities, materials, or equipment are necessarily the best available for the purpose.

ABSTRACT

Nearly two-thirds of the experiments performed at the NIST Center for Neutron Research (NCNR) utilize cold neutrons with wavelengths greater than 4 Angstroms. This report documents the development of the liquid hydrogen cold neutron source in the NIST research reactor. The source was designed to optimize the flux of cold neutrons transported to the scattering instruments in the guide hall. It was also designed to be passively safe, and operate simply and reliably. All hydrogen system components are surrounded with monitored helium containments to ensure that there are at least two barriers between the hydrogen and the atmosphere. Monte Carlo simulations were used to calculate the cold source performance and estimate the nuclear heat load at full reactor power. Thermal-hydraulic tests in a full-scale mockup at NIST Boulder confirmed that a naturally circulating thermosiphon driven by the 2 meter height of the condenser could easily supply the moderator vessel with liquid hydrogen while removing over 2000 watts. The cryostat assembly was designed to withstand any high pressure generated in a credible accident. It was fabricated to rigorous quality assurance standards, resulting in over 10 years of leak-free operation.

Contents

1.0 Introduction

The neutrons that are used for neutron scattering and other research applications at research reactors are those that have been slowed down from the range of MeV, at which they are created, to tens of meV by scattering in the moderator and reflector. In most reactors, the neutron energy spectrum is essentially Maxwellian, with a characteristic temperature somewhat higher than the actual temperature of the moderator (usually approximately room temperature). For such a spectrum, the mean neutron wavelength, energy and speed are 1.8 Å, 25 meV and 2200 ms^{-1}, values well suited to study the properties of condensed matter at the atomic scale, where interatomic spacings are approximately 1 Å, and characteristic vibrational energies are of order meV.

Over the past two-three decades, structures with characteristic lengths of 100 Å and correspondingly smaller vibrational energies, have become increasingly important for both science and technology. For example, polymers are being developed with totally new properties as substitutes for other more traditional metal materials for weight savings, nano-structures are being developed with novel properties for processing drug delivery plus other applications and biotechnology applications are increasing in importance. All of these structures have characteristic dimensions that are best matched by neutrons of longer wavelength, which also allow better resolution in energy to match the slower relaxation and vibration of the more massive objects. However, the fraction of neutrons with energies less than 5 meV in a normal moderator spectrum is less than 2 % of the total, which makes their use impractical, except in special cases. In order to address this problem, several groups around the world[1] have developed systems that place cryogenically cooled moderators called "cold sources" in the reflector of neutron sources. These cold sources shift the spectrum down in energy to a temperature somewhat above the moderator temperature, providing large gains in intensity for low energy neutrons.

The NIST research reactor, NBSR (National Bureau of Standards Reactor), was designed from the beginning with a provision to add a cryogenically cooled moderator system, or cold neutron source. The initial design, as discussed in NBSR-9[2] and NBSR-13[3], was a block of D_2O ice, cooled to approximately 25 K by circulating helium gas. A water cooled lead and bismuth gamma ray shield was included to reduce heating of the ice. The source was installed in the reactor in 1987. Its successful operation was a key to the development of the NIST Cold Neutron Research Facility, a large new experimental area constructed to take advantage of the longer wavelength neutrons produced by this source. The success of this facility, and the high national demand for cold neutrons, led to a design effort to develop a more intense cold neutron source, based on liquid hydrogen. The first version of this source was installed in the NBSR in 1994, and resulted in a gain in cold neutron intensity of a factor of seven. Further refinements of the design resulted in an additional gain of a factor of two for the unit installed in 2002.

This report documents the design and analysis of the latest version of the NIST liquid hydrogen source.

2.0 Design Basis

The design basis for the liquid hydrogen cold source is driven by the following requirements, listed in priority order:

- The finished cold source must satisfy the safety requirements of 10 CFR 50.59.
- The source must allow extraction of beams from all existing cold source beam ports (CT-E and CT-W), as well as from the insertion port, with full guide illumination to 10 Å.
- Operation should be simple and reliable, with minimal impact on reactor operation.
- The intensity of neutrons with energies less than 5 meV should be maximized.

Each of these requirements has several implications for the design of the liquid hydrogen cold source, which will be addressed in turn.

2.1 Requirements of 10 CFR 50.59

At the time of cold source design and construction, the requirements of 10 CFR 50.59 were:

- (a)(1) The holder of a license authorizing operation of a production facility may (i) make changes in the facility as described in the safety analysis report, (ii) make changes in the procedures as described in the safety analysis report, and (iii) conduct tests or experiments not described in the safety analysis report, without prior Commission approval, unless the proposed change, test or experiment involves a change in the technical specifications incorporated in the license or an unreviewed safety question.

- (2) A proposed change, test, or experiment shall be deemed to involve an unreviewed safety question (i) if the probability of occurrence or the consequences of an accident or malfunction of equipment important to safety previously evaluated in the safety analysis report may be increased; or (ii) if a possibility for an accident or malfunction of a different type than any evaluated previously in the safety analysis report may be created; or (iii) if the margin of safety as defined in the basis for any technical specification is reduced.

In order to comply with this requirement, the cold source design emphasizes simplicity, passive safety features, complete blanketing of all hydrogen containing components with the inert gas helium, and a vessel designed to withstand a hypothetical ignition of a hydrogen-air mixture without damage to the cold source thimble. Based upon experience in Europe, these requirements have led to a thermosiphon design, with gravity driven flow of liquid hydrogen from a condenser into the moderator chamber, removal of the heat (generated by the reactor) by boiling of the liquid and return of the vapor to the condenser. The hydrogen-containing components of this system have no moving parts, and the entire hydrogen inventory is contained in a closed system with no automatic or remotely operated valves or rupture discs. Hydrogen vapor returning from the moderator chamber is recondensed in a heat exchanger cooled by helium gas at 15 K, and then flows back down into the vessel under gravity. The hydrogen supply and return lines are sized to provide for two phase (liquid and vapor) flow in the return from the moderator chamber. This provides a very stable operating condition under changing conditions of heating, as shown for a source designed for the High Flux Reactor (HFR) at the Institut Laue Langevin[4] (ILL), and verified for the NIST geometry in a series of mockup tests[5] carried out at NIST-Boulder. A schematic view of this system is shown in Figure 2.1.

Note that all hydrogen-containing components, or components that could conceivably contain hydrogen, are surrounded by helium, including the ballast tank

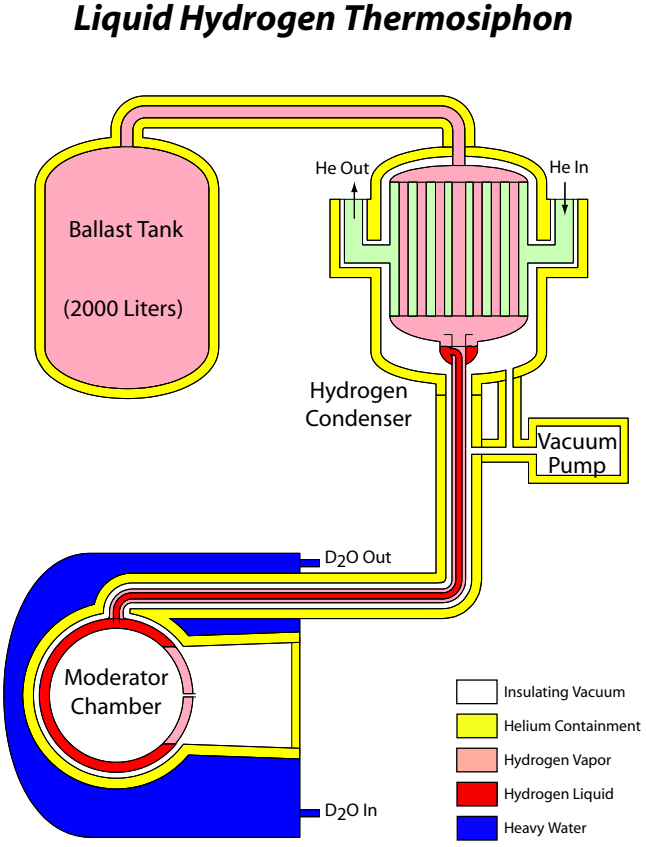

Figure 2.1 Schematic of NIST Advanced Cold Neutron Source, Unit 2.

(sized to hold the hydrogen gas at less than 0.5 MPa when the system is warm), and the vacuum pumps. There are at least two barriers to mixing of hydrogen with air, which prevents formation of a flammable mixture. In addition, all hydrogen containing components, including the lines from the moderator chamber to the condenser and ballast tank, are protected from damage by being surrounded by steel barriers or heavy, non-movable shields. This is the basis of the safety case – mixing of hydrogen and air is prevented to avoid any possibility of damage to the reactor. In addition, one of the vessels surrounding the moderator chamber, the helium vessel, is sized to withstand a hypothetical reaction of a room temperature mixture of air and hydrogen at 0.1 MPa, without any damage to the reactor vessel thimble that contains the source.

2.2 Extraction of Beams

The arrangement of the cold source thimble and beams in the original reactor design is shown in Figure 2.2. As can be seen from the figure, two horizontal beam ports (CT-E and CT-W) were included, separated by an angle of 33°, and crossing

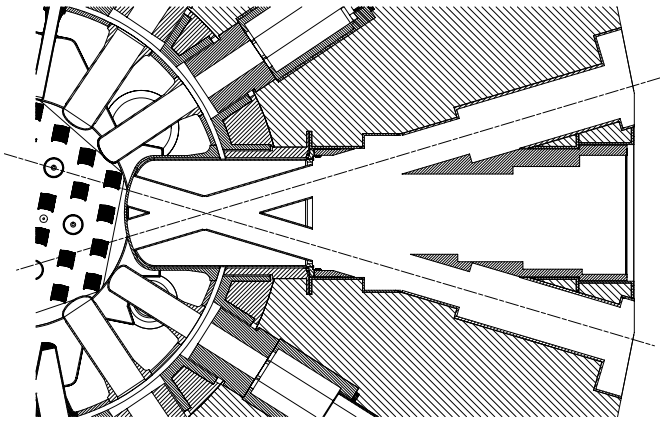

Figure 2.2. Original layout of the cold neutron port.

before the end of the thimble. This design was chosen to accommodate a large D_2O ice cold source, which would have a viewed surface at the point of the beam crossing. For a hydrogen source, the viewed surface should be much closer to the tip of the thimble, as a result of the much higher scattering cross-section for hydrogen than deuterium. The net result is that the viewed surface must be large, in both height (determined by the beam port diameter of 170 mm and the guide height) and width (determined by the crossing point of the beam port lines-of-sight and the guide width). In calculating the required sizes, guide coating with ^{58}Ni is assumed, which gives a critical angle of 0.02 radians at 10 Å. This adds nearly 80 mm to the required area in both dimensions, since the guides begin approximately 2 m from the end of the thimble, and the additional area is required to fully illuminate the guides. The required size of the viewed surface is approximately 300 mm × 300 mm, a size that imposes severe constraints on design. In order to make a moderator chamber with such a large, flat viewed surface, able to withstand the pressures involved (up to 0.5 MPa internal pressure), the material would have to be tens of mm thick, which would both reduce the intensity due to absorption and scattering and increase the heat load beyond reasonable values. One solution examined was to use an elliptical shell of at least 2:1 axial ratio, while a second was to connect a number of vertical tubes arranged to provide an almost uniform thickness moderator of appropriate dimensions. While either of these solutions would have worked, they both have serious defects. For the former, the thickness of hydrogen would have been far too large for optimum intensity, while for the latter, fabrication would have been quite complex, involving many welds, and the fluid flow in the thermosiphon would have been difficult do in a way that ensured safe, effective operation.

2.3 Simple, Reliable Operation

In our research on the causes of incidents and failures, it quickly became clear that human error and failure of non-passive devices were the most prevalent initiators. For this reason, the design studies focused on passive, fail-safe operation, with an absolute minimum of active components. It was decided that the reactor would not operate unless the cold source was operational, eliminating any backup cooling systems. This was done primarily to simplify the design of the in-pile components, as any backup cooling would have to involve gas cooling of the moderator chamber, implying a high velocity flow of helium. Experience with the D_2O ice source, which used high velocity gas cooling, and at Brookhaven National Laboratory, where a directly cooled hydrogen source operated for several years, showed that this was a source of problems

for several reasons. The most critical was that the gas would be flowing at high velocity through a region of high neutron flux, so that any erosion could lead to transport of radioactive material out of the in-pile components, presenting both a maintenance problem (due to internal contamination of the gas circulation system) and a possible health physics problem (if a seal material such as indium were to break off, become highly activated, and be transported out into piping in occupied areas). Another was that the gas circulation system would have to be jointed, to allow for maintenance, providing opportunities for leaks of contaminated gas.

Experience here and at other facilities was an important factor in the design if the NIST liquid hydrogen (LH_2) cold source. The only pipes that go into the in-pile area in the chosen design are the hydrogen supply and return, and D_2O cooling for the heavy walled vessels in the cryostat. There are no connections in any of these pipes – all joints are welded, and the welds were radiographed and helium leak tested at the time of installation. The hydrogen thermosiphon is operated under saturated conditions, so that the only relevant parameter is the vapor pressure, which determines the temperature, and the instrumentation is outside the high radiation fields. Finally, the thermosiphon is operated in a regime with two phase flow in the return line, providing stable operation over a wide range of heat inputs.

The helium gas used to condense the hydrogen is supplied by a closed cycle refrigerator with a compressor, coldbox, and expander turbine. The model chosen provides up to 3.5 kW of cooling at 14 K, which is far more than required, but which allows for consideration of a deuterium source at a future date. The refrigerator is controlled by a Programmable Logic Controller (PLC), with automatic startup, shutdown, and warmup functions, and is operated at a fixed cooling power. The cooling loop is controlled by the same PLC, which controls a valve regulating the flow of cold helium to the condenser (the remainder of the flow bypasses the condenser) so as to maintain a constant hydrogen pressure. This mode of operation maximizes refrigerator reliability, and provides rapid responses to changes in heat load (such as reactor power changes).

2.4 Maximize Intensity of Neutrons Below 5 meV

This consideration is of course the primary reason for installation of a new cold neutron source, but the solution is seriously constrained by the preceding requirements. In order to optimize this constrained design, it was necessary to iterate repeatedly, first calculating the neutronics for an idealized source geometry, then doing a rough mechanical design incorporating constraints, then repeating the neutronics calculations. Several concepts were considered before settling on the actual design used, which is shown in Figure 2.3. The fundamental concept is creation of a shell of hydrogen inside a mechanically efficient shape – first a sphere, then in the second version of the source, an ellipsoid of revolution. The large neutron scattering cross-section of hydrogen, along with the finite absorption cross-section, leads to the existence

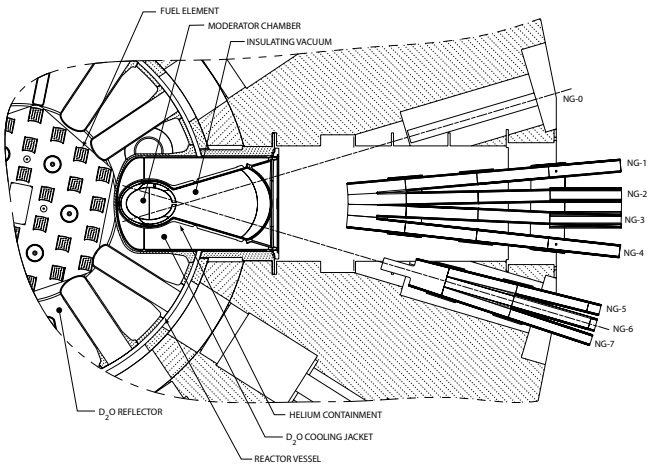

Figure 2.3. Layout of the Advanced Cold Neutron Source and guides.

of an optimum thickness of moderator material. There must be some material for the neutrons to scatter and thus lose energy, so that the yield of cold neutrons increases as the thickness increases from zero. However, as the thickness increases further, the yield of cold neutrons begins to decrease, as some of the neutrons slowed down in the first layers will not be able to reach the viewed surface because of scattering and absorption. The optimum thickness depends on the relevant cross-sections, which introduces another complication.

Hydrogen molecules exhibit well-defined states of

angular momentum characterized by rotational quantum numbers J=0,1,2…, and at low temperatures, in the stable equilibrium state, all of the molecules will be in the J=0 state, which has the lowest energy. As a result of the spin dependence of scattering, molecules with even angular momentum (para-hydrogen) have a small scattering cross-section, unless the neutron energy is large enough to allow excitation to a state of higher angular momentum, while molecules with odd J (ortho-hydrogen) have a large scattering cross-section for all neutron energies. As stated above, the equilibrium state would be almost all para-hydrogen at 20 K, and thus would have a low scattering cross-section for neutron energies less than 15 meV. This would imply that the optimum thickness could be quite large. However, there is a great deal of uncertainty about the actual state, with contradictory evidence[6.7] and most designers have assumed that the actual state is an equal mixture of ortho and para hydrogen[8]. Our studies indicate that the optimum thickness is approximately 30 mm, so long as the ortho content is greater than 40 % to 50 %, and the close agreement of our measured and calculated cold neutron intensities and energy dependence seems to confirm that the concentration is closer to normal (75 % ortho) than to para for our source. In order to extract the maximum number of neutrons from the shell, an entrance hole was included with minimal hydrogen in the path, as shown in Figure 2.3. The details of the neutronic design are given in Section 3.

3.0 Cold Neutron Performance and Nuclear Heat Load Calculations

The design of the NIST liquid hydrogen cold sources was guided by the results of Monte Carlo simulations of neutron and photon transport through detailed models of the reactor core and cold source thimble. Computer codes and platforms have evolved tremendously since the first Cold Neutron Source (CNS) calculations in the late 1980's. No effort will be made to detail chronologically all of the steps and miss-steps in the process. The first three parts of this section describe the currently-used methods for cold source development. The concluding sections outline the evolution of the source, and the parameters that were optimized in its development, with brief notes about early results using what are now outdated methods.

3.1 NBSR Modeling with MCNP

A three-dimensional, Monte Carlo Neutron Photon (MCNP[9]) model of the cold source thimble was first used at the NCNR for the development of a liquid hydrogen cold neutron source in 1989. A full core model was completed in 1993 accurately predicting the performance and nuclear heat load of the first LH_2 source, Unit 1. MCNP is a Monte Carlo neutron and photon transport code developed at Los Alamos National Laboratory (LANL) that is used for a wide variety of problems including criticality simulations. It features generalized surfaces and cells, so that complex geometries can be defined, along with continuous energy cross-section data. Hundreds of cross-section files with gamma-ray production data have been formatted for use with the code, including thermal neutron scattering kernels for all common reactor moderators, and four cold moderators. The most recent version, MCNP 5, includes seven kernels for ortho- and para-LH_2 in 1 K intervals from 19 K to 25 K (more information about ortho/para-hydrogen will be presented in later sections).

The core model has been continually modified and expanded, and it was used extensively in the reactor physics analysis of the NBSR submitted to the Nuclear Regulatory Commission (NRC) in April 2004 in support of the relicensing effort. All of the major features of the NBSR that affect the reactivity of the core are represented in great detail in this model including:

- A hexagonal array of the 30 fuel elements, 6 vertical thimbles, and the regulating control rod.
- All 1020 fuel plates, their Al cladding and D_2O-filled coolant channels, positioned in hexahedral repeating structures for the upper and lower sections of the core.
- Fifteen fuel material specifications representing each step in the fuel management pattern for the 7 and 8 cycle fuel elements.
- The four shim arms, which can be positioned at any angle between their scram and fully withdrawn positions.
- Nine radial beam tubes, two tangential beam tubes, the vertical beam tube, and the four in-core pneumatic 'rabbit' tubes.
- The large cryogenic beam port and the liquid hydrogen cold source(s).
- The reactor vessel, filled with D_2O, representing the moderator between the fuel elements, and the core reflector regions.
- Layers of lead and iron outside of the vessel, comprising the thermal shield, and a layer of concrete, for part of the biological shield.
- A portion of the D_2O tank, providing neutronic coupling with the graphite in the thermal column.

Many of the above features are shown in Figure 3.1. The lines of the hexagonal array are for computational purposes, locating the 30 fuel elements. Concentric areas surrounding the core are the D_2O reflector, the Al vessel, 5 cm of lead and 20 cm of iron comprising the thermal shield, and the first 20 cm of the concrete biological shield. Four cells between the inner

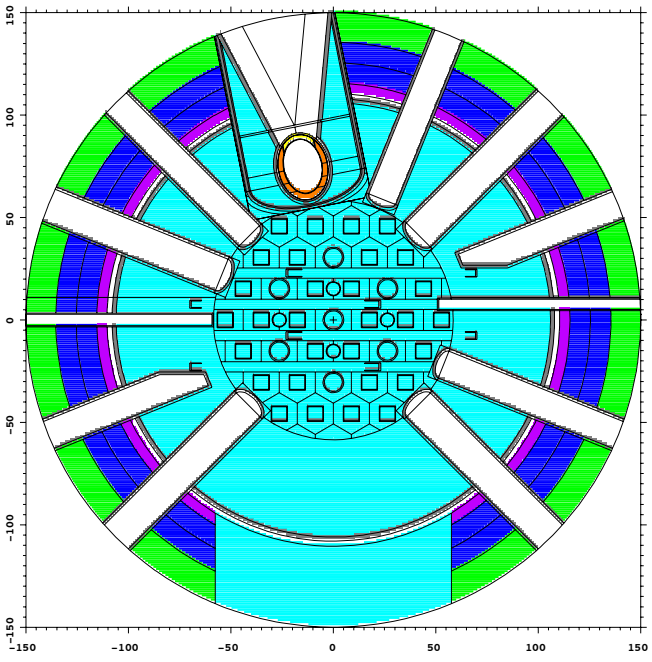

Figure 3.1. The MCNP model (in cm) of the NBSR core at its mid-plane, in the unfueled region.

most rows of fuel are excluded from the array to accommodate the cells of the Cd shim arms. Starting at 5 o'clock, and moving counterclockwise, the radial beam tubes are BT-1 through BT-9. Between BT-5 and BT-6 is the large cryogenic beam port, CT, containing the Unit 2 liquid hydrogen CNS. The axis of CT is 11.25° west of the y axis of the model, which is the north direction. Part of a D_2O tank leading to a graphite thermal column (not shown) substitutes for the thermal shield on the south side.

The MCNP model was provided to the Energy Sciences and Technology Department at BNL as a basis for their reactor physics and safety analysis study, Appendix A of NBSR-14, the updated SAR[10]. Section 3 of that appendix contains a thorough description of the MCNP model, including the fuel geometry and fuel loading scheme, control elements, experimental facilities, etc. The ^{235}U inventory in each fuel element was determined iteratively with three computer codes, MCNP, ORIGEN2[11], and MONTEBURNS[12], with MONTEBURNS managing the interactions between MCNP and ORIGEN2. The model has been carefully benchmarked, and was used to calculate the power distribution, reactivity coefficients, integral and differential reactivity worths of the shim safety arms and the regulating control rod, neutron fluxes in the experimental facilities, etc.

3.2 Neutron Performance Calculations

The figure of merit for judging the performance of a cold neutron source is the "brightness" of the source in the direction of the beams or guides to various instruments. Brightness, or $d^2\varphi/d\lambda d\Omega$, has units of neutrons/cm^2-s-Å-ster, when written in terms of wavelength, or $d^2\varphi/dEd\Omega$ with units of n/cm^2-s-meV-ster, when written in terms of energy. Specifically, it is the brightness of cold neutrons, E < 5 meV or λ > 4 Å, in the direction of the guides, with angles less than the critical angle for reflection from the ^{58}Ni-coated surfaces within the guides. The critical angle is given by $\theta_C = 0.002\ \lambda(Å)$ rad for ^{58}Ni. An MCNP current tally is used to calculate the brightness in a two-step process. In the first step, a lengthy criticality calculation generates a surface source file for neutrons entering the CT region. Much shorter calculations starting with the source file can exploit powerful variance reduction techniques to optimize the cold source geometry (see the MCNP input file, "unit2", in the appendix).

A surface source file containing the location, direction, energy and weight of the starting neutrons to be used for the MCNP calculation was generated in a KCODE calculation of the entire NBSR core including the region surrounding the CNS (Figure 3.1). The CT axis, y′, is 11.25° west of the y-axis. A coordinate transformation to y′ is needed for all the surfaces in the CNS region. Typically, the surface source is on the MCNP surfaces PY′ = 55.5 cm (a plane perpendicular to the y′ axis, 55.5 cm from the core center) and CY′ = 30.0 cm (a cylinder along the y′ axis with a 30 cm radius). Data for every particle crossing PY′ in the positive, +y, direction, and every particle passing into the CY′ cylinder are recorded in the surface source file. Such files may be very large, 500 MB, to obtain good statistical results. A track for a given neutron may pass into and out of the CT region many times. Data are recorded for each entrance.

A given surface file can be used to study the effects of small changes in the CNS geometry, using much shorter calculations. A large change, such as a modification in the D_2O cooling jacket, will change the reactivity of the core, and will require a new surface

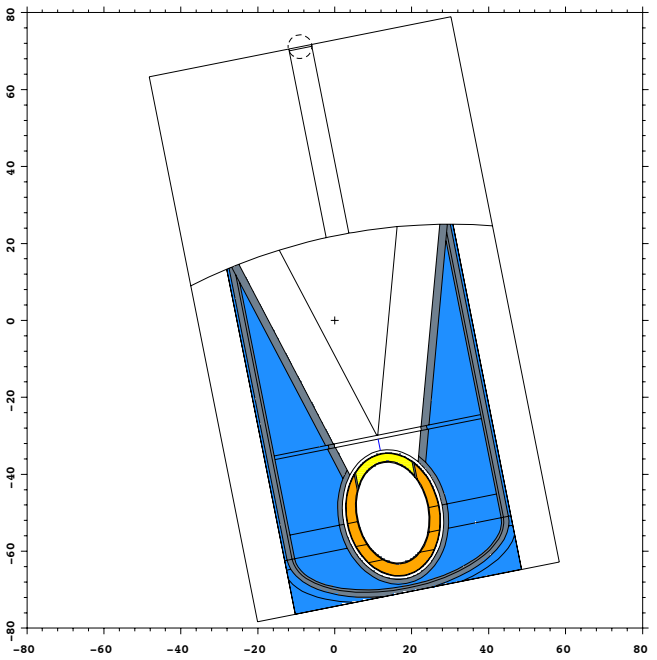

Figure 3.2. An MCNP geometry plot (in cm) of the cold source region containing the Unit 2 CNS.

source to be generated.

Figure 3.2 shows just the CNS region as specified in the input file "unit2" (the input file is listed in Appendix A of this document). The small circle at the top of Figure 3.2 is a DXTRAN sphere, just large enough to enclose the current tally surface, which is a 6 cm diameter circle perpendicular to the y′ axis and 124 cm from the center of the CNS. At every neutron collision, a pseudo particle is generated, and the probability that it will be scattered and transported to the DXTRAN sphere is calculated. Inside the sphere, pseudo particles are transported normally, contributing to tallies. Very few cold neutrons will be transported to the tally surface in analog MCNP; the neutron is killed if it does manage to enter the sphere. The DXTRAN feature is a powerful variance reduction tool described at length in the MCNP User's Guide. DXTRAN cannot be used in problems with repeated structures, preventing its use in the original KCODE calculation of the NBSR core. As another variance reduction measure in "unit2", the neutron importance is increased from 1 to 27 as neutrons move toward the LH_2 cells. The probability that a fission neutron will be transported to the tally surface is about 10^{-7}. A combination of generating a surface source and using it, together with MCNP variance reduction techniques, provides tallies with reliable statistics without generating billions of source neutrons.

The tally surface is located near the entrance of the in-pile piece of neutron guides NG-1 through NG-4. These tallies provide both a relative measure of the performance of various CNS geometries, and a way to calculate the absolute brightness of the source. Brightness is independent of the location of the tally used to compute it. Once the brightness is determined, the fluence anywhere in the beam line can be determined. The direction cosine bin of the current tally should be approximately equal to $\cos \theta_C$, where θ_C is the critical angle of the guides for the longest wavelength to be "fully illuminated" by the source. Most of the NCNR guides are coated with ^{58}Ni (or ^{58}Ni equivalent super-mirror for the majority of their length) which has a θ_C = 0.02 rad for 10 Å neutrons. (The MCNP user specifies direction cosine bins, rather than an angle; the angle is between the neutron direction vector and a vector normal to the tally surface.)

The size of the cold source with respect to the guides, determines whether or not the guides are fully illuminated. Consider a guide of width, w, located a distance, D, from the source. To be fully illuminated, the cold source width must exceed $w + 2 \times D \times \theta_C$. For example, if guides with w = 6 cm are to be fully illuminated to 10 Å by a source at a distance D = 110 cm, the source width must be $W_{CNS} > 6 \text{ cm} + 2 \times 110 \times 0.02 = 10.4$ cm. The exit hole of Unit 2 is 15 cm wide so the guides are fully illuminated to at least 10 Å. The tally surface should also be fully illuminated to 10 Å, so we chose a cosine bin between cos (0.02) = 0.9998 and 1.0000. The width of the cosine bin is then $d\mu = 0.0002$. A larger value of $d\mu$ is sometimes used for the brightness calculations to obtain better statistics, but as the full illumination condition is relaxed, the cold neutron brightness will appear to decrease.

To approximate the beam intensity at the guide entrance, the current tallies are divided by the tally surface area, 28.27 cm^2, and multiplied by the 20 MW normalization factor of 1.525×10^{18} neutrons/sec per starting neutron (MCNP starting particles in the KCODE calculation). The default MCNP normalization is per starting particle, so the tallies are independent of the length of the calculation. *MCNP normalization is preserved in the process of generating a surface source and using it in a subsequent problem.* The user can easily verify this with identical tallies in both the source generation calculation and problems using the source.

Specific tallies needed to compare competing geometries are given in the "unit2" input file in the appendix. When using the DXTRAN feature for a current tally, the surface must lie completely within the DXTRAN sphere. The cosine bins of the tally and size of the surface must be chosen to exclude illumination of the tally surface by the exterior of the cold source or any room temperature part of the reactor structure. A 6 cm diameter tally surface was chosen, approximately 1.25 m from the source, with the smallest cosine bins of either 0.9998 or 0.9996. Twenty energy bins of 1 meV or 5 meV were chosen

to provide either the cold neutron spectrum or the thermal neutron spectrum, respectively. The same tallies are used for all CNS calculations.

Sample Brightness Calculation:

Let the brightness be $d^2J/dEd\Omega = B$. Its units are n/cm^2-s-meV-ster, and its value should not depend on the distance of the tally surface from the source, if the tally surface is on the beam axis and is fully illuminated as mentioned above.

Let $F(E,\Omega)$ be the MCNP current tally per unit area in energy bin dE and cosine bin $d\mu$ times the reactor normalization at full power, 1.525×10^{18} at 20 MW.

Then $F(E,\Omega) = B \times dE \times d\Omega$, where $d\Omega = 2 \times \pi \times d\mu$.

So $B = F(E,\Omega)/[(2\pi)\ dE\ d(\cos\theta)]$.

For the case of Unit 2, $F(E,\Omega) = 1.9 \times 10^8$ n/s cm^2, for $0 < E < 1$ meV, and $0.9998 < \theta < 1.0000$. Then we have dE = 1 meV, $d(\cos\theta) = d\mu = 1 - 0.9998 = 0.0002$, and $B = 1.5 \times 10^{11}$ n/cm^2-s-meV-ster.

3.3 Nuclear Heat Load Calculations

MCNP can also be used to estimate the energy deposited in the LH_2 and the Al vessel with the NBSR at its full power of 20 MW. The sources of energy are:

1. Fast neutrons.
2. Fission gamma rays.
3. Capture gamma rays.
4. Fission product gamma rays.
5. Activation product gamma rays.
6. Activation beta particles.

The code will only directly tally the prompt contributions to the heat load, namely items 1, 2, and most of 3 (some cross section files lack capture gamma-ray production data). Since the activation product responsible for most of items 5 and 6 happens to be ^{28}Al, these contributions can also be determined. MCNP 5 includes an aluminum cross section file (13027.62c) with the 1.78 MeV gamma ray accompanying the beta decay of ^{28}Al added to the prompt capture photon production data. This extra photon will always be present in a steady state case because ^{28}Al has a 2.2 minute half-life and will rapidly reach saturation in the cryostat assembly and reactor components. Likewise, the ^{28}Al beta particle contribution can be calculated by tallying the $^{27}Al(n,\gamma)^{28}Al$ reaction rate, which will be equal to the ^{28}Al decay rate, and multiplying by 1.25 MeV, the average beta-particle energy. It is assumed that all of the beta-particle energy is deposited in the cell in which it is created.

Gamma rays from fission products are not included in any of the cross section sets provided with MCNP. To estimate the contributions of item 4, an ENDF5/B ^{235}U cross section set (92235.50c) was modified at Oak Ridge National Laboratory (ORNL) to add "prompt" photon production data (92235.02c) characteristic of the fission product gamma rays in equilibrium in HFIR (High Flux Isotope Reactor) fuel[13]. These data are used for heat load calculations only.

Table 3.1. Nuclear heating (in watts) in the moderator vessel.

	LH_2 (324 g) - Watts	Al (2840 g) - Watts
Neutrons	104	3
Beta particles	-	308
Gamma rays	185	815

The energy deposited in the Unit 2 moderator chamber from neutrons, beta particles, and gamma rays (prompt and delayed), is summarized in Table 3.1.

The calculated heat load is 1415 watts, based on MCNP results using the modified cross sections with delayed gamma rays described above. Indirect measurements indicate 1150-1200 W, so the measured heat load is 81 % to 85 % of the calculated value. The same can be said for the Unit 1 model heat load calculation, 950 W. It over-estimated the measured heat load, 865 W, by about 10 %. (The measured heat load is obtained indirectly by comparing the output of the refrigerator return gas heater with and without the reactor operating. Since some of the refrigerator parameters change during the transition, the method

leads to a wide range of measured values. This is discussed further in the Section 7, CNS operations.)

3.4 Evolution of the Liquid Hydrogen Sources

As mentioned in Section 2.2, the requirement of full illumination of the CTE and CTW beams intersecting outside the CT thimble, dictated that the source dimensions would be large. An early candidate was a double row of vertical tubes, approximating a plane source that was roughly a 30 cm square close to the front (reactor side) of the thimble. A second possibility was a vertical cylindrical annulus, similar to the second generation CNS in the Orphée reactor at Saclay[14] or a spherical annulus. Ultimately we chose a 32 cm OD spherical annulus that differed from the Saclay source in that the shell had a 20 cm exit hole through the LH_2 facing the neutron guides. (The source at Saclay illuminates beams on opposite sides.) The 32 cm annulus with the exit hole is referred to as Unit 1 in this report.

Several parameters were varied in a series of early MCNP calculations in an attempt to optimize the source performance: diameter, LH_2 thickness, exit hole size, LH_2 density (or void fraction in the boiling liquid) and the ortho-LH_2 content of the cold moderator. The latter two may be easy to vary in calculations, but they are not so easy to control or measure in practice. The outside diameter was chosen to be as large as possible given a number of engineering constraints:

- The annulus needed a 5 cm "bubble-cap" vapor separator above the sphere connecting to the LH_2 supply and return lines (see Section 4.2).
- It needed to be as close as possible to the front end of the cryostat assembly.
- The inside radius of the CT thimble is 27.5 cm.
- Surrounding the source there were three additional vessels, vacuum, helium containment for a 2 mm to 3 mm layer of He, and D_2O jacket containing about a 2 cm layer of D_2O to cool the assembly.

Neutron optics dictated the size of the exit hole. Its diameter had to exceed the guide height + $2 \times D \times \theta_C$. The exit hole in Unit 1 had a 20 cm diameter; it was changed in the elliptical geometry of Unit 2 to be 20 cm high by 15 cm wide.

The optimum thickness of the LH_2 annulus depends on both the void fraction and the ortho/para ratio. An overall density of 0.63 g/cm^3 (90 % of the nominal LH_2

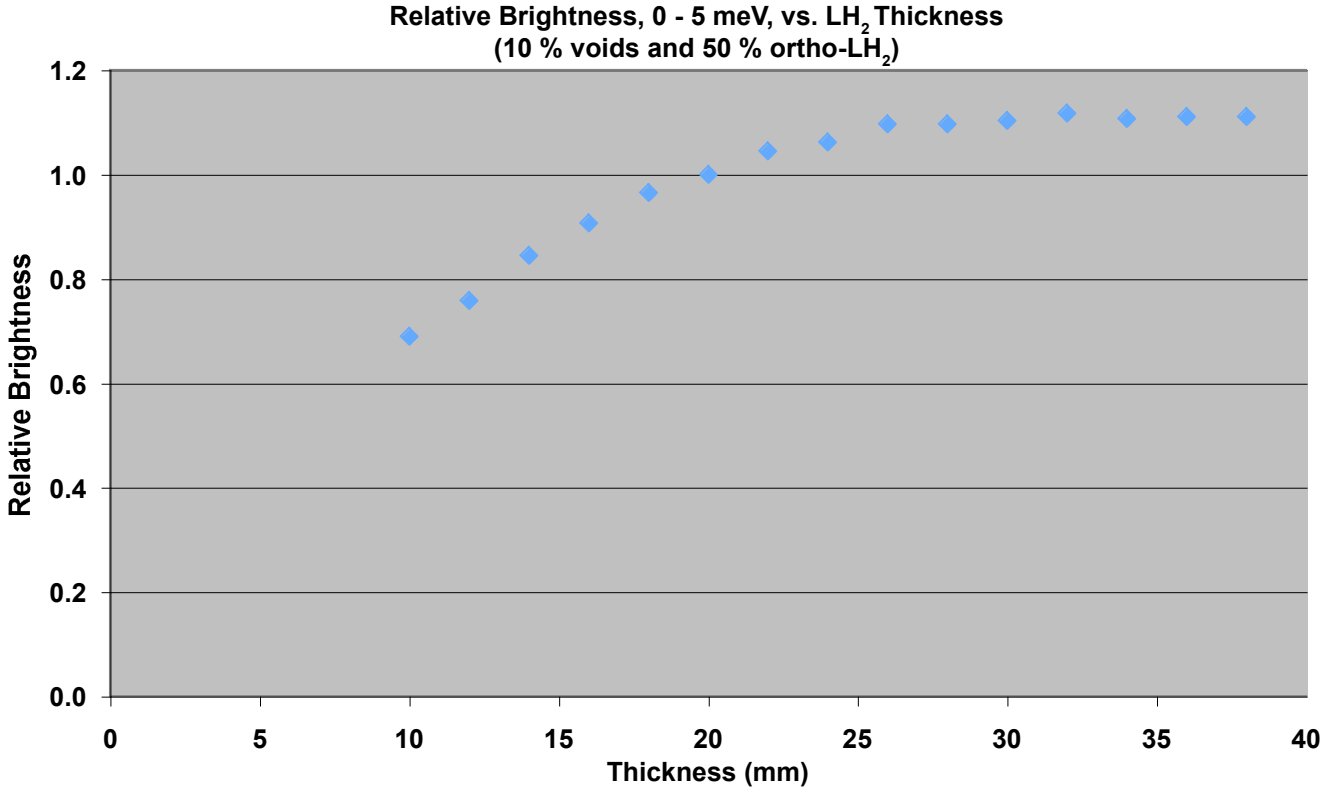

Figure 3.3. Relative brightness versus the thickness of the hydrogen moderator, Unit 1.

density), and a 50/50 ortho/para content, were chosen for the thickness optimization calculations. Figure 3.3 is a plot of relative brightness vs. the thickness of the LH_2 annulus for Unit 1. The LH_2 volumes of the 20 mm, 30 mm, and 40 mm thick annuli are 5.0, 6.9, and 8.4 liters, respectively. Although the maximum gain occurs at a thickness of 32 mm, we chose 20 mm as a compromise between neutron performance and hydrogen inventory. (A 1000 g inventory at 5 bar was self-imposed in the initial request for a NRC preliminary review). Increasing the thickness from 20 mm to 30 mm, for example, increases the inventory by nearly 40 %, but only increases the gain by 11 %. At the time, the estimated operating pressure of the source was between 1 and 2 bar, so the 30 mm vessel was rejected because at 2 bar, there would have been very little excess LH_2.

Later, the maximum thickness of Unit 2 was increased to 30 mm without increasing the inventory because the moderator chamber is smaller, a 32 cm by 24 cm ellipsoidal annulus. In either case, if the hydrogen converted entirely to para-LH_2, the thickness would have to be considerably greater, 50 mm to 80 mm.

As mentioned in Section 2.4, the scattering cross section for ortho-H_2 is much greater than that of para-H_2 at neutron energies less than about 15 meV. It is not surprising, therefore, that the gain and the cold neutron energy spectrum from the source vary considerably over the range of possible para-H_2 concentrations, 25 % for normal (room temperature) hydrogen to 100 % at 20 K. In the absence of ionizing radiation, LH_2 molecules would convert slowly to over 99 % para, because it has the lowest energy level. If, however, the molecules are dissociating and recombining at high rate, particularly in a two-phase system, the ortho content may be as large as 50 % to 75 %. Figures 3.4 and 3.5 show the effects of the presence of para-LH_2 in the Unit 1 source. The conversion of the moderator to 100 % para causes the brightness to drop 40 %, and a noticeable shift in

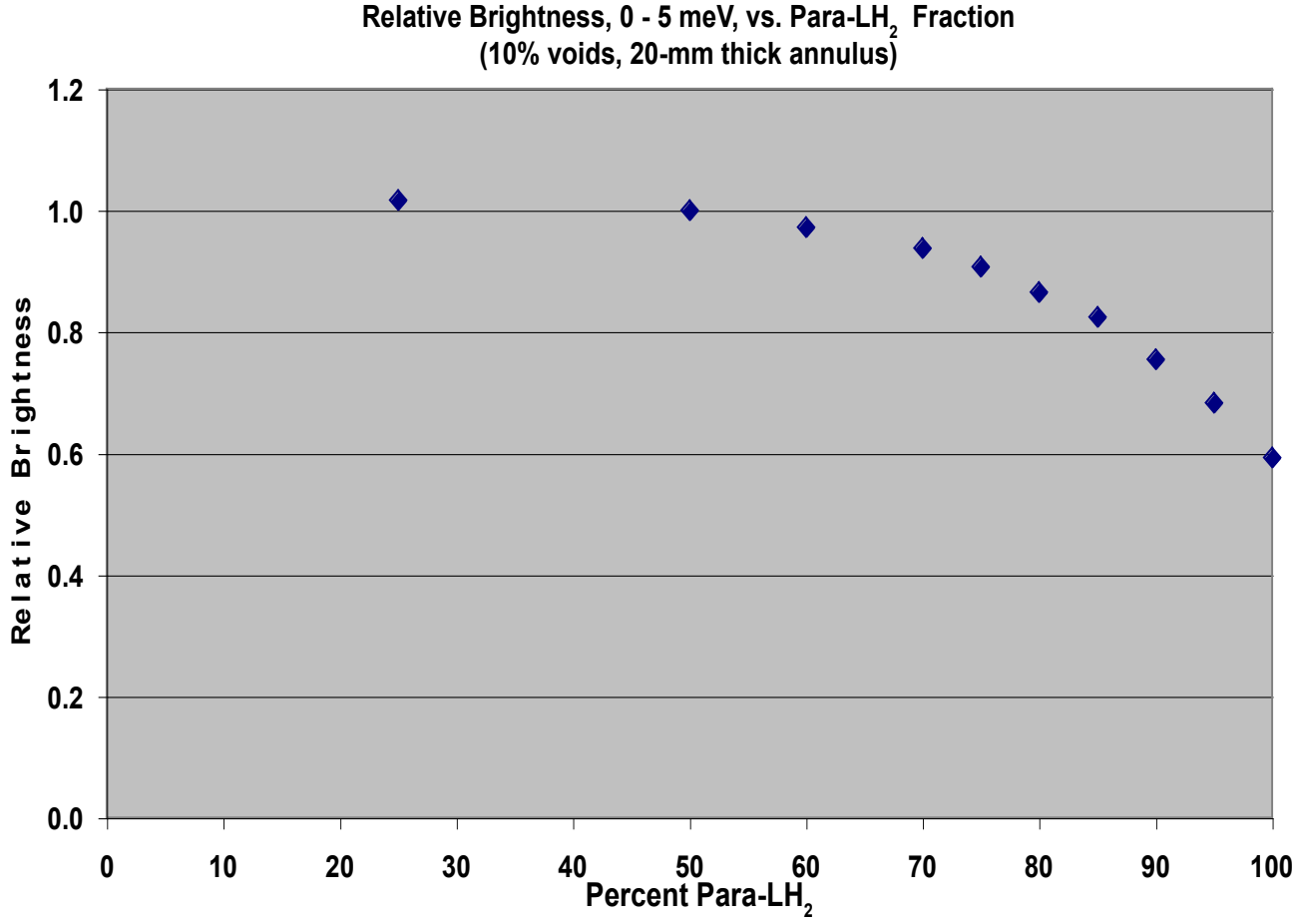

Figure 3.4. Brightness of the Unit 1 CNS as a function of the para LH_2 content.

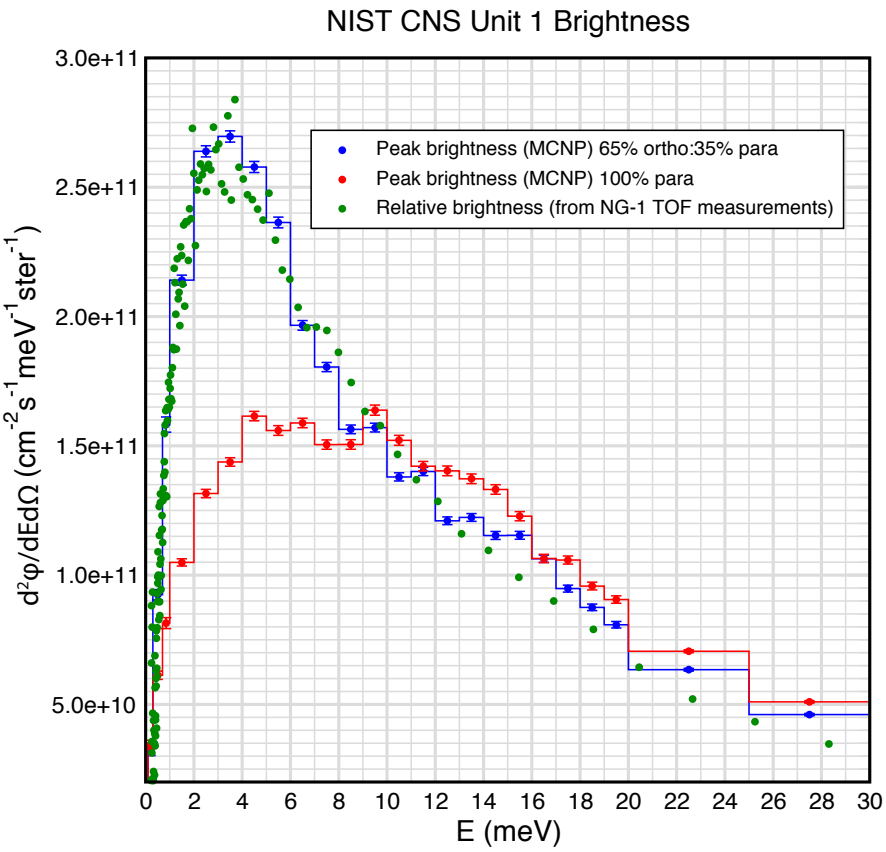

Figure 3.5. Measured TOF spectrum (April 1996) and MCNP calculations for 35% and 100% para-hydrogen in Unit 1. The TOF data have been renormalized showing that the shape of the measured spectrum is very simialr to the MCNP prediction for the 65% ortho-LH_2 case.

the neutron energy spectrum to an under-moderated state. Because the scattering cross section of ortho is so much greater than para, just 15 % ortho results in 82 % of the normal LH_2 brightness. From the shape of the measured time-of-flight spectrum in Figure 3.5, it is clear that the ortho content is sufficient to dominate the scattering in the moderator. Additional evidence of the large ortho content will be presented in the section on operating characteristics.

The void fraction due to boiling in the liquid hydrogen also affects the brightness, as shown in Figure 3.6. To verify that the annular vessel would not result in an excessive void fraction or thermal hydraulic instabilities, a full scale mockup was built at the NIST campus in Boulder for series of tests (see Section 4.3). Measurements of the mass of LH_2 vs. heater power indicated that the average void fraction would be about 10 % at the anticipated 800 watt heat load. As seen in Figure 3.6, there is only an 8 % decrease in brightness as the void fraction increases from 0 to 20 %.

In the first weeks of operating Unit 1, it was observed that reducing the system pressure resulted in a brightness increase of up to 5 % at the longest wavelengths. This result seems to conflict with the density dependence (Figure 3.7) above, because a pressure increase will reduce the bubble size in the boiling liquid. The flux increase, however, is due to decreased scattering of cold neutrons out of the beam directed at the guides, as the molecular density in the H_2 vapor decreased. The phenomenon is further evidence that the LH_2 and vapor are largely composed of ortho-hydrogen. Para-hydrogen, with its very small scattering cross section at low energies, is nearly transparent to cold neutrons. MCNP calculations show that brightness increases with increasing pressure if the vapor is 100 % para, as shown in Figure 3.7. A 50-65 % ortho-LH_2 concentration in the vapor, however, is shown to be consistent with the observed behavior.

Fixed-Source vs. Surface-Source Calculations:

Most of the early optimization work on Unit 1 was done using a fixed source of neutrons rather than the surface-source method described above. A source subroutine was added to the MCNP code to start thermal and epithermal neutrons from the outside surfaces of the CNS region. The spatial distribution of these neutrons was dictated by neutron flux profiles taken from the original SAR of the reactor, NBSR-9[2]. Starting neutrons were distributed uniformly over the base of the cylinder defining the region (55.5 cm from the core center), and distributed with a linearly decreasing probability along the cylindrical surface, as the distance from the core increased. In the absence of a model of the reactor core, this source subroutine

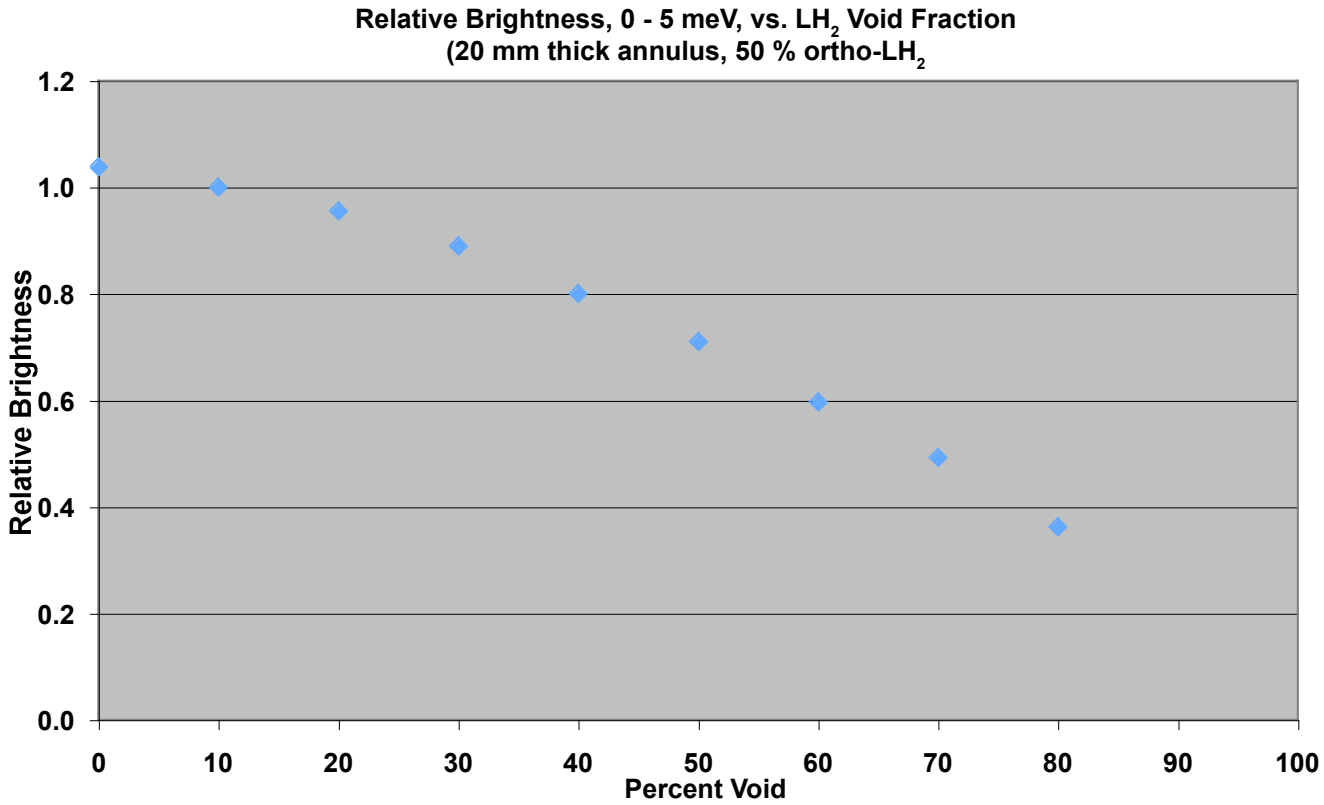

Figure 3.6. Brightness versus void fraction for the Unit 1 source.

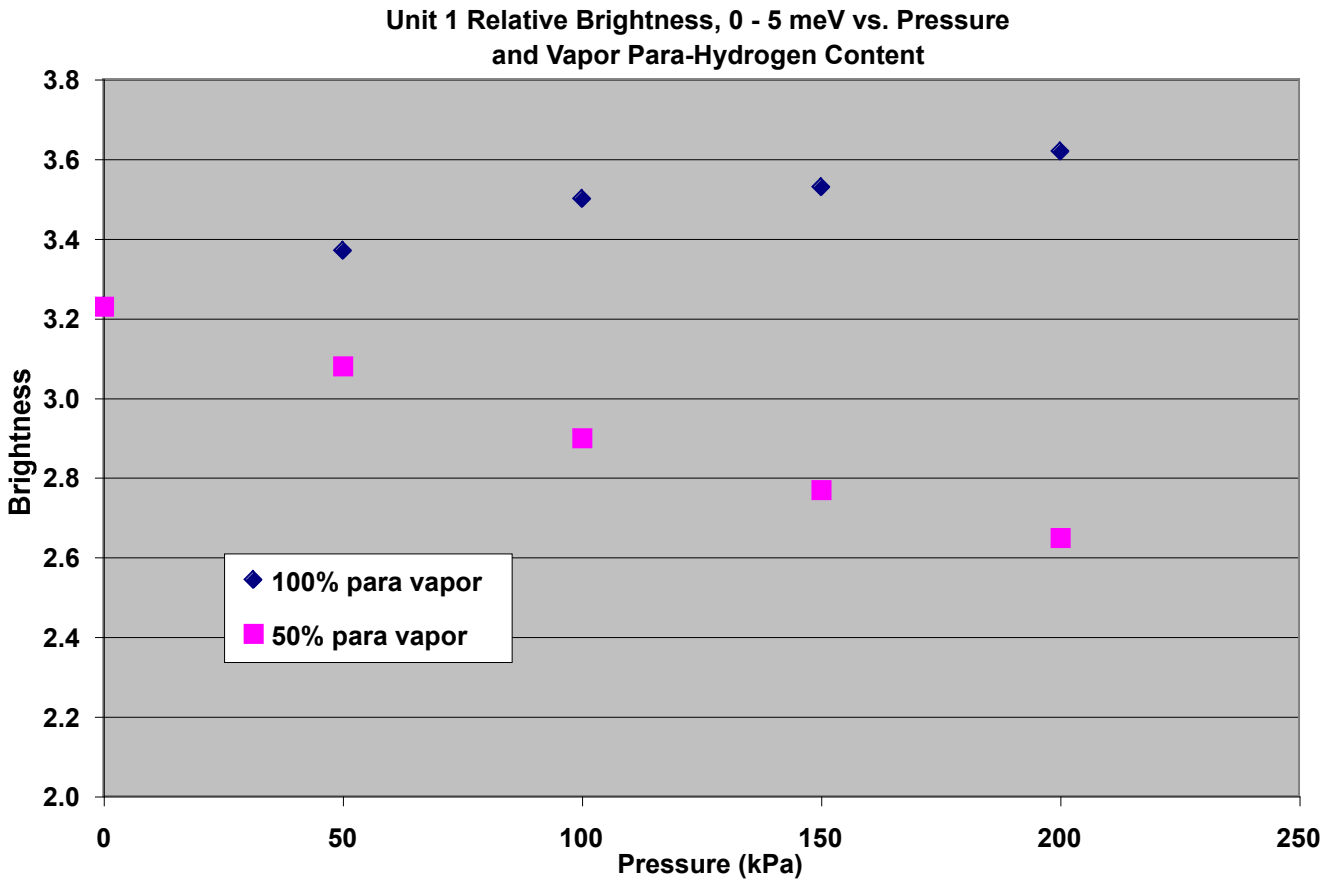

Figure 3.7. Brightness versus pressure for 100% and 50% para-hydrogen vapor (the liquid density held constant at 90%).

mimicked the flux expected around the CT thimble. There was no effort to normalize the subroutine to reactor power.

Although the fixed source calculations could not provide absolute values for the source performance or the nuclear heat load, they did allow us to compare the relative behavior of the candidate geometries, and calculate the effects of thickness, density and ortho-para ratio. The geometry of Unit 1 was determined by the fixed source calculations.

The first model of the core was used to estimate the nuclear heat load in Unit 1 in 1992. By that time, the thermal hydraulic tests were well underway in Boulder (see Section 4.3), and the 3.5 kW refrigerator was installed. A heat load of 800 W to 900 W was calculated, assuming that the fission product gamma ray heating was equal to the prompt fission gamma ray contribution.

The whole-core model confirmed the expected cold neutron gain of 22 for Unit 1 with respect to an empty cryostat, but predicted a 25 % lower gain with respect to the existing D_2O source than did the fixed source calculations (6.7 rather than 8.8). The discrepancy arises because the fixed source is insensitive to the impact of the cold source itself on the neutron flux in the adjacent fuel elements in the core. Unit 1 introduced a large void in the reactor reflector compared to the D_2O source, lowering the thermal neutron flux in the northwest corner of the core. In fact, the whole-core model revealed that there was a one-time loss of about 0.6 % reactivity in the core when Unit 1 replaced the D_2O source, worth about 2 days of full power operation. As the core model was improved, preliminary design work began on a second generation LH_2 source even as Unit 1 was being installed.

The Advanced Liquid Hydrogen Cold Source:

Modifications incorporated in Unit 2 resulted from improved computational models and experience gained in the operation of Unit 1. Calculations demonstrated that filling a portion of the insulating vacuum space of Unit 1 with D_2O, so the source was partially surrounded, would increase the neutron flux throughout the cold source region and increase the brightness by over 40 %. Experimenting with the operating pressure of Unit 1 showed that the vapor within the inner sphere was scattering at least 10 % of the cold neutrons from the direction toward the guides.

A lengthy series of calculations was needed to study and optimize the neutronic coupling of the core and the source. An ideal limiting case, although totally impractical, is a source like Unit 1, with no vapor in the center, nearly surrounded with D_2O, and a very small exit hole. Such a source could provide one small beam with a brightness of 3.4 times that of Unit 1. Since the

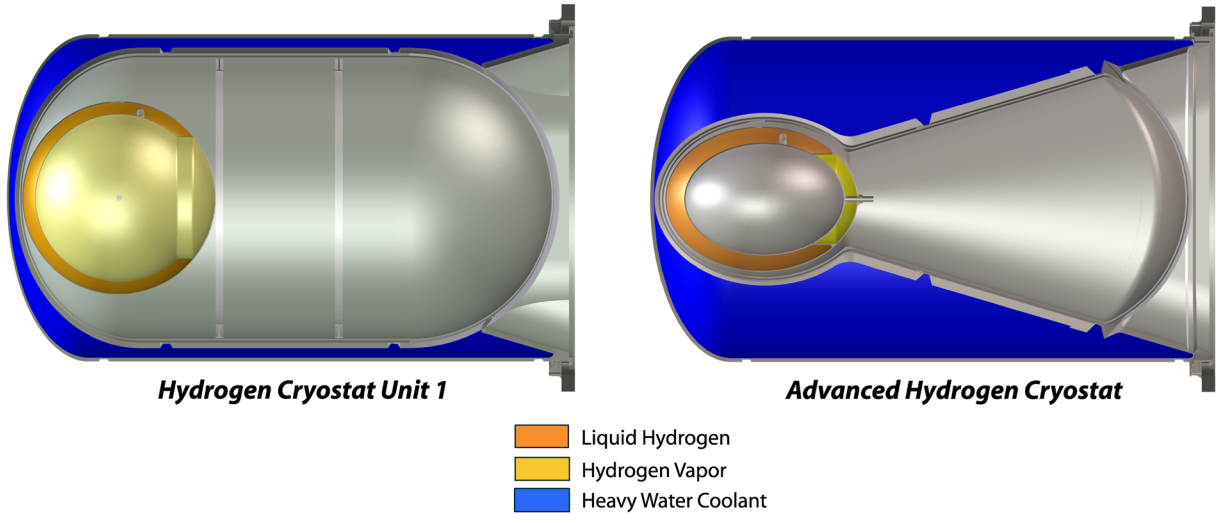

Figure 3.8. Comparison of the Unit 1 assembly (left) and that of the Advanced Cold Neutron Source (Unit 2).

cold neutron beam ports through the biological shield of the NIST reactor span a range of 16.5° on either side of the axis of the center cryogenic port, we needed to balance the conflicting goals of surrounding the source with D_2O and fully illuminating the existing guides. MCNP is ideally suited for this task, but the process required many, lengthy criticality calculations because the addition or subtraction of a few well-positioned liters of D_2O changed the reactivity of the core (k_{eff}), the thermal neutron flux in the region, and even the fuel utilization.

Engineering constraints must also be considered in the MCNP calculations. The moderator chamber is surrounded by a vacuum vessel, that is surrounded by a helium containment vessel, strong enough to withstand the design basis accidental detonation of liquid hydrogen and solid oxygen. The helium vessel determines the extent of the D_2O volume. Thus, through an iterative process, the conceptual design had to be modified as the complex mechanical design was finalized.

The geometry of the advanced source differs from Unit 1 in many key respects, as shown in Figures 3.8 and 3.9. The most important change is the addition of 60 liters of D_2O to the cooling jacket, partially surrounding the moderator chamber. This substantially reduced the area of the void through the reactor reflector, increasing the thermal neutron flux in the cryostat region about 40 %. Unit 2 is an ellipsoidal, rather than spherical, annulus, with major axes of 320 mm, and a 240 mm minor axis in the transverse horizontal direction. This 5 liter annulus is between two nearly concentric Al-6061 ellipsoids; its average thickness is 25 mm. The center of the inner ellipsoid is offset 5 mm, however, so that the annulus is 30 mm thick near the core, and 20 mm

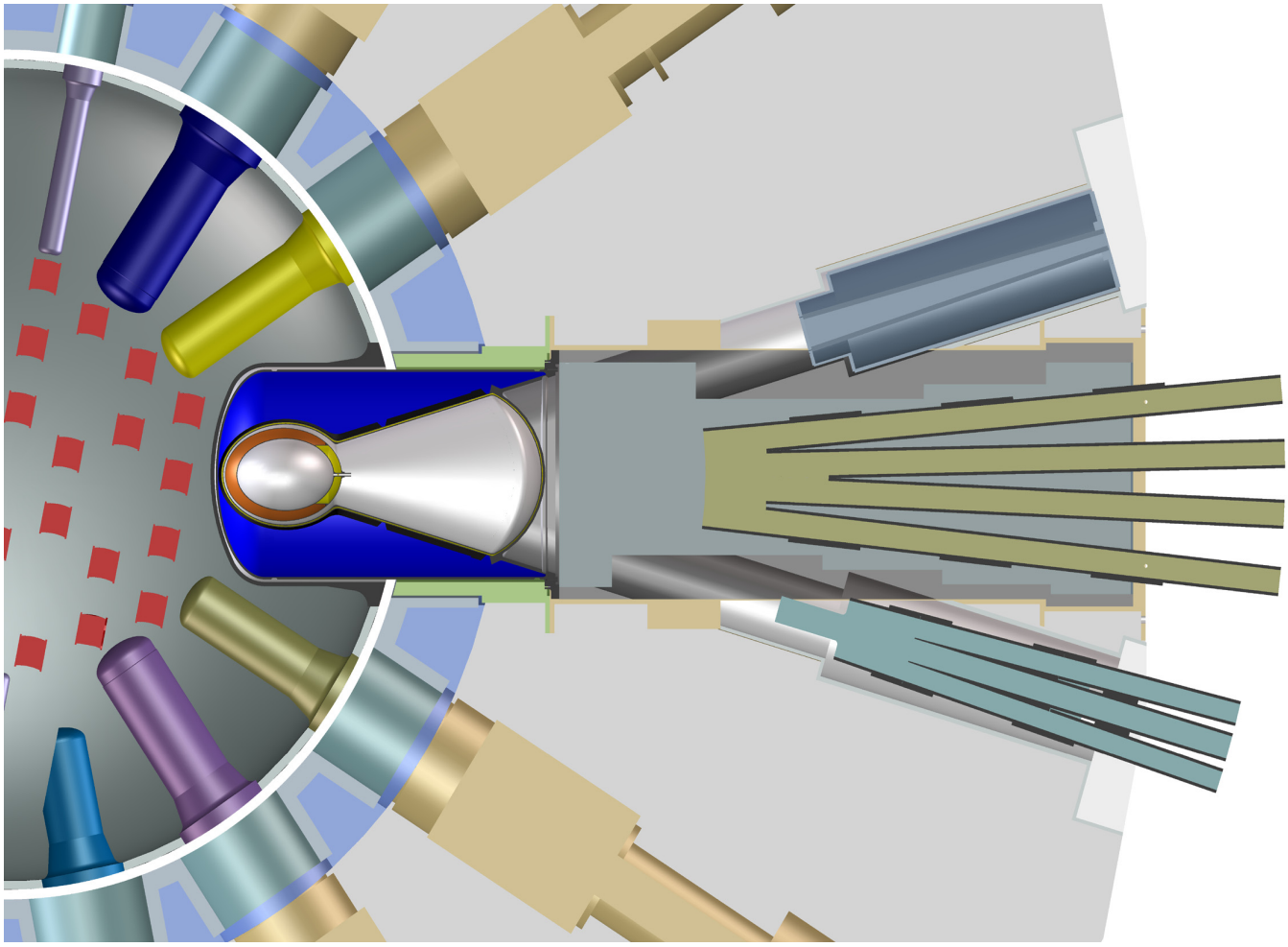

Figure 3.9. Plan view of the Advanced Cold Neutron Source. The cryostat assembly was inserted horizontally into the cryogenic beam port. The cold neutron beam ports intersect at a point near the exit of the thimble, about 20 cm from the center of the LH_2 vessel.

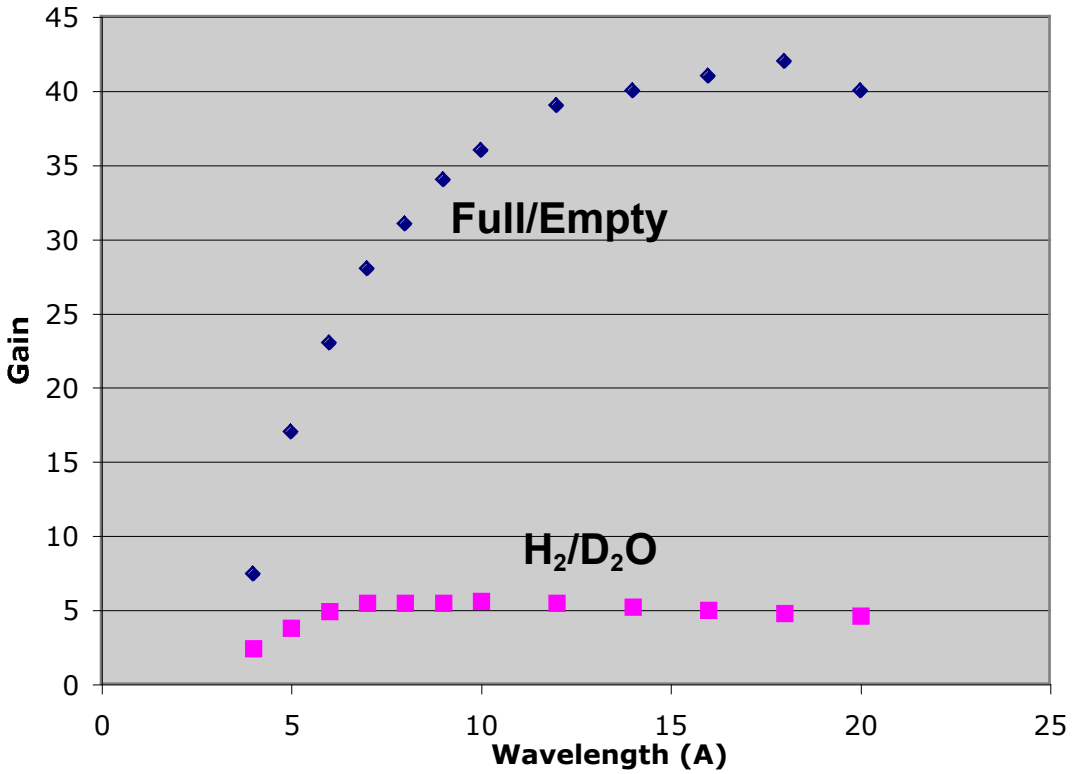

Figure 3.10. Neutron gain versus wavelength for Unit 1. The bottom curve is the gain with respect to the old D_2O source, and the top curve is the gain with respect to the source while warm.

thick at the exit hole. The inner ellipsoid is evacuated through a small vacuum port. For structural reasons, hydrogen vapor fills the elliptical exit hole (200 mm by 150 mm), but in Unit 2, the cold neutron beam will pass through only 20 mm of vapor, rather than 300 mm. These changes in the moderator chamber added another 20 % to 25 % gain.

An ellipsoidal annulus provides three advantages. Because it has a smaller volume, more D_2O can be introduced in the cryostat assembly. It is also possible to increase the LH_2 thickness while maintaining the same volume as Unit 1. An elliptical shape is also desirable from a neutron optics standpoint; the neutron guides at NIST are all rectangular, most are 60 mm wide and 150 mm tall, so they are still fully illuminated with the smaller cold source volume. A disadvantage was that the mass of the moderator chamber increased over that of Unit 1, from 2.1 kg to 2.8 kg, because the inner vessel had become part of the hydrogen boundary.

A separate calculation, presented in Section 3.3, was required to determine the nuclear heat load in the chamber when the reactor is operating at 20 MW. For the new moderator chamber described above, the calculated heat load is 1400 W. It increased as a result of the additional mass of aluminum and the higher neutron flux. From our previous attempts at a benchmark for Unit 1, however, the MCNP result overestimated the heating by 10 % to 15 %, so we expected that 1200 W to 1300 W would be deposited in Unit 2. Based on our tests at Boulder, the increased heat load over Unit 1 would be easily removed by exploiting our excess refrigerator capacity. The measured heat load was 1150 W to 1200 W.

Unit 2 was first operated in March, 2002. Only one aspect of its behavior was unexpected. It was thought that with most of the H_2 vapor removed, there would be an increase in brightness as the system pressure increased, owing to the reduced void fraction in the LH_2. Instead, just like Unit 1, the flux decreased as the pressure was raised. Even though there is only 20 mm of vapor in the exit hole, the loss from the vapor scattering still outweighs the gain due to the lower void fraction. Therefore, the source is operated at nearly the same pressure as Unit 1 (90 to 100) kPa.

3.5 Source Performance

The neutron performance of the source has been evaluated in many ways, including gain over the previous D_2O ice source, gain full to empty, absolute flux, and cold neutron spectrum. The measured gains for Unit 1 are shown in Figure 3.10 as a function of neutron wavelength. Agreement with calculation was highly satisfactory, and the cold neutron gains (full/empty) are as high as those seen for any hydrogen source. The gains measured at all of the instruments were fully consistent with those shown here, which are those measured at the NG-7 30 m SANS. The intensities at approximately 2.5 Å for the SPINS triple axis spectrometer were equal to or better than those at the best spectrometers at thermal beam ports at similar resolution (note that the NIST guides are not curved, providing excellent continuous measurement capability from 2.5 Å to 6 Å)

Another benchmark for source performance is the total capture neutron flux in the guides, an integral measurement that is most sensitive to the longest wavelengths (e.g. for a 45 K Maxwell-Boltzmann spectrum, over half of the capture flux comes from neutrons with wavelengths longer than 10 Å). Hydrogen sources are certainly inferior to deuterium sources at the longest wavelengths because of absorption and, as stated earlier, the primary region of interest is below 10 Å. For the Unit 1 source, the

Table 3.2. Capture flux measurements from Unit 1 at various guide locations.

Guide - location	φ_c^{meas}/cm^{-2}s^{-1}
NG-0 (NDP in C-100)	2. 6 x 10^9
NG-1 (Reflectometer)	3.0 x 10^9
NG-2 (Before filter)	3.4 x 10^9
NG-3 (Before SANS filter)	1.7 x 10^9
NG-4 (Shutter position)	2.7 x 10^9
NG-5 (Entrance guide hall)	2.3 x 10^9
NG-6 (Entrance guide hall)	2.3 x 10^9
NG-7 (Reflectometer)	1.9 x 10^9

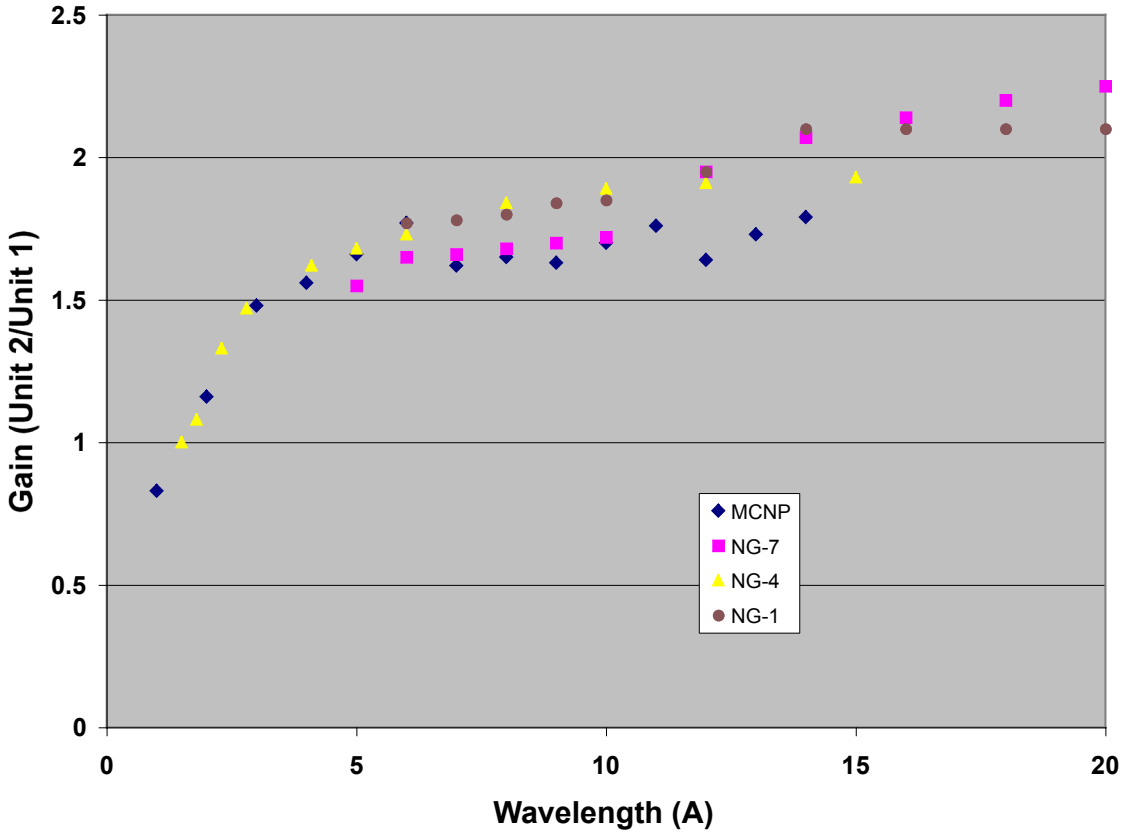

Figure 3.11. Measured and calculated gains of the Advanced Cold Neutron Source. Some gains exceeded predicted values because improvements were made to the neutron guide system.

capture flux measured inside the neutron guide hall (35 m from the source) was 2-3 x 10^9 n/cm^2/s, see Table 3.2. Allowing for guide losses and for the high ortho/para ratio in the gas as discussed above, this was in satisfactory agreement with the calculated value of 4 x 10^9 n/cm^2/s, assuming no losses.

A time-of-flight measurement of the cold neutron spectrum was obtained at the end of NG-1, and plotted against the MCNP estimates in Figure 3.5. The TOF data has been corrected for solid angle, guide acceptance and reflectivity, and absorption in aluminum windows, to determine the source brightness. Both the shape and intensity of the measured spectrum agree very well with MCNP calculations in which the ortho content of the LH_2 was 65 % (best fit). Simulations with 100 % para-hydrogen predict intensities above 4 Å to drop by a factor of two. All of the performance measurements are consistent with our conclusion that the liquid hydrogen is maintained with at least 50 % ortho.

The neutronic performance of the new source was benchmarked by duplicating flux measurements made with the Unit 1 cold source at several Guide Hall instruments. Figure 3.11 is a plot of the cold source gain, defined as the ratio of intensities between Unit 2 and Unit 1, as a function of neutron wavelength. The figure includes the gain factors measured at three spectrometers and the gains calculated using MCNP. While the agreement is excellent, the measured gains were actually somewhat greater than predicted, especially at long wavelengths. This additional gain is likely due to the new guide sections replaced during the cold source installation, an effect not included in the MCNP models. The new cryostat design also substantially reduces the number of fast neutrons from the cold source resulting in improvements in instrument signal-to-noise levels.

4. Thermal Hydraulic Design

4.1 Design Criteria

The first and over-riding design requirement was simple, robust operation under varying conditions of heat load (e.g. reactor on/off), which immediately focused the design on a liquid hydrogen thermosiphon. In this design, which has been used at many facilities, heat is removed by allowing cold hydrogen to flow into the moderator chamber under gravity, forcing warmer hydrogen (vapor, liquid, or two phase) out of the chamber to a secondary source of heat removal (condenser, heat exchanger). The first step in the design was to establish the likely minimum and maximum heat loads, as described in the previous section. Rather quickly, the neutronics design led to results that established the likely mass of hydrogen and cryostat metal that would be in the high flux area, enabling initial studies of the thermal hydraulic design.

4.2 Initial Design

Originally, the maximum expected heat load of Unit 1 was determined to be 1500 W, with a probable value of less than 1000 W. An operating pressure of approximately 100 kPa to 200 kPa was chosen as a design goal, as a compromise between higher pressures which tend to reduce the void fraction and lower pressures which tend to reduce scattering losses from the vapor in the exit path. This choice also yields a reasonably sized storage vessel, and allows the use of containment helium pressures only slightly above barospheric. The latter condition ensures that any leak is from the helium space into the hydrogen volume, and that monitoring of the helium pressure will give indications of a leak, while minimizing the design pressure for the containment system.

Since the cold source was to be installed into an existing horizontal beam port, the next step was to calculate the length of horizontal piping that would be required, and then to size the piping using the physical constraints on the location of the condenser, which in turn sets the available driving head for the thermosiphon. At this stage, the configuration of the lines leading into the source also had to be specified (to obtain a length, and to ensure that adequate radiation shielding would be in place). The final piping design, which differs only in detail from the original conceptual design, is shown schematically in Figure 2.1. For reasons of space constraints, it was decided to go with a design in which the liquid flowing to the source passed through an inner tube, while the return (gas or two phase mixture) passed through a concentric annulus surrounding the supply line. In this design, the supply and return lines act as a relatively efficient counter-flow heat exchanger. This design has several advantages:

- Compact design to meet space constraint.
- Good thermal isolation of the supply line.
- A nearly isothermal system, so that all thermodynamic variables are determined by pressure alone (allowing measurement of only one variable, outside any high radiation area).
- Once flow is established, the operating point is stabilized by the properties of the supply and return lines acting as a counter flow heat exchanger.

And it has some disadvantages (some of which were only discovered in later tests):

- Fabrication and assembly is complex.
- Establishment of initial flow and re-establishment of flow after an upset is made difficult by the heat exchanger effects.

For design purposes, a total length of 5 m, of which 1.5 m is vertical, was assumed. Using these values, a preliminary design consisting of a ½ inch (1.27 cm) diameter inner tube, surrounded by a 1¼ inch (3.175 cm) diameter tube was chosen. This provided flow areas of approximately 1 cm^2 for the liquid supply line and 4 cm^2 for the return line. Using single phase estimates of pressure drop, this design would allow for a maximum heat load of more than 2500 W at full flow, limited only by the tubing pressure drops. This model was used in the tests described below. More recent calculations, using the as-built drawings, and a model for two phase flow developed by Dukler[15], give the results shown in Figure 4.1. In these calculations, the pressure drop within the moderator chamber itself is neglected, since the flow area is approximately 200 cm^2. Note that the total flow through the system consists of the liquid going to the moderator, and the two phase return, driven by the head arising from the difference in density of the liquid and two phase fluid. At approximately 3000 W, the fluid leaving the moderator chamber is all vapor, and a further increase

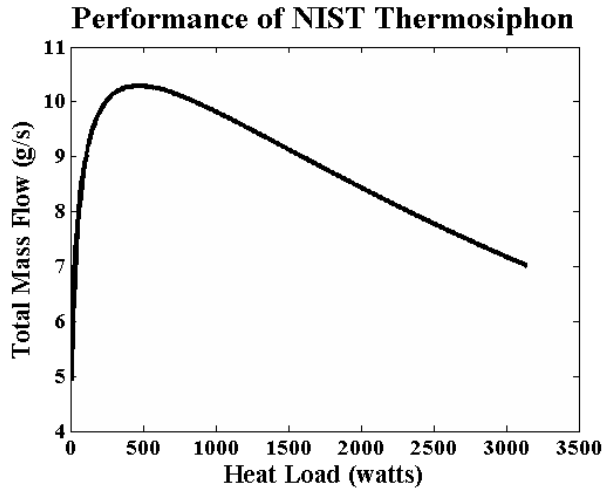

Figure 4.1. Calculated performance of the thermosiphon for the NIST liquid hydrogen cold source.

in heat would empty the chamber and flow would cease.

A key parameter in the neutronics performance of this system is the void fraction present in the moderator chamber as a result of vapor bubbles rising through the liquid. The vapor lowers the effective density of the hydrogen, and reduces the effective moderator thickness. Although this can be partially rectified by making the moderator annulus thicker, the intensity in the NIST reactor drops monotonically with distance from the center of the reactor, so that this strategy is not fully effective, and at some point, will result in reduced intensity. The geometry of the concentric spheres provides a constant flow area for the vapor over the height of the inner sphere; however, above this level, the area rapidly decreases, and is at a minimum where the vapor return line attaches to the outer sphere. This causes a large acceleration of the vapor, which tends to carry along extra liquid into the return. This could lead to a relatively large volume at the top of the source that is almost entirely vapor, decreasing source performance. In an attempt to improve performance, a "bubble cap" (phase separator) was added at the top of the moderator, as shown in Figure 4.2. This addition provides a space where the area again increases, allowing the vapor to expand, and liquid to strike the top of the cap, and drain to the bottom of the cap, where holes allow the liquid to return to the moderator, in counter-flow. The supply line ended in the exit of the vapor line from the outer sphere, inside the cap as shown in Figure 4.2.

In order to choose a nominal thickness, an estimate of the expected void fraction is needed. One estimate can be obtained by using the prediction for the terminal velocity of bubbles rising in a swarm of other bubbles[16]:

$$U = (1-\alpha)^{1/2}\, 1.53\, [\sigma g(\rho_L-\rho_G)/\rho_L^2]^{1/4}$$

where:

α = the void fraction

σ = the surface tension

$\rho_{L,G}$ = the density of the liquid, gas

The void fraction α is simply given by the superficial velocity U_{GS} of the vapor (volume of vapor generated/s over the flow area) divided by the terminal velocity U. For the estimated heat load of 1 kW (which gives the total gas volume generated over the entire height) and

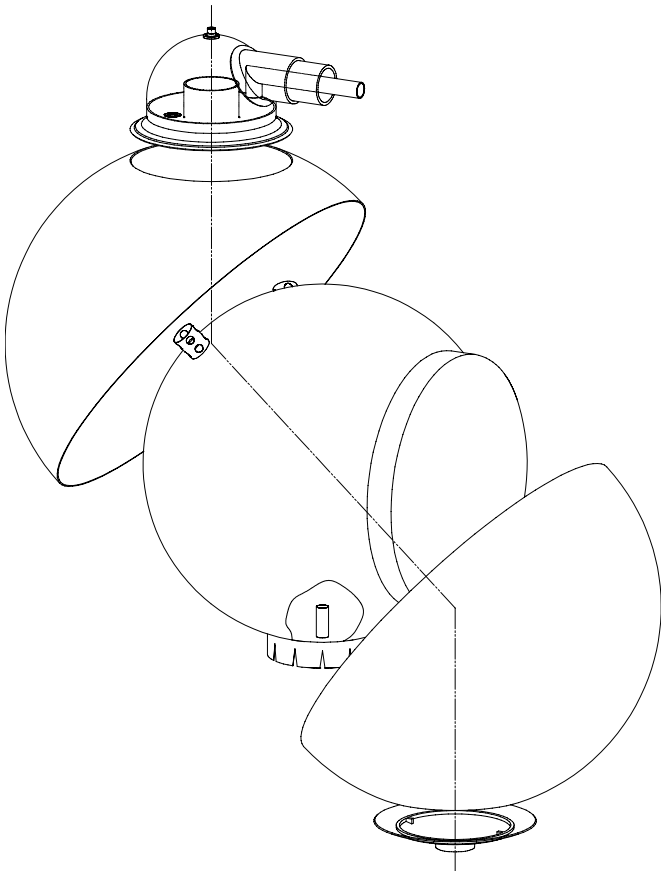

Figure 4.2. Original design of the first hydrogen cold source moderator chamber (spherical annulus).

an approximate flow area of 200 cm^2, the <u>average</u> (i.e., the superficial velocity at mid-plane, corresponding the one-half the heat load) superficial velocity U_{GS} = 4 cm/s at 0.1 MPa.

Therefore,

$$\alpha = U_{GS}/U = U_{GS}/(1-\alpha)^{1/2}\, 1.53\, [\sigma g(\rho_L-\rho_G)/\rho_L^2]^{1/4}$$

This leads to a predicted average void fraction of 28 %, which could be reduced to 20 % by increasing the pressure to 0.15 MPa. This was the preliminary design – to operate the source at approximately 0.15 MPa, and to optimize the pressure by observing the neutron intensity as a function of pressure. The initial thermal hydraulic design also assumed that the thermosiphon would be operated with single phase flow in both the supply (liquid) and return (vapor) leg by controlling the hydrogen inventory and pressure.

4.3 Thermal Hydraulic Tests at NIST Boulder

As a result of the uncertainties involved in the novel shape of the moderator chamber volume, a full scale mockup of the cryostat and transfer lines was built and tested at the Boulder site of NIST. The details of the mockup, tests and calculations have been published as a NIST internal report[5]. The mockup (of the original spherical shell system) was constructed from two standard, commercially available glass spherical flasks of volume 12 liters and 22 liters. This gave an annulus of almost 2 cm, as in the planned source, but a larger total volume of 6.755 liters rather than the 5 liters planned for the actual source. The nuclear heat load was simulated by a resistance heater consisting of a flat nichrome ribbon (with dimensions chosen such that the heat flux at 2 kW input was less than one-forth of the critical heat flux for departure from nucleate boiling) wound loosely around the inner glass sphere, as shown in Figure 4.3. As a result of the slightly larger diameter of the test system as compared to the planned source, the flow area between the two spheres is 1.137 times as large as that for the actual system, and the volume is 1.35 times as large. The very close match of the annular gap gives high confidence that the results obtained will be representative of the actual system. As shown in Figure 4.4, the entire moderator chamber was mounted on a balance scale, so that the actual mass of hydrogen in the system could be measured under operating conditions.

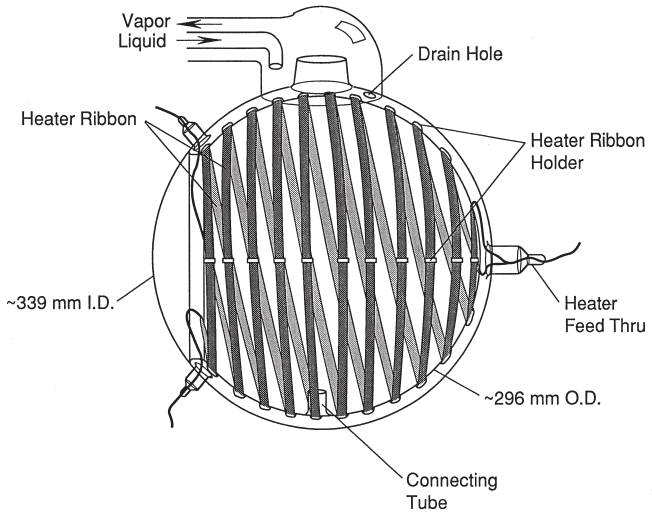

Figure 4.3. NIST-Boulder moderator test vessel.

After some initial difficulties achieving an adequate insulating vacuum preventing liquid from flowing to the vessel, the vessel was successfully filled with LH_2 and void fraction measurements as a function of heater power were made. A second test was made to assess the ability of the thermosiphon to restart following a temporary interruption of the LH_2 supply. Even when the heater was turned off, however, with the supply line configured as shown in Figure 4.3, the *flow of LH_2 to the vessel could NOT be restarted until all the liquid in the vessel had evaporated*. It was not possible to overcome the backward flow of vapor up the supply line. This failure led directly to an important design change, namely, to extend the LH_2 supply tube to the bottom of the vessel.

A smooth tube was added to extend the liquid fill line to the bottom of the annulus, and two complete runs were obtained in which the input power could be varied and other parameters tested. In the course of arriving at this test geometry, a corrugated tube was used initially to extend the fill line, and filling could not be achieved. This result clarified one of the primary issues with this design – the effect of the coaxial supply and return lines. In this design, it is difficult to change the operating point because the transfer line acts as a counter-flow heat exchanger, making changes difficult (such as getting the entire system cold). During the successful filling of the system, the vessel was cooled by individual liquid drops "dancing" down the fill line, in a manner analogous to liquid nitrogen on a floor. This provided the necessary imbalance in the system to allow cooling, and showed clearly that corrugated lines (i.e. bellows) would totally inhibit filling. All bellows used in the system are lined with

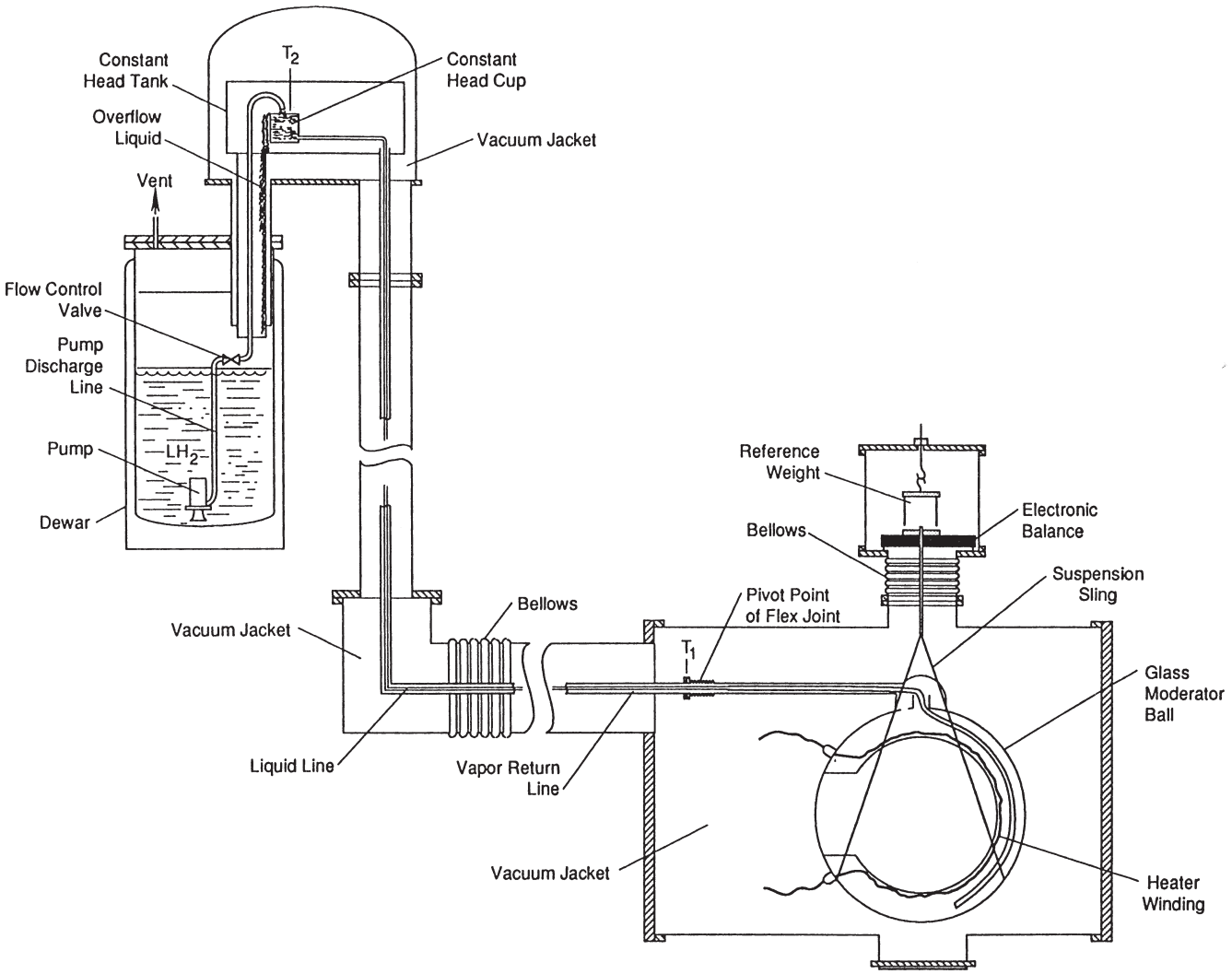

Figure 4.4. Diagram of the NIST-Boulder test configuration.

a smooth insert to reduce friction, and there are no bellows in the liquid supply line. Although attempts were made to operate with limited hydrogen flow, this proved impossible. However, by keeping the supply line full (by constantly overflowing the constant head cap), stable operation was routine, under low to high (2200 W) heat load. Following a heat input change, the system immediately stabilized at a new flow condition, with no instability of any kind. This was true even for almost instantaneous large power changes.

During each of the tests a video record of the boiling behavior was recorded for later analysis. This record was especially illuminating regarding the modes of boiling and bubble rise, which are notoriously difficult to model properly. Among the more salient observations from these video records are the following:

- The bubbles rise in a spiral path around the vertical axis, completing 1/8 to 1/4 of a revolution during their rise.
- The total rise time of a bubble from the bottom of the sphere to the top is of order 1 s, implying an approximately constant velocity of approximately 35 cm/s.
- The bubbles seem to be of uniform size, approximately 1 cm in diameter.
- Bubbles tend to follow each other during their rise.
- The areal distribution of bubbles seems to be uniform, and relatively stable at any height.
- Up to 2200 W, there was no liquid-vapor interface in the spherical annulus.
- The bubble cap on the top of the sphere did seem to accomplish some phase separation.
- With the constant head in this test, the return line flow was always two phase up to 2200 W input power.

The void fraction as a function of input power at 85 kPa (barospheric pressure in Boulder) was measured by observing the weight of hydrogen in

the chamber, and determined to be almost linear, reaching approximately 20 % at 1800 W. The effect of pressure on mass in the chamber at an input power of 860 W was measured over a limited range up to 125 kPa, and the mass was found to increase almost linearly. Experimental difficulties prevented a detailed examination of void fraction as a function of pressure, but a model was proposed that indicated a maximum in mass, in the chamber, should occur at 150 kPa.

Based upon this model, and earlier experience in the design of a cold neutron source for the Institut Laue Langevin[4], it was decided to operate the NIST source with a sufficient inventory of liquid hydrogen that flow would be self-limiting, *i.e.* by providing the equivalent of the constant head cup at the top of the hydrogen supply line, as shown in Figure 4.5. This required a design for the condenser that provided

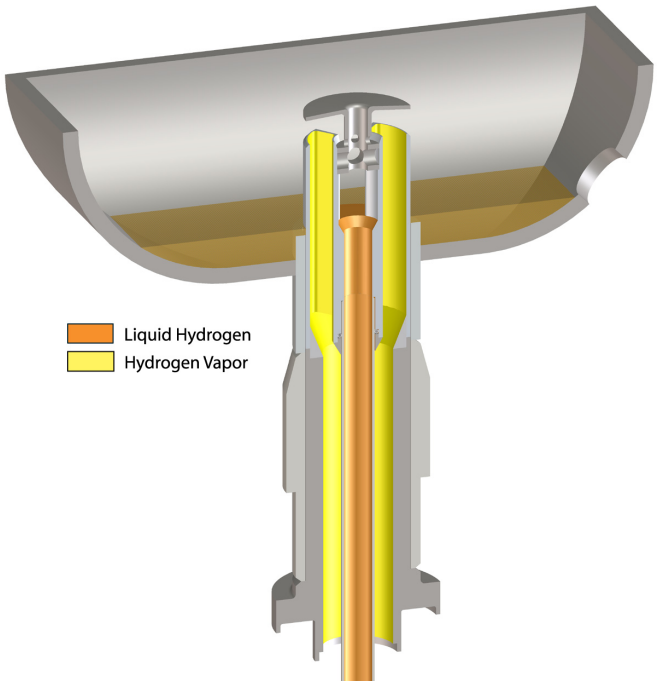

Figure 4.5. Arrangement of hydrogen supply and return lines at the bottom of the hydrogen condenser.

room for excess liquid, so that there would be no need to control the inventory too closely. Further, the inlet liquid line was extended to the bottom of the annular space, allowed restarting of flow after an interruption caused, for example, by a refrigerator upset. Finally, the decision was made to plan on a hydrogen pressure near 150 kPa, but to check for the value that gave the best intensity with neutrons.

4.4 Other Components (Condenser, Ballast Tank, Hydride Storage)

While sizing all of the non-cryostat components, the decision was made to allow for future changes, such as development of a liquid deuterium source, which was estimated to require 3.0 kW to 3.5 kW of cooling capacity. Therefore, a design effort was begun to develop a condenser capable of at least that amount of heat transfer from cold helium gas to the hydrogen vapor. During the commissioning of the refrigerator, the plate-type heat exchangers used for that system were being examined, and the engineer from the manufacturer suggested that the same company could make a condenser to our specifications. The actual condenser is a hydrogen reflux condenser, consisting of multiple welded aluminum plates in counter-flow geometry, providing 5.042 m^2 of heat transfer area for the hydrogen side and 3.526 m^2 for the helium side. This provides 848 W/K at 5.16 K logarithmic mean temperature difference, or 4375 W, thus yielding a 25 % margin over the 3.5 kW requirement. The effective length of each plate is 291 mm. The entire assembly is contained in a stainless steel vacuum jacket, with connections for helium transfer lines, a reflux line for hydrogen, and two junctions to allow connection of the condenser to a remote storage tank and gas handling system. As shown in Figure 4.5, the hydrogen line from the condenser comprises an inner supply line along with a concentric, annular return line, that attaches to the condenser by means of a specially designed fitting incorporating a weir over which the liquid must flow. The height of the weir is chosen such that any oxygen impurities would be trapped there, rather than going into the moderator chamber and exposed to high radiation.

The amount of liquid hydrogen present on the plates is of interest, since that provides a reservoir for liquid during operation, and affects the inventory required. To calculate this volume, it is necessary to estimate the thickness of the film formed on the heat transfer plates. From standard texts[17], the film thickness δ is given by:

$$\delta = \left[4\,\mu k y (T_G - T_W)/(g h_{fg} \rho(\rho - \rho_v))\right]^{1/4}$$

where:
μ = viscosity of liquid = 1.32×10^{-5} kg-m^{-1}s^{-1} at 100 kPa and 20.2 K
k = thermal conductivity = 0.0989 W-K^{-1}m^{-1}
y = distance from top of plate (m)
$T_{G,W}$ = gas, wall temperature
h_{fg} = enthalpy of vaporization = 445.5 kJ/kg
ρ = liquid density = 70.8 kg/m^3
ρ_v = vapor density = 1.33 kg/m^3

This yields an average thickness of $0.8 \times 0.00018 \times y^{1/4}$, or 10^{-4} m for the plate length used, which, when combined with the total plate area of 5 m^2, gives a volume of 0.5 liters of liquid on the plates during operation.

The NIST source is designed so that there are no active components required in the hydrogen system during the entire cycle, from all gas at room temperature at a moderator chamber full of liquid. This requires provision of a "ballast tank" that can contain all of the hydrogen at room temperature and a modest pressure (0.5 MPa). The tank is sized at 2 m^3, and is filled to a warm pressure such that when hydrogen is liquefied to fill the moderator, the supply and return lines, and the reservoir at the bottom of the condenser, the pressure drops to approximately 0.1 MPa. As is true for all parts of the design, the entire system, (including piping and valves) is surrounded by a blanket of inert helium gas. In addition, all parts of the gas handling system are protected from accidental damage by steel panels, heavy shielding blocks, routing below the floor surface, or other means. The ballast tank itself is located outside the radius of the reactor crane, and protected from damage by steel plates.

4.5 Helium Refrigerator

A helium gas refrigerator was purchased from CVI Incorporated in 1990, and installed at NIST in the early 1990's. It was designed for a capacity of 3,500 watts at a supply temperature of 14 K, before the LH_2 cold source was designed. A PLC controller made it a fully automated system. In 1995, it was upgraded and expanded to monitor and control cold source operation (see Section 6) and in 1998 a second, backup compressor was added.

System Components:

Originally, the refrigeration system was made up of three skid-mounted modules, plus a gas charging and storage system, and various ancillary components. The skid-mounted modules are respectively the Compressor modules (now two modules), the Final Oil Removal/Gas Management module and the Cold Box module. The gas charging/storage system consists of a low-pressure storage tank and a connection to high-pressure He cylinders maintained by the reactor operations group. Ancillary equipment (major components are shown in Figure 5.1) includes the following items:

- Interconnecting piping for the skids.
- A 22712 liter (6000 gal) LN_2 tank, and a vacuum jacketed pipe to the Cold Box.
- A free standing motor starter enclosure.
- Uninterruptible power supply (UPS) for the compressor motor controls.

Two identical compressor modules consist of Sullair Model C20LA704-26 single stage, positive displacement, oil flooded (lubricated and cooled) rotary screw compressors, bulk oil separators, helium 'after' coolers, oil coolers, two oil pumps per compressor, filters, valves, piping, instrumentation and controls. Only one compressor at a time can be operated, but, in the event of a failure, a manual switch to the second one can be accomplished in a few minutes. Water to cool the compressor oil is supplied from a separate pump module can provide up to 757 lpm (200 gpm). The compressors are ultimately cooled by the reactor cooling tower using an isolated pump system, Helium Compressor Secondary Cooling (HCSC), served by a plate-type heat exchanger and the reactor secondary coolant.

The Final Oil Removal/Gas Management module is also installed in the Compressor Building. It consists of three coalescer vessels with internal elements, a carbon adsorption bed with internal particulate filters, three control valves, piping, instrumentation and controls. Control valves are needed for mass inventory control and bypass capability (discharge pressure control).

The vacuum insulated coldbox contains the heat exchangers, valves, piping, a purifier and a turbine expander. The coldbox is horizontally oriented with turbine and valve penetrations in the vacuum vessel. A single turbine is accessible for operation and maintenance without breaking the vacuum in the

coldbox. Helium purification is accomplished with an 80 K purifier, which is regenerated without removal from the coldbox. The turbo molecular pump and the rough vacuum pump located on the coldbox module are used to maintain a vacuum of order 10^{-5} Pa within the coldbox. A 10.8 kW heater in the return line is programmed to maintain 18 K at the return gas inlet of heat exchanger HX-3, and a load bypass line from the turbine to the heater allows variable flow rates to the condenser to follow the CNS heat load.

A 16990 liter (600 ft^3) low-pressure helium storage tank is used as a reservoir to store helium when the compressor is shut off. The high-pressure cylinders assure a nearly inexhaustible supply of "zero" grade He, also required to operate the NBSR.

The Helium Refrigerator layout is shown in Figure 5.1. The coldbox module is located in room C-100 of the reactor building. Nearly 100 m of vacuum jacketed piping connects it with the hydrogen condenser, also in C-100, on the north face of the reactor. The compressors and final oil removal modules are located in the compressor building with all controls for operation at ground level. The motor control centers are also located in the compressor room. The low-pressure gas storage tank is situated adjacent to the Compressor Building on a concrete pad on the north side, and the high-pressure He cylinders are likewise adjacent to the building but on the south side.

Process Description:

High purity helium gas from the high-pressure cylinders is supplied to the low-pressure storage tank and regulated at a pressure somewhat higher than the compressor suction pressure. Helium enters the refrigerator cycle, on the suction side of the compressor, through a controller-operated valve. Helium gas is compressed by the rotation of two intermeshing helical rotors, one lobed (the male rotor) the other fluted (the female rotor). As the rotors turn their point of contact progresses along their axis, causing an axial movement of the helium gas introduced at the suction pressure and trapped in the inter-lobe volume. The inter-lobe volume progressively decreases, increasing the gas pressure, as it advances down toward the discharge port. Oil is injected along the periphery of the rotors to seal, cool and lubricate. The screw compressor also is equipped with a slide valve for capacity control. When the slide valve is closed, all of the gas introduced into the rotors is compressed, and when partially open, a fraction of the helium is bypassed to the suction side.

On exiting the compressor, the oil laden helium gas enters the oil separator. Here it impinges against a baffle that separates the bulk of the oil by gravity into a sump. The oil is removed from the sump and directed through a water-cooled heat exchanger and particulate filters to the oil manifold where it is re-injected into the compressor. The gas over the sump then passes through a first stage coalescer, reducing the oil content to the order of 100 µg/g. This stream is then water-cooled (in the after-cooler) before going to the final oil removal system. The final oil removal system consists of three coalescers in series, that remove the oil aerosol to approximately .001 µg/g followed by an activated carbon adsorber for the removal of any vapors (decomposition products and trace contaminants).

Following oil removal, the high-pressure helium flow (approximately 165 grams/sec for 3500 W) enters the coldbox, which thermally insulates the cold components of the refrigerator. Helium enters the coldbox at a pressure of 19.0 barospheres and is cooled to near LN_2 temperature in the first heat exchanger (HX-1) by receiving refrigeration from the low pressure return stream as well as the cold GN_2 boil-off from HX-2 (see Figure 4.6). The stream is further cooled to 79 K in HX-2 by heat exchange with boiling LN_2. The helium then passes through an activated carbon adsorber (purifier) for removal of impurities before being further cooled to approximately 20.7 K in HX-3 by counter-flow exchange with the low pressure return stream. The process gas enters the turbine expander at approximately 18.8 bar and 20.7 K and is expanded to approximately 5.42 bar and 14 K, removing approximately 4760 watts from the process gas and thus producing the required refrigeration. The expander discharge is split, going to the load as well as bypassing the load and entering the inlet of the return gas heater. The return gas heater supplies additional heat to bring the total return gas temperature to the control setpoint of 18 K. The

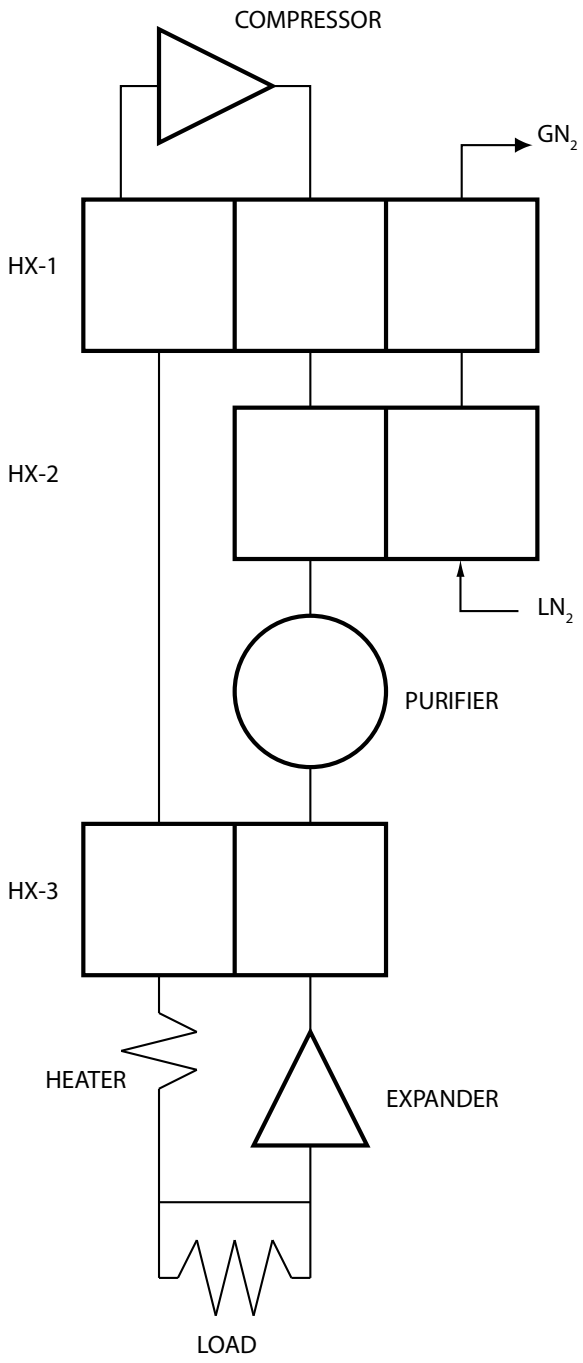

Figure 4.6. Simple flow schematic for the 3.5 kW helium refrigerator. See Figure 6.2 for typical operating temperatures and pressures.

stream then returns through heat exchangers HX-3 and HX-1 to the compressor suction and the cycle is complete.

Generally, the compressors are not operated fully loaded because the Unit 2 heat load is only one third of the refrigerator capacity. A refrigerator power of about 2500 W is more than adequate to cool the condenser, make up the 500 W to 700 W heat leak in the coldbox end, He transfer lines and condenser and still require a few hundred watts from the return gas heater. The interaction between the CNS and the refrigerator is presented in Section 6.

5.0 Mechanical Design

The advanced hydrogen cold source facility was designed to be reliable, maintainable and above all safe. The success of the first cold source, D_2O ice, installed in the mid 1980's, provided the momentum for the development of the Cold Neutron Research Facility and for the hydrogen cold sources. The D_2O ice source operated successfully for several years and provided valuable experience, insight and knowledge in the design and operation of a cold source facility. The D_2O cold source consisted of a complex maze of tubes, valves, pumps and gas systems presented to the operator through a variety of interfaces. An integral part of the facility was a 1 kW helium refrigerator that provided the means to cryogenically cool the block of ice. Included with the refrigeration system and coupled to it was a liquid nitrogen cooled helium circulator (small refrigerator) that was used to keep the ice frozen should the main refrigerator fail to operate.

Due to the complexity of the D_2O ice cold source system considerable time and effort was required to start, maintain, operate and even shutdown the facility. Preparing the cold source for operation required making ice by transforming a fixed inventory of heavy and light water, cooled with liquid nitrogen, into a layered block of frozen moderator material. The ice-making process was complicated and time consuming and required meticulous attention to procedure to ensure success. Failure to adhere to the prescribed procedure could abort the ice-making session and possibly damage the cryostat beyond repair. The old helium refrigerator, designed and built more as an experimental model than a production unit, also required a great deal of attention to start, cool down and bring the block of D_2O ice to an operating temperature of 25 K. The refrigerator system was manually operated, as were all the systems of the cold source facility, and therefore required constant attention for a considerable period of time until the system and cold source reached their operating temperatures. After the systems reached equilibrium, refrigerator operation required only inspection and data collection at regular intervals. Automatic data acquisition was not available for the refrigerator or cold source and therefore process information was recorded manually by reactor operations staff.

Normal operation of the cold source also required a cold source operator to manually perform a slight warm up of the source to force a controlled release of stored energy from the ice. This operation was performed every forty-eight hours to prevent a spontaneous release of energy from occurring that could adversely affect the operation of the refrigerator causing a shutdown and requiring even further operator intervention. Shutdown of the cold source involved slowly warming the refrigerator to melt the ice, warming the water and then subsequently draining the water into a radiation shielded holding tank. After several days the water could be safely removed from the holding tank for proper disposal. A fresh mixture of light and heavy water would then be prepared for the next freeze cycle. Other significant maintenance tasks for the refrigerator and cold source included extensive oil vapor removal procedures from the highly inadequate oil coalescers downstream from the refrigerator compressor and regeneration of the cover gas sweep hydrogen system getters.

The complexity of the D_2O ice cold source coupled with the poor reliability of the 1 kW helium refrigerator and associated components plus the quest for improved cold neutron performance drove the development of a hydrogen cold source system that had to be functionally simple. The entire system also had to be dependable, easy to operate and maintain and above all safe.

The 3.5 kW refrigerator purchase specification required a rotary screw type compressor for efficiency and reliability, extensive oil removal capability to ensure a clean system, a gas bearing turbine for reliable operation and zero maintenance, operator initiated automatic operation for easy cool-down, warmup and recovery from one central location, fast cool-down and warmup, corrosion resistant materials to minimize or eliminate required part replacement, extensive instrumentation and automated data collection to help anticipate problems before they develop into failures.

For the hydrogen cold source, simplicity in design was achieved principally by changing moderators from

ice to liquid hydrogen. Utilizing a thermosiphon to circulate the liquid hydrogen between the moderator chamber and the condenser greatly simplified the system and allowed for the a completely passive design. The vast matrix of valves that existed in the earlier D_2O source was replaced by just a few that are used only for initial charging of the system with hydrogen, isolating the cryostat and buffer tank during major system upgrades or decommissioning the system and subsequent hydrogen removal. In addition, there are no pressure relief devices of any kind; the hydrogen enclosure is hermetically sealed to assure the integrity of the system. During normal operation the valve handles are removed to prevent accidental operation (the valves have only been used a few times in the past ten years). Since the cold source is a passive design operator intervention is never required to maintain the safety of the system. Should cooling fail (refrigerator failure) the hydrogen will boil off and safely return to the buffer tank.

To ensure a reliable and safe cold source, quality assurance played a crucial role from the very beginning through a judicious approach to system operation and the meticulous selection of materials, equipment, services and processes. This methodology has provided many years of safe and reliable cold source operation. A quality assurance plan was developed that provided a comprehensive approach to quality management and yet provided methods that were by design simple, easy to implement and execute. Some of the basic elements of the plan called for certified material and processes, comprehensive tests to ensure reliability and rigorous standards for acceptance.

All materials procured for the fabrication of the cold source were certified in their composition and mechanical properties (e.g., strength and elongation). Equipment was chosen based on reliability, simplicity of operation, availability and low maintenance. Heat trebarents and other processes performed on

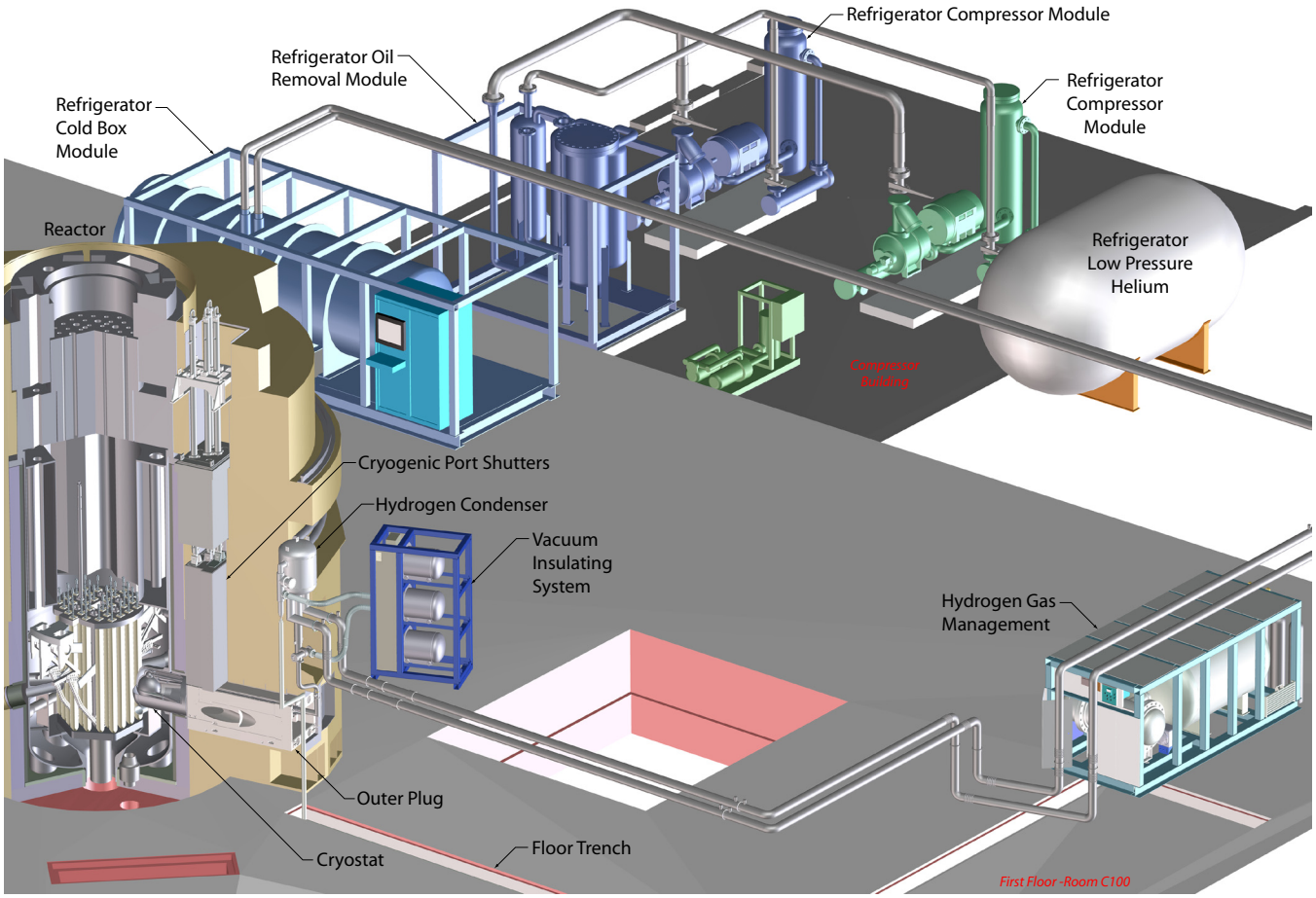

Figure 5.1. The NCNR cold source facility.

cryostat components by outside vendors also had to be certified.

Non-destructive testing of system components and assemblies focused mainly on leak testing using a helium mass spectrometer to ensure system integrity. Additional tests included x-ray radiography on all in-pile welds, cold and warm thermal soaks on all cryogenic components and assemblies, and when needed, dye penetrant and ultrasonic tests. Pneumatic proof pressure tests were also performed on the completed assemblies. In addition, prototypes of the hydrogen moderator chamber and helium containment vessels were subjected to high pressure (hydraulic) tests designed to measure their burst points. The moderator chamber ruptured at a pressure of 27 bar while the helium vessel survived a pressure of 88 bar and remained intact with only slight deformation.

Extremely high standards for accepting components and assemblies for the hydrogen cold source increased confidence in the reliability of the finished product. As an example, the NCNR leak tests provided for a nominal acceptance helium leak rate of 10^{-9} std-cc-s^{-1}. Although quite stringent, in reality, any leak that was encountered during testing was repaired to a zero leak rate (no leak detected). The result was a cold source assembly free of known leaks.

The cold source facility, shown in Figure 5.1, consists of several major component assemblies:

- In-pile cryostat assembly.
- Cold hydrogen transfer line.
- Condenser.
- Hydrogen gas management system.
- Vacuum insulating system.
- 3.5kW helium refrigerator.

The in-pile assembly, installed in the cold port of the NCNR reactor, is comprised of the hydrogen cryostat mated to a stainless steel shield and support, the outerplug. The condenser and cold hydrogen transfer line are mounted to the face of the reactor immediately above the cold port. Located away from the reactor in the northwest corner of room C-100 is the hydrogen gas management system. A warm hydrogen transfer line, protected in a trench in the C-100 floor, connects the condenser to the gas management system. A dual pump vacuum system sits atop the guide shields (guide shields not shown in figure) and provides the thermal insulation for the cryogenic system components, the condenser and the hydrogen cryostat. The coldbox module of the 3.5 kW helium refrigerator resides along the west wall of C-100 while the compressors and ancillary refrigerator equipment are located in a separate building immediately adjacent to the west wall of the reactor confinement building.

5.1 Hydrogen Cryostat Assembly

The advanced hydrogen cryostat is an all-welded assembly consisting of a moderator chamber surrounded by a closely fitting insulating vacuum jacket, a similarly shaped helium containment jacket and a large water-cooling jacket.

The in-pile cryostat assembly was fabricated almost entirely of aluminum alloy 6061. This alloy was chosen for the following reasons:

- Superior cryogenic properties; ductile at low temperatures, high thermal conductivity.
- Resistant to hydrogen embrittlement.
- Radiation tested; years of experience with this alloy in high radiation fields.
- Neutronic properties; relatively low capture cross-section.
- Ease of fabrication; high speed machining possible, weldable.

To enhance safety and reliability, the use of mechanical joints in the hydrogen cold source system was greatly minimized. The in-pile cryostat assembly is devoid of all mechanical joints. The hydrogen system from the cryostat to the ballast tank, including the valves, is joined entirely with welds with the exception of a few high vacuum/high pressure mechanical joints.

Section VIII, Rules for Construction of Pressure Vessels, of the ASME Boiler and Pressure Vessel Code provided a design methodology for preliminary sizing, vessel wall thickness and allowable pressure of the vessel shells. This also provided for the initial design feedback (geometry, mass) to the neutronic calculations. In addition, the ASME code also furnished material requirements such as maximum allowable stress and operating temperature envelope. Since the unusual shape of these vessels did not readily lend itself to easy structural analysis, finite element techniques utilizing solid and surface models, were used to analyze the pressure vessels under a variety

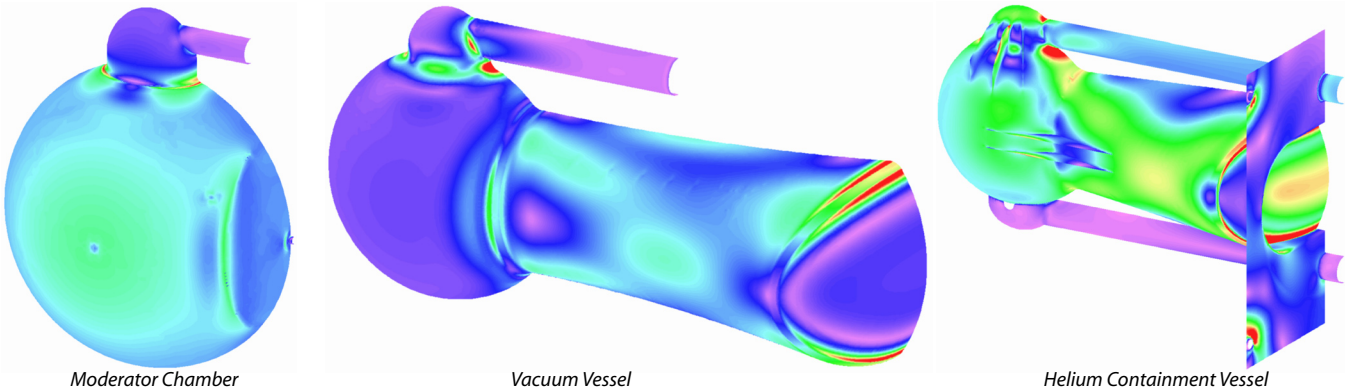

Figure 5.2. FEA results for the moderator chamber, vacuum and helium vessels.

of internal and external load conditions. Figure 5.2 shows typical von Mises stress results from finite element analysis (FEA) for the moderator chamber, vacuum vessel and helium containment vessel.

The advanced solids based computer aided design (CAD) program that was used to generate a variety of models for FEA was also used to provide solids based models for computer aided machining (CAM). All of the cryostat vessel parts were fabricated on computer numerical control (CNC) machines programmed directly from the 3-D design model files. Large pieces of aluminum alloy 6061 plate stock were whittled down to form the thin shell components that were subsequently welded together to form the individual pressure vessels in the cryostat assembly. Heat trebarent was used between machining steps, as necessary, to relieve residual stresses and therefore reduce part warpage. After machining was complete, the parts received a final heat trebarent that brought the finished pieces to a T4 material condition before they were welded together.

The right image of Figure 3.8 is a cross-sectional plan view of the cryostat tip showing the inner and outer vessels of the moderator chamber, the insulating vacuum, helium containment and the water-cooling jackets. Both the vacuum and helium vessels are extended beyond the moderator chamber along the neutron beam to form the neutron beam window.

Considerable effort went into the design and analysis stage of the cryostat to reduce the mass of the moderator chamber, and thereby minimizing the heat load on the hydrogen system and eliminating any adverse effects that might occur on the performance of the thermosiphon. The liquid hydrogen moderator is arranged in the shape of an annulus formed by the inner and outer thin-walled shells. The annulus has a non-uniform thickness ranging from 2.0 cm to 3.0 cm and an approximate volume of 5000 cm^3 (5 liters). The inner vessel of Unit 1 cold source was open to the annulus and filled with hydrogen vapor during operation. In the advanced design the inner vessel is open to the insulating vacuum space at the rear of the vessel. Evacuating the inner vessel eliminated the hydrogen vapor and increased the cold neutron flux. The liquid hydrogen supply line and vapor return line enter at the top of the chamber. The inner vessel has a small opening in the rear and is held in place by the outer vessel end cap. The closed space formed between the downstream inner vessel shell and the end cap is open to the annulus and filled with hydrogen vapor during normal operation. (The end cap design was later modified for the backup cryostat by eliminating the hole that vented the space between the inner vessel and the cap to the hydrogen annulus. Instead, this small space is also opened to the insulating vacuum jacket.)

The insulating vacuum vessel closely follows the shape of the hydrogen moderator chamber with a nominal operating thermal insulating gap of 0.25 in (6.4 mm). When warm, the front or upstream end of the moderator chamber will bump or barely touch the vacuum vessel. As the system cools, the hydrogen supply and return tubes contract and pull the moderator chamber away from the vacuum vessel providing a uniform clearance gap all around the chamber.

The rear section of the vacuum vessel is extended along the neutron beam line to the end of the cryostat tip where it forms a window for the neutrons to exit. A tube exiting horizontally from the top of the vessel extends the insulating vacuum along the path of the concentric hydrogen lines. It also serves as the sole mechanical support for the moderator chamber and as a pump-out line for the insulating vacuum system. The support system is designed to restrict movement of the moderator chamber to along the axis of the hydrogen line as the temperature of the hydrogen system changes.

The insulating vacuum jacket is completely surrounded by a helium containment jacket that serves to prevent the possibility of undetected air from entering the hydrogen system and also serves as a containment for any adverse hydrogen-oxygen event.

From an engineering standpoint, the most significant task in designing a cold source with a helium jacket is that it leaves one shell, in this case, the vacuum vessel, without direct cooling to remove the energy deposited from neutron capture and gamma radiation. The moderator chamber shells are cooled by the liquid hydrogen, the helium shell is cooled by the circulating heavy water, but the vacuum jacket has no direct thermal cooling and has to rely on thermal radiation to the moderator chamber shell or conductive cooling to the helium vessel. If the energy deposited in the vacuum vessel could not be removed effectively then the shell temperature would exceed the allowable design operating condition (100 ˚C) and compromise the integrity of the system. The amount of energy lost to the moderator chamber through radiation is insignificant, and furthermore not the preferred mode of heat removal for the vacuum shell. Fortunately, dimensional constraints from the size of cold port thimble (there is only so much room to work in) and the desire for a significant heavy water presence outside the helium vessel, relegated the gap between the vacuum and helium vessels to a small one. Since the gap was too small to take credit for reliable thermal convection, conduction through the helium layer is the only viable method of removing the heat from the vacuum shell. The gap was made as small as possible to enhance the thermal conduction. This allowed for acceptable heat removal and vacuum vessel wall temperature and yet still permitted the unit to be assembled without too much difficulty. Without taking credit for any heat transfer from free convection or thermal radiation, a helium gap of 0.25 cm is sufficient to remove the heat generated in the vacuum vessel without exceeding the maximum allowable working temperature. To further improve the margin of safety, the effective thermal conductivity through the helium filled gap was increased by filling the space between the vacuum and helium vessels with multiple layers of expanded aluminum. This material is commonly used to make air filters for HVAC and electronic cooling systems. The material is very soft and conforms easily to complex shapes such as the vacuum and helium vessel assemblies.

The helium containment jacket consists of a thick vessel and tubes that completely surround the vacuum vessel and pump-out line. The helium jacket, like the insulating vacuum jacket, consists of an elliptically-shaped vessel with a large extended portion along the beam line. The entire helium vessel with the vacuum and moderator chamber inside is cantilevered off the helium vessel rear support plate that forms the downstream end of the cryostat. Since this assembly is also the primary protection or safety barrier between the moderator chamber and the reactor beam port, the helium vessel was designed to withstand an internal static pressure of 8270 kPa (1200 psi) before rupturing.

The cryostat water-cooling system is designed to remove the nuclear heat generated in the vacuum, helium and water vessels. Water for cooling the cryostat assembly is supplied by the reactor auxiliary D_2O system and delivered to the water vessel through the helium vessel rear support with a 2.67 cm (¾ inch) Schedule 40 pipe and distributed inside the jacket through a manifold and four 1.27cm (½ inch) tubes.

Before the exterior hydrogen, drain, water-cooling and thermowell lines were added, the cryostat tip assembly was placed in a large laboratory oven for heat-trebarent (artificial aging). This procedure was designed to bring the T4 temper aluminum to a T6 temper and strengthen the parent material in the weld heat-affected zones.

5.2 Outer Plug Assembly

The cryostat assembly is attached to a reusable stainless steel plug and radiation shield, shown in Figure 5.1, This support also contains several openings for the neutron beams as well as the new reactor cold port shutters. The plug was designed at the NCNR and fabricated by an outside contractor. Two welded subassemblies and two large machined pieces are the principle components of the plug assembly. Stainless steel plates were welded together to form the top and bottom sections of the plug. After welding, these subassemblies were machined to the required dimensions. The two side pieces were machined from solid stainless steel plate. Final machining was accomplished with these four main pieces bolted together. Heavy concrete was used to fill all the hollow sections of the top and bottom subassemblies.

The plug also has four adjustable wheels to facilitate easy installation and removal. Four long connecting rods are used to secure the cryostat assembly to the front of the plug. Attachment is made from the downstream or "cool" end of the plug. This allows the plug to be reused a number of times for different cyrostat tips therefore saving considerable hot plug storage space.

5.3 Cold Hydrogen Transfer Line Assembly

The cold hydrogen transfer line comprises the section of super-insulated vacuum-jacketed concentric annular tubes along the face of the reactor from the condenser assembly to the in-pile cryostat assembly, see Figure 5.1. These tubes are also surrounded by a layer of helium. Stainless steel alloy 304 is used for all components except for the hydrogen vapor line components which used alloy 316, an alloy slightly more resistant to hydrogen embrittlement. The transfer line has several special sections that provide for the thermal expansion and contraction of the hydrogen liquid and vapor tubes. Pump-out ports for connection to the insulating vacuum system are available through this assembly for the cryostat and condenser insulating vacuum jackets. The transfer line provides an over-lapping vacuum break that separates the two vacuum spaces yet maintains the integrity of the vacuum and insulation without thermal shorts. In a similar fashion, the helium containment systems of the cryostat and condenser are split and are so designed to eliminate all direct paths from the barosphere to the vacuum jacket, an important safety feature.

5.4 Hydrogen Condenser Assembly

The hydrogen condenser assembly utilizes a cold gas stream from the helium refrigerator to liquefy the hydrogen used to moderate neutrons and cool the cold source moderator chamber. Under normal operating conditions, cold helium gas enters the heat exchanger at approximately 15 K and at a pressure of 3 bar. There it is warmed by condensation of hydrogen and returns to the refrigerator coldbox at approximately 20 K. Liquid hydrogen drains to the bottom of the heat exchanger into the phase separator region, allowing the incoming vapor stream to expand and any liquid carried over to be separated and returned to the cryostat through the liquid supply line. The operating point for the condenser is controlled by the incoming helium temperature and mass flow, which in turn are regulated by the system hydrogen pressure.

The condenser, like the moderator chamber, is surrounded by an insulating vacuum jacket, which in turn, is surrounded by a helium containment jacket. The entire assembly is mounted to the reactor face above the cold port, Figure 5.1, and surrounded by a protective shield, also mounted to the reactor face.

The insulating vacuum and helium containment jackets each contain pressure vessels that were designed to withstand any hydrogen-oxygen event. Each vessel was designed using Section VIII of the ASME Boiler and Pressure Vessel Code.

The hydrogen condenser is a brazed plate-fin heat exchanger made entirely of aluminum. With working pressures for the helium and hydrogen sides of 2070 kPa and 986 kPa respectively, and a 3.5 kW heat transfer capability, the condenser can easily handle the heat load required for successful operation of the NCNR hydrogen cold source. Pressure drop across the condenser is less than 7 kPa at a helium flow of 162 g/s (3500 watts). As shown in Figure 5.1, the inlet and outlet pipes for the refrigerated helium stream are on either side of the heat exchanger core. Two inch

stainless steel pipe ends are attached to the aluminum pipes on the condenser through Bi-Braze transition joints. A 3.81 cm diameter drain tube for collection of the condensed hydrogen and delivery to the cryostat is located at the bottom of the condenser.

A hydrogen phase separator is installed in the drain tube at the bottom of the condenser to separate the return vapor coming back from the cryostat from the liquid supply to the cryostat. A partial cross-sectional view of the separator, shown in Fig 4.5, illustrates how the vapor return flow from the cryostat is split away from the fill tube into two chimneys. Liquid hydrogen pools at the bottom of the condenser as shown in the figure and flows between the two vapor chimneys and into the fill line to the cryostat. An umbrella is installed on top of the separator assembly to prevent condensate, either impurities or hydrogen, from dripping from the condenser core directly into the supply or return lines.

5.5 Hydrogen Gas Management Assembly

The hydrogen gas management assembly and the warm hydrogen transfer line connecting it to the rest of the system are located on the first floor of the confinement building, room C-100 and are shown in Figure 5.1. The system consists of four principle assemblies: the ballast tank, the valve tank, the warm hydrogen transfer line and the protective frame assemblies. The ballast tank assembly contains a large double-walled gas reservoir to safely hold the entire hydrogen inventory. The valve tank assembly provides the means for isolating the ballast from the cryostat and connection ports for charging and removing the gas from the system. The protective cage assembly consists of steel plates and frame surrounding the hydrogen containing components to protect them from accidental damage. Also included is the necessary instrumentation to assure that hydrogen fill and removal operations are performed safely.

All sections containing hydrogen are completely surrounded by a helium blanket. This is designed to prevent undetected air from entering hydrogen system. The plumbing design allows the hydrogen system to be separated into sections when the system is not operating (i.e. during maintenance) to limit the volume of gas available when the system is most vulnerable to accidental rupture, since shields may be removed.

The warm hydrogen transfer line piping from the ballast tank to the reactor biological shield lies inside the existing floor trench, where it is protected from any possibility of accidental rupture. At the face of the reactor biological shield, the line passes through the massive radiation shielding to the condenser, that is also surrounded by a protective steel enclosure. Since the cold source system is not operated unless the shielding is in place, the entire hydrogen system is enclosed by protective shielding that will prevent the possibility of damage as a result of any external occurrence while the system is cold, and the inventory of hydrogen available for release is large. When the system is warm, 98 % of the hydrogen is in the ballast tank. Before any shielding is removed, the hydrogen is protected from release by closing the pair of manual isolation valves shown schematically in Figure 5.3. This design protects against a massive spill of the inventory to the confinement building, with the possibility of delayed ignition and detonation. Furthermore, any remaining hydrogen in the warm hydrogen line, condenser and cryostat is easily removed with portable metal hydride storage units.

The ballast tank assembly consists of two pressure vessels, a hydrogen vessel within a helium vessel. The vessel assembly was designed and constructed by an outside contractor to meet NCNR cold source specifications and the requirements of Section VIII of the ASME Boiler and Pressure Vessel code. The hydrogen vessel is a large, 2 m^3, all-welded cylindrical pressure vessel, completely contained and supported inside the slightly larger helium vessel. Each vessel is fabricated from a rolled cylinder with a 2:1 elliptical head welded at each end. Each vessel has a wall thickness of 0.95 cm. Stainless steel alloy 316 was used for the components of the hydrogen vessel and alloy 304 used for the helium vessel. Six spacers center and support the hydrogen tank inside the helium vessel.

Hydrogen enters and exits the inner vessel through a single 6.03 cm (2 inch) pipe located in the center of one of the elliptical heads. Helium flows into the outer vessel through a 16.83 cm (6 inch) pipe concentric to

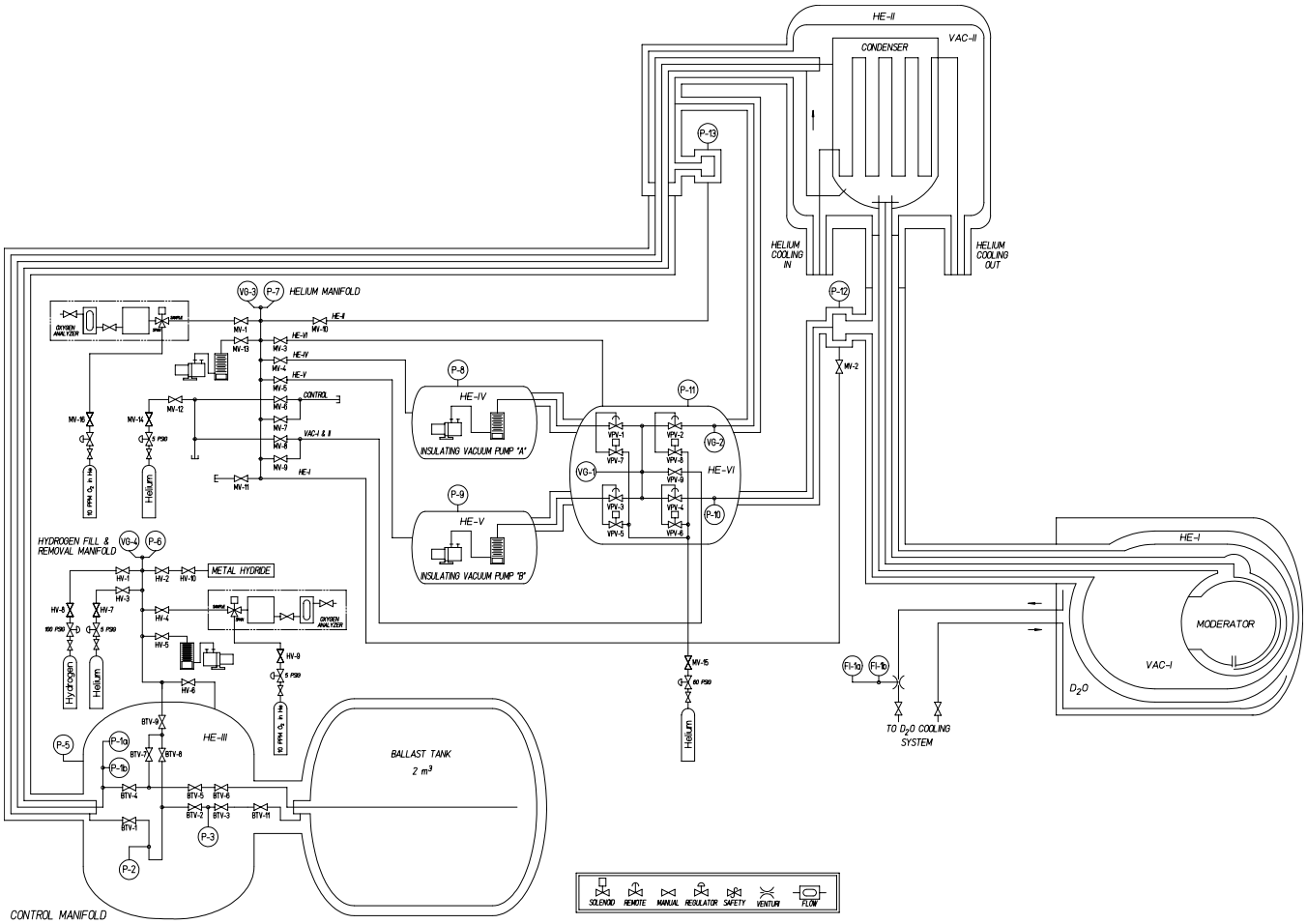

Figure 5.3 Advanced hydrogen cold source plumbing diagram.

the hydrogen fill pipe.

The assembly rests on two supports welded to the cylindrical section of the helium vessel, which in turn are welded to cross members of the protective steel frame.

The valve tank assembly is a flanged pressure vessel containing the system control valves and sensors to monitor the system pressures.

The pressure vessel is essentially a stainless steel tank composed of a flanged center cylindrical section, fabricated from 304 stainless steel, with flanged elliptical stainless steel heads bolted to each end of the tank body. There are numerous penetrations in the tank body to accommodate the mechanical feedthroughs to operate the variety of control valves and electrical feedthroughs to handle the signal requirements of the electrical equipment and instrumentation sensors. There is a large opening in the rear of the tank body for a pipe connection to the hydrogen ballast tank assembly. In addition, a penetration at the bottom of the tank body receives the warm hydrogen transfer line rising from the floor trench beneath the gas management assembly.

5.6 Insulating Vacuum Pump Assembly

The insulating pump assembly consists of two identical vacuum pump tank assemblies, one valve tank assembly, a support frame with plumbing, and several flexible hose assemblies. The vacuum pumps and vacuum valves are located inside vessels filled with helium. Each helium containment is physically separated and monitored. The assembly can pump on either of the two insulating vacuum systems or both simultaneously and is accomplished using the valves located in the valve tank assembly. An external manifold and plumbing assembly is used to evacuate and fill the helium containments surrounding the cryostat, condenser and vacuum pumps. Since the

pumps operate in sealed helium containments, each tank environment is cooled with a small heat exchanger supplied with plant chilled water to prevent the pumps from overheating.

6.0 Instrumentation and Control

A console on the coldbox module houses the main PLC controller (Allen-Bradley PLC-5/40) monitoring the refrigerator and cold source instrumentation. Two PCs are also located at the console providing an interface with the entire system (RSView). Most alarms regarding abnormal conditions are generated by the PLC, but there are two reactor rundown signals that are directly wired into the reactor console. The PLC is programmed to automatically step through the procedures to cool the system to operating conditions, warm it to ambient temperatures, and shut off the compressor. All components of the Instrumentation and Control system receive AC power from an Uninterruptible Power Supply (UPS).

6.1 Programmable Logic Controller (PLC)

The main PLC was part of the refrigerator operating system provided by CVI. It is located in the console next to the coldbox, the area where the CNS team operates the system. The PLC is mounted in one of two racks of instrumentation modules used for analog and digital input and output for the refrigerator and Compressor 1. The refrigerator was installed long before the cold source, and was tested and operated as an independent system for over two years. (A 1960's vintage refrigerator was still being used to cool the D_2O cold source; that system was removed in 1994.) A second PLC was included with the refrigerator turbine package to monitor its inlet and exhaust pressures, bearing, brake, and seal gas pressures, exhaust temperature, and speed. This turbine PLC determines the run/alarm/trip status of the turbine, conveyed as digital data to the main PLC.

The PLC is programmed in ladder-logic code in which most steps (called rungs) consist of a conditional inquiry followed by an action if the condition is true. A printed page of the software has the appearance of a ladder. Many subroutines are used to perform specific tasks such as startup and shutdown, block transfers of data, etc. The original software and database were created by CVI, but subroutines were added in 1995 to include CNS data monitoring and control, and again in 1998, to add Compressor 2 instrumentation and logic. Regardless of the operating status of the refrigerator, the program is always being executed at a rate of about 50 times per second. Data memory locations are not necessarily updated at that rate, however, as block transfers of analog I/O are performed asynchronously through memory buffers; most are updated at least every 5 seconds. The program can be modified as it is running, with due caution, of course, so new logic may be tested instantly. The modified program is then downloaded to a PC where the most recent versions are stored.

As the system was expanded, remote PLC racks were added to the data highway, shown in Figure 6.1. Rack 4, located on the condenser enclosure, close to the insulating vacuum system, contains data modules for the vacuums, condenser temperatures, helium containments, thermocouples in the cryostat assembly, as well as AC outputs for controlling the vacuum valves. Rack 5, located in the pump house, receives compressor cooling water flow rates and temperatures. Rack 6, in the compressor building, was added when Compressor 2 was installed. At the same time, the compressor motor control centers were each upgraded with a smart motor controller (SMC), communicating power, current, line voltage, and faults to the main PLC as Racks 7 and 10.

6.2 Control Program

As mentioned above, the ladder-logic program consists of a main program and many (34) subroutines. A list of the source code is well over 100 pages. Many of the subroutines simply execute data block transfers, and floating point data manipulations to express parameters in familiar units. Other subroutines are PID controls that compare a process value to its set point, and adjust the output of a component to maintain the variable at its set point. (PID is the acronym for Proportional-Integral-Derivative, in which the strength of the feedback is calculated using any or all of the three algorithms. Proportional is the simplest as the feedback is directly proportional to the difference between the variable and its set point.) Still other subroutines contain the sequence of steps necessary for the refrigerator to perform its functions, cool the refrigerator, recover from trips, generate alarms, etc. A few of these subroutines are described below to present an overview of the program.

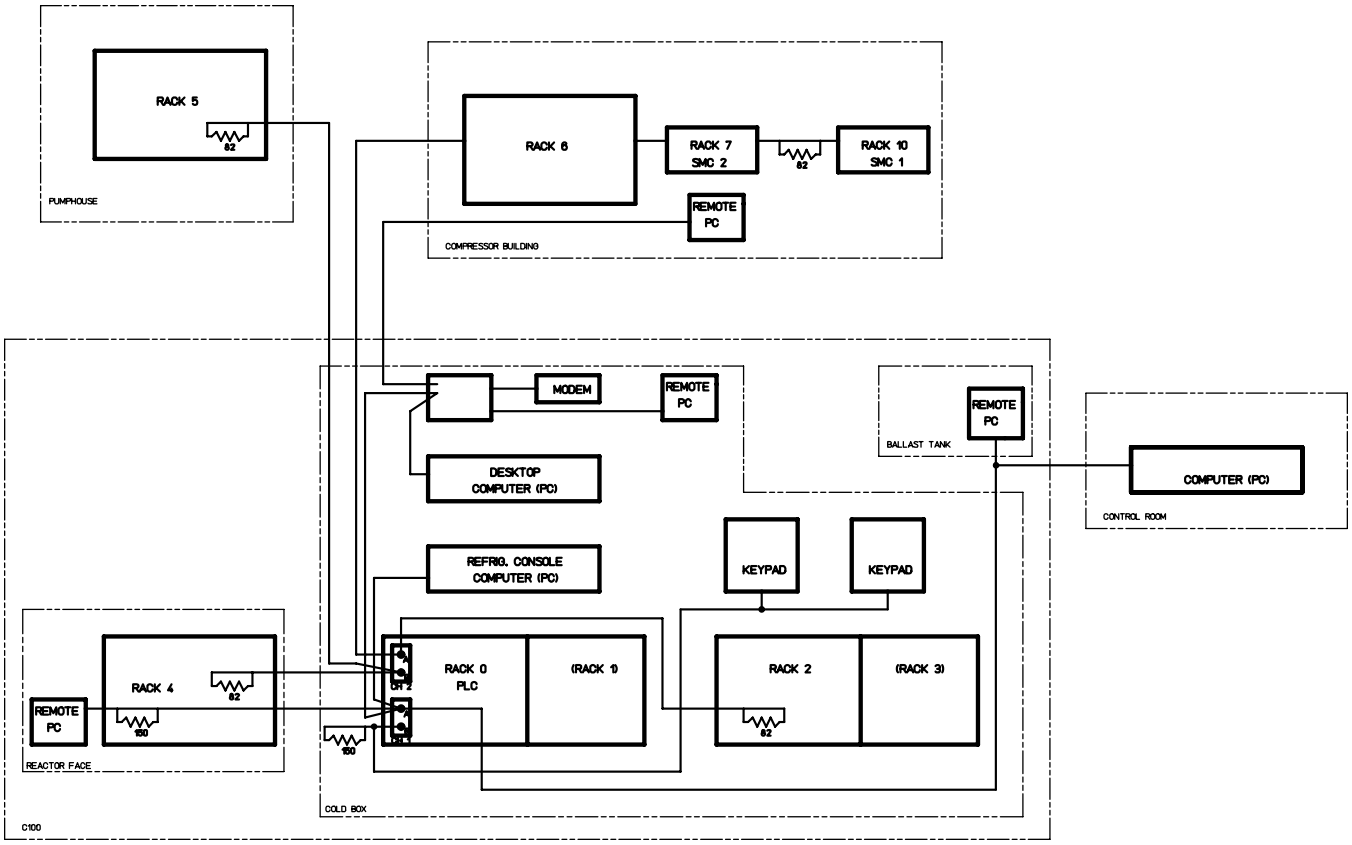

Figure 6.1. Data Highway configuration for the helium refrigerator and cold source.

Main Program:

Most of the rungs in the main program are jumps or conditional jumps to various subroutines for data transfer. Since block transfers take seconds to complete, and the program cycles in milliseconds, a block transfer command is not executed until the previous transfer command has been completed and has set its 'done' bit. A conditional jump is one which occurs only if the user has selected it, such as a jump to the cool-down sequence.

Auto-Cool:

This subroutine executes a sequence of numbered steps required to bring the refrigerator to its normal operating conditions from a shutdown and warm state, its presumed starting point. It specifies suction and discharge set points, opens bypass valves, starts the flow of liquid nitrogen, starts and loads the selected compressor, realigns bypass valves as temperatures drop, starts the turbine when it is cold enough, closes the turbine bypass valve, and cools the load to 20 K, finally changing status from the Cool-Down mode to the Auto-Operate mode. Along the way, most of the hydrogen is liquefied and eventually flows into the moderator chamber as the thermosiphon starts. The process takes about fours hours and usually requires no human intervention.

Auto-Warm:

The Auto-Warm subroutine was included to be able to warm the turbine to ambient temperature in three hours. It simultaneously opens the turbine bypass valve and closes the turbine inlet valve, increases the return heater set point to 300 K, and jumps into the compressor shutdown routine when the heater inlet temperature reaches 290 K. This sequence leaves HX-1 and HX-2 quite cold, however, so to warm the entire coldbox, the sequence is cancelled and valves are realigned manually; this process takes (6 to 7) hours to complete.

Shutdown:

The compressor is shutdown 'softly' by this subroutine in (6 to 8) minutes. The discharge pressure set point

is reduced slowly to 1240 kPa psia before unloading the compressor slide valve. It cools by operating at low power briefly before the motor is turned off.

Helium Mass Inventory:

Three proportional-integral-derivative (PID) controllers maintain the suction and discharge pressure set points, by operating the Mass-In, Mass-Out and Bypass valves. If the suction pressure is lower than the set point, the Mass-In valve opens allowing additional He to enter the suction line from the low-pressure storage tank. If it is too high, the Mass-Out valve opens, and He flows from the discharge line into the tank. The Bypass valve allows flow from the discharge line to the suction line if the discharge pressure is above its set point.

Cold Source:

The interaction between the refrigerator and the CNS is greatly simplified by the facts that both are controlled by the same PLC, and that a single variable, hydrogen pressure, is used to control the cold helium flow through the load lines to the condenser. This PID uses only proportional feedback, and the subroutine has only eight lines. A built-in load bypass line in the coldbox, and the return gas heater, already programmed by CVI, are also vital components in this scheme. The bypass valve is always left partially open, so that most of the flow can be accommodated when the condenser load is small, that is, when the reactor is shutdown. As reactor power increases, the increasing hydrogen pressure drives the PID to incrementally open the load line valve, and more cold helium flows to the condenser, where it is warmed a few Kelvin. The bypass and load flow streams mix before entering the return gas heater. The heater maintains the return helium temperature at 18 K, and it substitutes for the absent load when the reactor is shutdown. In this way, the refrigerator cooling power is nearly constant as the system follows the condenser load. No human intervention is required for the reactor startup or shutdown, or during a reactor scram.

Trouble Alarms:

Section 6.4 contains a thorough description of the thirty trouble alarms generated by the PLC when parameters are outside their normal range. All of the alarms are generated in one subroutine added to the program in 1995. The bits of three words of memory are used for the individual alarm conditions. The subroutine also utilizes two other pairs of memory words to bypass cold source alarms and to acquire "handshakes" from the RSView interface acknowledging that the alarms were recorded.

Restart:

A brief power interruption can cause the compressor motor to trip. When the power is restored, however, it is desirable to restart the refrigerator and resume CNS operation. If the refrigerator is in the Auto-Operate mode, but neither compressor motor is operating, a 20 second timer starts when the high voltage is restored. If the power stays on, the Auto-Operate mode is cancelled and the Auto-Cool mode is initiated (above). The compressor is restarted and the turbine starts as soon as the compressor is loaded because it is already cold. It takes 15-20 minutes to re-condense the hydrogen, so the reactor may be restarted (see Section 7 for a detailed account of the recovery process).

Compressor 2:

The last subroutine added to the program includes several data block transfers from Racks 6, 7 and 10 needed to integrate the new compressor and SMC's into the system. Compressor 1 transducers are directly wired to the console. Data from both are constantly read, so the subroutine must also identify which one is supposed to be operating. A compressor is "selected" when it receives high voltage; that bit is latched until the other compressor has high voltage, indicating a manual switch was performed.

6.3 User Interface

Two local PCs and several remote PCs provide the graphical user interface (GUI) with the main PLC. The windows-based software compatible with a database in the Allen-Bradley line of PLCs is RSView. RSView allows the user to create elaborate graphical representations of system components displaying

temperatures, pressures, the status of valves and motors, etc. Control "buttons" can be created such that a mouse click can initiate or terminate actions, or enable or disable automatic control of a component. Data entry fields can be called prompting the user to enter a new set point for a parameter subject to automatic control, or a new output level for a component in manual control. Messages regarding alarms and trips are displayed at the bottom of each screen.

RSView also performs data logging, providing the ability to display trends in past or current data. Any of the 420 I/O tags in the RSView database can be logged with frequencies ranging from seconds to days. Data files can be exported to spreadsheets for archival documentation. Section 7 contains plots of logged data from startup tests.

Information is displayed on seven major system component screens, a startup screen, and a screen to display previously defined trends. The component screens and some of their functions are:

- Overview – General layout of components; no control functions
- Compressor – Suction and discharge gas temperatures and pressures; motor power, line currents and voltage; cooling system temperatures and flows.
- Oil Removal/Gas Management – Suction and discharge process variables; sub-screens to change set points or manually control gas management valves.
- Coldbox – Temperatures and pressures at many points such as turbine inlet and exhaust, etc.; status of valves and LN_2 system; sub-screens to change set points for hydrogen pressure, return gas temperature and purifier temperature; ability to manually operate bypass valves. See Figure 6.2.
- Turbine – Speed, exhaust temperature, and local pressures from the turbine PLC; turbine alarm/trip status; no control functions.
- Vacuum – CNS insulating vacuums and most He containment pressures; control of vacuum manifold valves.
- Hydrogen System – Hydrogen pressure, condenser and moderator chamber temperatures; cryostat assembly temperature and D_2O coolant flow; reactor power; control of the hydrogen set point or

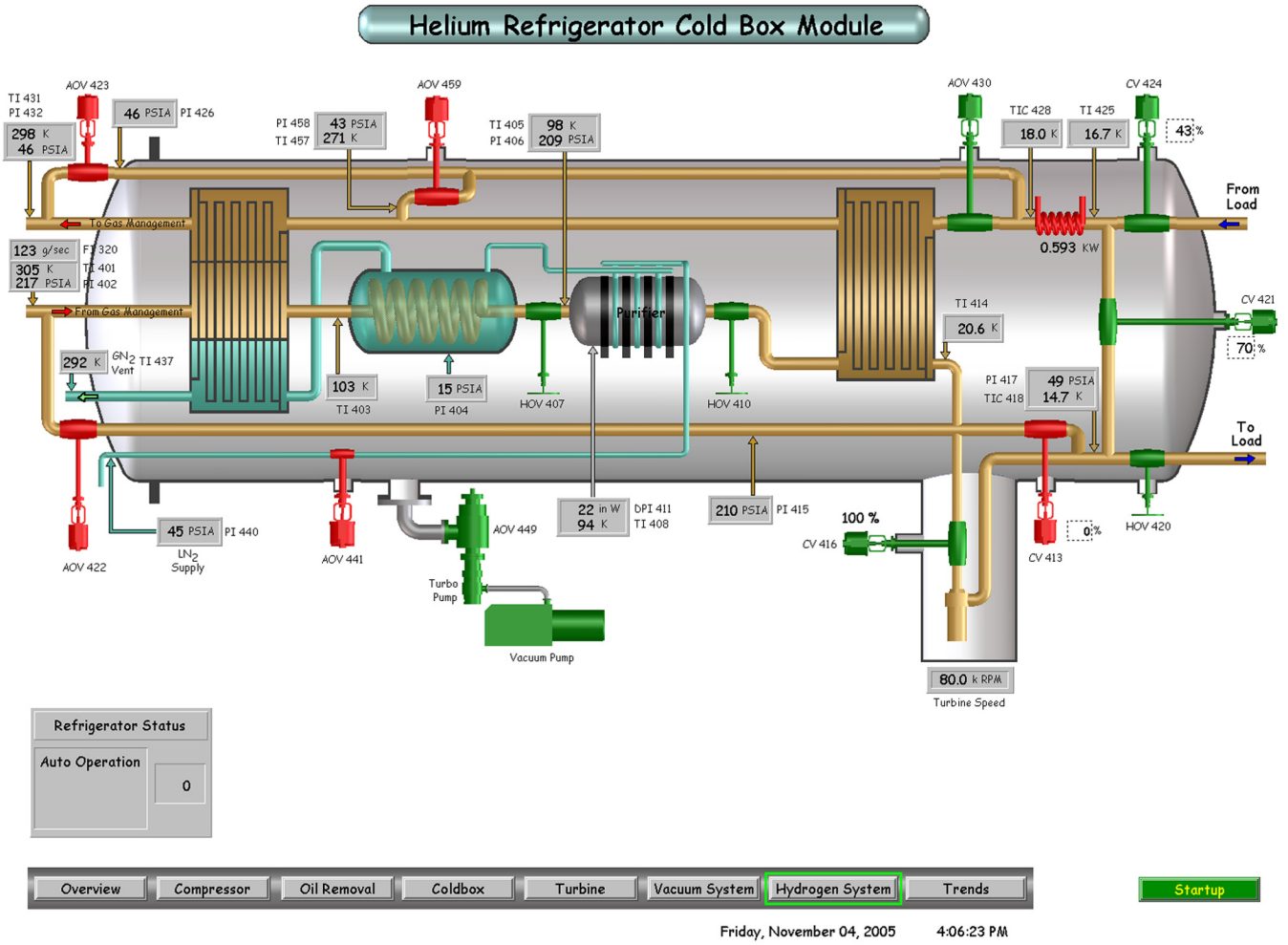

Figure 6.2. Refrigerator Coldbox screen.

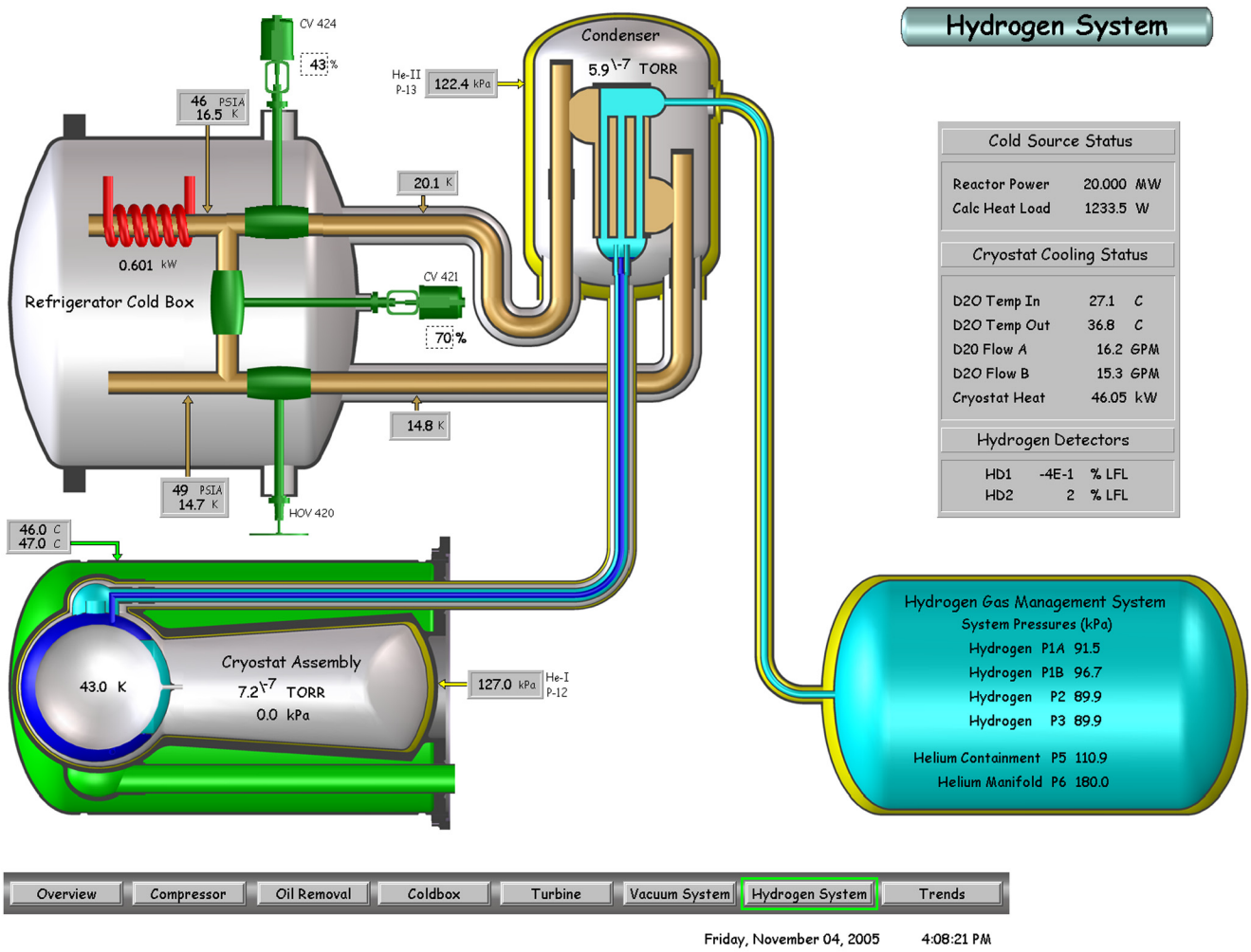

Figure 6.3. Hydrogen System screen.

manual operation of load line valve. See Figure 6.3.

The Startup screen gives access to compressor and refrigerator controls. A user can initiate or cancel the Auto-Cool, Auto-Warm and Shutdown subroutines in the PLC program, or manually start, stop, load, or unload the compressor. One can reset refrigerator or cold source trouble alarms, and access still another screen that can be used to bypass any of the cold source alarms. The activities launched from the Startup screen are critical for proper operation of the cold source (and the reactor!), so great care has been taken to ensure that the CNS operator will not mistakenly upset the system with an inadvertent keystroke or mouse click. Three or four mouse clicks are required to reach a control screen and initiate a critical action.

There are two versions of RSView. RSView-Works is used to establish the database, create the display screens, create data logs and trends, and monitor and control the cold source and refrigerator. RSView-Runtime is used only to monitor and control the system. It is installed in the reactor control room, and on the office computers of the CNS team members. Remote PCs connect to the data highway via the Building 235 intranet. Very remote PCs, in the homes of Cold Source Contacts, connect to one of the two local PCs using secure software that allows the home PC control of the local PC, at the refrigerator console. The contact can then monitor and control the system from home. Remote access is needed to respond to trouble alarms reported by the reactor staff after office hours.

6.4 Rundowns and Trouble Alarms

In the event of a refrigerator or auxiliary D_2O pump failure, the reactor power must be reduced to avoid overheating the moderator chamber or the cryostat assembly. Two rundown signals exist, therefore, to protect the cold source. A compressor or turbine

trip will stop the flow of LH_2 to the moderator chamber, resulting in a rapid increase in pressure. Two hydrogen pressure transducers are connected to the reactor protection system to generate redundant rundown signals when the pressure reaches roughly 135 kPa (5 psig). Likewise, two differential pressure signals from the D_2O orifice flow meter provide redundant rundowns if the flow drops below 18.9 lpm. Rundowns are appropriate, rather than reactor scrams, because the temperature increases are not rapid in either case. To keep the reactor critical and speed the return to full power, the reactor shift supervisor may bypass either rundown signal when the reactor power has dropped to 200 kW. A return to normal operation is permitted when the failure has been corrected. Further, following a refrigerator trip and restart, the reactor power can be increased to 2 MW if the hydrogen pressure has started to decrease and it continues to decrease. The return to full power must wait until all cold source trouble alarms have cleared.

In addition to the two rundown signals, there are thirty abnormal cold source or refrigerator conditions that generate alarms through the ladder-logic code executed by the PLC. These alarms annunciate in the reactor control room, indicating that some physical parameter is outside its normal range, but the signals do not directly affect reactor operation. The reactor operators are instructed to phone the Cold Source Contact, who will decide if the problem requires a shutdown, immediate repairs, or if the problem can wait until the next work day or next reactor shutdown for a fix. Tables 6.1 and 6.2 list all the alarms; they are briefly described below.

Hydrogen Pressure:

There are redundant alarms if the hydrogen pressure is above or below its normal range with the refrigerator in its Auto-Operate mode. These alarms could be due to a refrigerator failure, in which case there will be other alarms, or could indicate the control system is malfunctioning. Three additional alarms are generated if there is low hydrogen pressure when the condenser temperature is far above the hydrogen boiling point (normally when the system is shutdown); these would alarm if there was a large hydrogen leak.

Table 6.1 Cold Source Alarms from the PLC.

Cold Source Trouble Alarms	
1	VG > 13.3 Pa -- Gross Lost Vacuum
2	HD-1 or HD-2 > 20 % LFL -- Hydrogen leak in C-100
3	VG-1 and VG-2 < 10^{-7} Pa -- No AC Power to Vacuum Gauge
4	Flow - A < 18.9 lpm -- Loss of D_2O Cryostat Cooling
5	Flow - B < 18.9 lpm -- Loss of D_2O Cryostat Cooling
6	105 < P-5 < 115 kPa -- Ballast Tank Containment Leak
7	P-8 < 105 kPa -- Pump 'A' Containment Leak
8	P-9 < 105 kPa -- Pump 'B' Containment Leak
9	P-11 < 105 kPa -- Vacuum Valve Containment Leak
10	P-12 < 105 kPa -- Moderator Containment Leak
11	P-13 < 105 kPa -- Condenser Containment Leak
12	VG-1 > .133 Pa -- Poor Vacuum
13	VG-2 > .133 Pa -- Poor Vacuum
14	P1-A not 65 kPa to 125 kPa -- Abnormal Hydrogen Pressure
15	P1-B not 65 kPa to 125 kPa -- Abnormal Hydrogen Pressure
16	P1-A < 375 kPa, Condenser > 250 K -- Hydrogen Leak
17	P1-B < 375 kPa, Condenser > 250 K -- Hydrogen Leak
18	PLC Rack 2 or Rack 4 Fault -- Alarm Disabled
19	P-3 < 375 kPa, Condenser > 250 K -- Hydrogen Leak
20	P-1a Data Transfer Error -- Alarm Disabled
21	P-1b Data Transfer Error -- Alarm Disabled
22	VG Data Transfer Error -- Alarm Disabled
23	He Data Transfer Error -- Alarm Disabled
24	D20 Tin > 50 °C or Tout > 60 °C, Reactor > 1 MW -- Loss of Cooling
25	Pump 'A' or 'B' Containment Temp > 27 °C -- Loss of Cooling

Table 6.2 Refrigerator Alarms from the PLC.

Refrigerator Trouble Alarms	
1	Turbine or Compressor Trip in Auto-Operate Mode
2	Compressor Trip after Step 40 in Auto-Cool Mode
3	Compressor Trip in Auto-Warm Mode
4	Compressor Trip during Auto-Shutdown
5	Compressor Oil Temp > 50 °C
6	HCSC Flow < 189 lpm with Compressor Operating

Insulating Vacuum:

There are two levels of vacuum alarms, 'poor' vacuum and 'lost' vacuum, with set points of .133 Pa and 13.3 kPa, respectively. A poor vacuum may be due

to a malfunctioning pump or very small leak, which might be rectified by using the standby pump. A lost vacuum is insufficient insulation, and could indicate a hydrogen leak. The lost vacuum alarm is the only alarm that causes an active response; it seals the vacuum vessels by closing all the vacuum valves, and it stops cooling the condenser by closing the refrigerator load line valve. (A rundown signal would quickly shutdown the reactor, also, if it was operating.) Two additional alarms could indicate vacuum system problems. If both gauges indicate vacuum less than 10^{-6} Pa, an alarm indicates a loss of AC power. Finally, if either pump containment is too warm, an alarm indicates a problem with the chilled water system.

Helium Containment Pressures:

There are low-pressure alarms for all of the He containments that would indicate leaks to the barosphere or into the vacuums. In addition, there is a high-pressure alarm on the ballast tank containment, He-III, which could indicate a direct hydrogen leak. (Since He-III has the reference pressure for two hydrogen differential pressure transducers, the allowable pressure range in He-III is just 10 kPa.)

Cryostat Assembly Cooling:

In addition to the rundown, there are redundant low D_2O flow alarms. There are also high temperature alarms for the D_2O coolant to indicate insufficient cooling of the cryostat.

PLC Rack Faults:

If the PLC is not being updated because block transfers of data are failing, the PLC may continue to use the most recent value of the parameters it received, which would disable alarms using these data. Fortunately, the block transfer control software sets a fault bit if the transfer is not successfully completed. Four alarms were included to monitor the transfers of data from input modules for the vacuum gauges, the He containment pressures, and two separate modules with hydrogen pressure inputs. In addition, another alarm is generated if the PLC fails to communicate with either Rack 2 or Rack 4.

Hydrogen Detectors:

There are two hydrogen detectors monitoring room C-100, one just above the ballast tank, and one on the ceiling over the condenser. If either indicates the presence of hydrogen at a concentration of 0.8 %, 20 % of the Lower Flammable Limit (LFL), there are local audible and visual alarms, and there is a cold source trouble alarm annunciated in the control room. The output of the detectors is then automatically displayed on the PCs. If the H_2 level continues to increase, the operators will have C-100 evacuated and shutdown the reactor.

Refrigerator Trouble:

There are six refrigerator alarms, four of which are generated by a turbine or compressor trip in the four modes of automatic operation. The two remaining alarms indicate problems with the compressor cooling system. Since the reactor secondary and cooling tower comprise the ultimate heat sink, an alarm on the secondary flow to the heat exchanger indicates low flow. There is also an alarm if the compressor oil temperature exceeds 50 °C. (Each compressor is internally protected, as well, against high discharge temperature or pressure, low suction pressure, low oil pressure, and high oil temperature. The SMCs protect the compressor motors from operating with low or high line voltage or high current.)

The above PLC alarms are connected to the annunciator panel in the control room in a fail-safe manner. That is, the alarm is actually generated by the absence of an "All Clear" signal from the PLC. Alarm conditions set bits in words that give these memory locations non-zero values, and cause the PLC to stop generating the all clear signal. In this way, the alarms are generated if the PLC is disabled or loses AC power.

7.0 Startup and Operation of the Liquid Hydrogen Cold Sources

The startup of the first LH_2 CNS occurred in 1995, and Unit 2 started in 2002. This section contains summaries of the initial startup of each unit and their operating records. It is a record of safety and reliability. There have been no accidents or hydrogen leaks of any kind. Over its 38 reactor cycles Unit 1 was unavailable for only 14 of the days the reactor was scheduled to operate (1440 days); that is better than 99 % reliable. Unit 2 has had 100 % reliability. A chronological list of cold source milestones is presented in Table 7.1.

7.1 Authorization

As design work on the Unit 1 LH_2 source was nearing completion in 1992, a description of the system then envisioned was forwarded to the Non-Power Reactors Project Directorate in the Office of Nuclear Reactor Regulation of NRC, for an opinion as to whether the installation of the source could proceed under the provisions of 10 CFR 50.59 (see Section 2.1). Our proposal was sent to a group in INEL for review, and after a round of questions, and a small modification in the piping, we received a favorable reply from NRC on May 17, 1993. In the meantime, a separate outside review panel of experts in cryogenics, reactor safety, and nuclear radiation transport calculations, came to NIST in March, 1993 for a second independent appraisal of the proposed source. That panel strongly recommended the installation of the source to the Chief of the Reactor Radiation Division (now NIST Center for Neutron Research) and to the NBSR Safety Evaluation Committee (SEC). The SEC reaffirmed its support for the proposed source in Meeting 318 on May 6, 1993.

An Engineering Change Notice (ECN #413) was prepared for the committee, and it was approved on October 3, 1994. Finally, in early September of 1995, the SEC reviewed the startup and operating procedures, and approved the loading of up to 5 bar of hydrogen into the system and operation with liquid hydrogen in the NBSR. The ECN required startup tests in the first reactor cycle to measure:

Table 7.1 Liquid Hydrogen CNS Milestones.

Date	Milestone
26-Oct-1994	Unit 1 installed in CT beam port
8-Dec-1994	Condenser mounted on reactor face
26-Jun-1995	Ballast tank and hydrogen manifold complete
3-Aug-1995	Refrigerator connected to CNS
8-Sep-1995	Insulating vacuum system installed
12-Sep-1995	725 grams of hydrogen loaded into system
	First filling with LH_2
25-Sep-1995	Reactor startup with refrigerator OFF; 10 MW limit
27-Sep-1995	First reactor cycle with LH_2 source
5-Oct-1995	Power reaches 20 MW
6-Oct-1995	Thermosiphon restart tests; failed at 250 kPa
20-Oct-1995	Test of ortho/para catalyst pump
23-Oct-1995	Reduced operating pressure to 105 kPa
6-Nov-1995	End of first cycle
4-Apr-1996	Turbine inlet valve fuse blown - 1 lost day
19-Nov-1996	Late cycle compressor trip - 2 lost days
3-Mar-1997	Approx 18 g of hydrogen removed to hydride unit
26-Mar-1997	Add hydrogen to return to 725 g
23-Nov-1997	Turbine speed circuit failed - 2 lost days
25-Feb-1999	Start first cycle with Compressor 2
26-Feb-1999	Comp 2 and Comp 1 fail - 1 lost day
10-Aug-2000	600-Amp breaker fails - 1.5 lost days
25-Aug-2001	EOC #38; last day of operation of Unit 1
28-Aug-2001	18 g of hydrogen removed from source & condenser
2-Nov-2001	Unit 1 removed; stored in high-radiation cavity
23-Nov-2001	Unit 2 installed
29-Jan-2002	Ortho/para catalyst and pump removed
16-Feb-2002	Unit 2 ready; add hydrogen to 500 kPa
19-Feb-2002	First fill of Unit 2 with liquid hydrogen
6-Mar-2002	Start 1st cycle on Unit 2; 20 MW; P = 134 kPa
	Test of thermosiphon restart
14-Apr-2002	Lower pressure to P = 115 kPa
24-Apr-2002	100 grams of H-2 removed to hydride; P = 425 kPa
2-May-2002	Start 2nd cycle at P=100 kPa
24-Aug-2004	14 g of hydrogen removed; not replaced

1. The moderator chamber temperature with the refrigerator shutdown and its insulating vacuum backfilled with helium.
2. The power deposited in the cryostat assembly based on D_2O flow and ΔT.
3. The rate of increase of the assembly temperature with no D_2O flow.
4. The response of the system to a reactor startup, power increase, rundown and scram.
5. The optimum steady-state temperatures and pressures of all components at 20 MW.
6. The recovery rate of the system following a refrigerator trip.

7.2 Startup and Operation of Unit 1

By September 12, 1995, installation of all of the components of the cold source was complete. One minor deviation from the system described in Section 5 was made; the Vacuum Valve containment vessel, He-VI, was filled with nitrogen (also inert) rather than He because the cold cathode vacuum gauges failed in a helium environment. (The gauges were modified six months later, and He has been used in all of the containments since then.) The volume of the hydrogen system was measured earlier by loading the system with known quantities of helium; precise mass measurements were made on three He gas cylinders before and after filling the ballast tank with each. The volume of the ballast tank is 2009 liters (± 0.25 %), the volume outside of the tank (moderator chamber, condenser and piping) was 48 liters (± 4 %), and therefore the total hydrogen volume of Unit 1 was 2057 liters.

After checking the operability of the area hydrogen monitors, about 725 grams of hydrogen was loaded into the system, resulting in a pressure of just over 425 kPa at room temperature. With the reactor shutdown the refrigerator was started and the source was filled with LH_2 about four hours later that same day, September 12. Since the hydrogen pressure PID was still unfinished, there was considerable experimentation with the load and bypass valves. The vessel filled rapidly with LH_2 once the thermosiphon started following a pressure spike as liquid rushed into the warm vessel (see Section 7.3, also). The refrigerator was then shutdown and the LH_2 slowly boiled away overnight, the system returning to its starting pressure about twelve hours later. From the rate of pressure increase, the thermal radiation heat load was determined to be only 9 W.

Startup Tests:

Startup tests with the refrigerator shutdown began on September 25, 1995. The vacuum surrounding the moderator chamber was backfilled with He to allow some heat transfer through the vacuum and He jackets to the D_2O coolant. The moderator chamber temperature was measured indirectly by isolating the chamber, condenser, and connecting lines (48 liters) from the ballast tank, and measuring the hydrogen pressure in this part of the system as the chamber (17 liters) was warmed by the reactor. At 1 MW, 5 MW, and 10 MW, the measured temperatures were 40 ˚C, 67 ˚C, and 114 ˚C, respectively. Test 1 determined the conditions under which the reactor could have operated with the Unit 1 CNS and refrigerator shutdown:

- Moderator chamber filled with hydrogen (or helium) to at least 60 psia.
- Insulating vacuum and containment helium-filled to at least 45 psia.
- Normal auxiliary D_2O cooling maintained.
- Reactor power not to exceed 10 MW.

This was the only time ever that the reactor has been operated above 200 kW with the CNS warm.

Test 3 was also performed that day. At 10 MW the D_2O flow was secured and the cryostat assembly temperature rose 5 ˚C in 45 seconds. Extrapolating to 20 MW, the heating rate at full power would be 13.3 ˚C/min. Since the average D_2O temperature is less than 35 ˚C at 20 MW, at least 5 minutes would be needed to reach the boiling point. Test 3 verified that a low-flow (18.9 lpm) reactor rundown provides more than adequate protection against overheating. The cryostat heat load at 20 MW, Test 2, was later determined to be 27 kW to 30 kW; it is constantly monitored and displayed.

Following these tests, the insulating vacuum was reestablished and the refrigerator was started the following day. On September 27, the first reactor cycle with the LH_2 source began. Since it was also the first cycle with new plate-type primary heat exchangers, the power was limited initially to 10 MW. The source performed as expected and preliminary gain measurements indicated that instruments in the guide hall were receiving up to 40 times the beam intensity

measured two days before, with the source warm.

A week later, with the reactor at 20 MW, the response of the cold source to a refrigerator failure (Test 6) was simulated by twice interrupting the flow of cold helium to the hydrogen condenser. Before the start of this test, the hydrogen pressure was maintained at 134 kPa through the action of a controller on the He load line return valve. The cold neutron flux was monitored at the NG-7 SANS. In the first case, the valve was closed and the hydrogen pressure was allowed to increase to 200 kPa before the valve was restored to its automatic mode, 47 seconds later. The pressure decreased immediately, returning to its initial value in about 3 minutes, and the flux dropped about 2 %, before returning to its initial value. We repeated the test, but allowed the pressure to rise to 250 kPa before returning the valve to its automatic mode (87 seconds). Again the pressure immediately started to decrease, but the flux had dropped to only 10 % of its initial value, prompting a verbal request that the reactor be shutdown. The sharp decrease in neutron flux, even as the hydrogen pressure was decreasing, indicated that the liquid was not refilling the moderator chamber.

As a result of these tests, a maximum reactor rundown set point was established at 200 kPa. In addition, the reactor is not restarted after a hydrogen pressure rundown, until either all of the alarms have cleared, or the operators have discussed the situation with the Cold Source Contact. It became clear in the first cycle, that a turbine or refrigerator trip would always lead to a reactor rundown. Later, the set point was lowered to 130 % of the operating pressure to speed the recovery from such a trip.

Optimization:

The hydrogen pressure was varied to optimize performance. Increasing the hydrogen pressure caused the long-wavelength intensity to drop, so the pressure was lowered to about 105 kPa, where it remained for the life of the Unit 1 source. The hydrogen recirculation pump, designed into the system to counteract the feared conversion of ortho-LH_2 to para-LH_2, was twice tested for many hours during the first cycle. Its operation had no measurable effect on the beam intensity, and the system was never used subsequently. The pump and catalyst were removed in 2002 before the startup of Unit 2.

Both of the above phenomena support the conclusion that the LH_2 and vapor are NOT completely converted to para-hydrogen in the source (see Section 3 and Figure 3.5). In addition, if the LH_2 were to gradually convert to para, we would expect to observe the cold neutron flux decrease at the instruments during the first few days of a reactor cycle. No changes are observed over the 38 days. Finally, if the LH_2 were to convert to para quickly, in a few hours, there might not be any drop to be observed during a cycle. However, a refrigerator trip and recovery would mix the presumed para vapor from the source with the normal hydrogen remaining in the ballast tank. The cold neutron intensity after a trip would be greater than it was previously. This has never been observed, either. One can only conclude that the ortho content of the LH_2 is always maintained at a fraction high enough to cause the scattering to be dominated by ortho.

Reliability:

A review of the operating logs for Unit 1 shows that there were 46 refrigerator trips during its 38 cycles. Two of these were turbine trips only (failed inlet valve fuse and speed circuit) and the remaining 44 were compressor trips, usually caused by storm-related AC power interruptions. Only nine of these trips caused ^{135}Xe poison shutdowns (30-40 hours), resulting in about 14 days lost (though some days were just postponed); thus the reliability of the Unit 1 CNS was 99 %. A few trips coincided with other reactor system failures that prevented restarts.

Of the 44 compressor trips, the system restarted itself eighteen times, and was successfully restarted manually fifteen times. The manual restarts involved either re-initiating the Auto-Cool program, or, on eight occasions starting in January 1999, switching compressors and restarting Auto-Cool. It takes less than 5 minutes to make the switch, so unless the trip comes in the last few days of a reactor cycle, there is ample time to change to the other compressor and start it, rather than diagnose the failure of the first

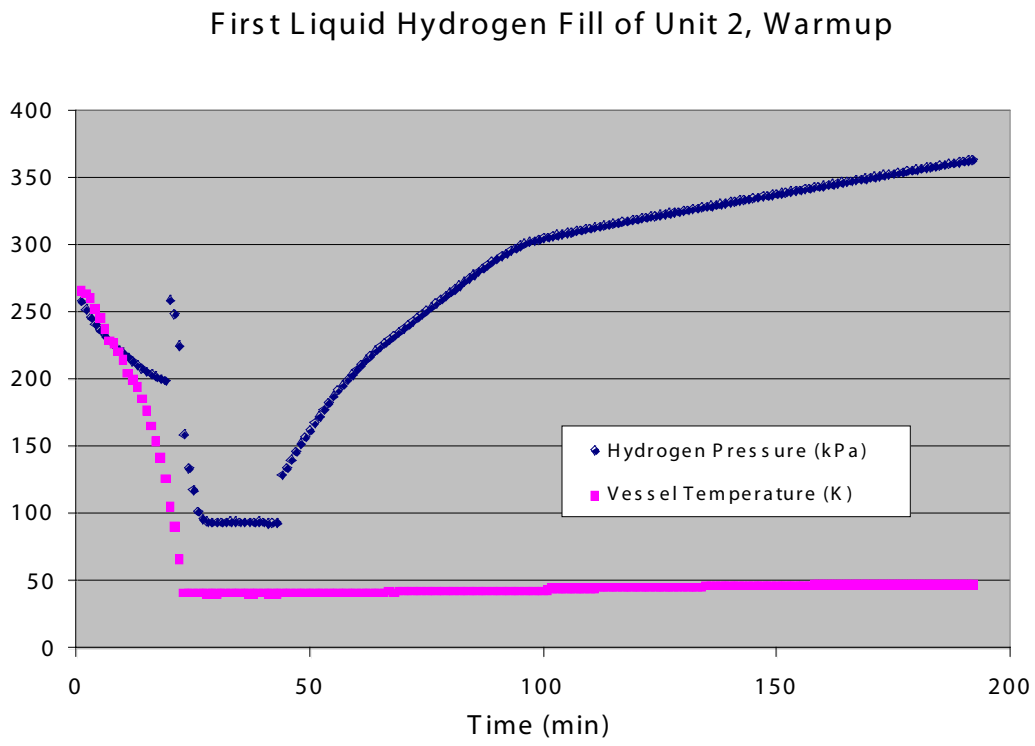

Figure 7.1. Hydrogen pressure and Unit 2 moderator chamber temperature as the thermosiphon starts for the first time.

compressor to restart. The cold source can recover completely 15 to 20 minutes after the refrigerator restarts.

7.3 The Advanced Liquid Hydrogen Cold Source, Unit 2

Unit 1 was replaced during a six-month shutdown in 2001-02. It had not reached the end of its life, nor was there anything wrong with Unit 1. The Advanced LH_2 Cold Source was installed because it was expected to increase the brightness by 70-80 %, as described in Section 3. A new cask and transfer system were built for the removal of Unit 1, and the entire job of pulling it from the reactor, transporting it to its storage vault, and securing it safely inside the vault was accomplished in 5 hours on November 2, 2001. Only the cryostat assembly was replaced; the condenser, ballast tank, refrigerator, vacuum system etc. are still in service. We needed only to sever the D_2O and LH_2 supply lines to free Unit 1 from the reactor, and rebuild these lines to connect Unit 2 to the existing components. Authorization for the change was sought and received in the form of an Addendum to ECN #413, as there were no unreviewed safety questions.

Thermosiphon:

Having removed the large volume of H_2 vapor from the inner vessel, it was anticipated that the optimum operating pressure for Unit 2 would be 150-200 kPa. Accordingly, once the system was completely reassembled, over 100 more grams of hydrogen were added, increasing the pressure at STP to 500 kPa, and the total inventory to 825 g. The new source was first filled with LH_2 on February 19, 2002. A plot of the hydrogen pressure and moderator chamber temperature as the thermosiphon started is shown in Figure 7.1. Unit 2 behaved very much like Unit 1, although the pressure was a little higher, and, this time, the thermocouples on the LH_2 vessel survived the installation welding. As the condenser cooled toward 20 K, LH_2 collected beneath and between the plates, prevented from filling the vessel by the back pressure created as droplets evaporate in the lines and vessel. An unstable equilibrium existed 25-30 minutes until a larger quantity of LH_2 reached the vessel where it boiled rapidly, producing the 60-kPa (10-psi) pressure spike. Sometimes there are two or three spikes, and sometimes a spike is barely noticeable, but the start of the thermosiphon is unmistakable because

the pressure drops very quickly to its set point. The temperature of the vessel also drops rapidly to 20 K (the thermocouples, however, indicate 40 K).

Immediately before the thermosiphon started, when the pressure was just under 200 kPa, about 60 % of the inventory had liquefied, 510 g, corresponding to 7 liters of LH_2. Very little of this had reached the moderator chamber, which was still quite warm, so the condenser plates were completely flooded; the hydrogen side of the condenser has a volume of 6.4 liters, and there is only a 0.5 liter plenum below it. Once the thermosiphon was operating, the pressure dropped to 95 kPa, indicating that there were nearly 9.5 liters of LH_2 in the system. Given that the vessel holds 5 liters and there may be another 2 liters available under the condenser and in the transfer tubes, the condenser plates were still nearly half flooded. We operated the first cycle at 135 kPa, which would have left the plates one-third covered with LH_2. (Later, we reduced the inventory to 695 g, but it is very likely that we still operate with 20-25 % of the condenser flooded.)

Still referring to Figure 7.1, the refrigerator was shutdown 20 minutes after the thermosiphon started, and the hydrogen slowly boiled away. The resulting pressure rise appears to occur in three distinct regimes. For the first 12-14 min, until the pressure reached 200 kPa, the thermal radiation heating rate was about 70 W. At this point, the condenser plates were no longer flooded, but the transfer tubes and vessel were full of liquid. For the next hour, the heating rate decreased from 40 to 20 W, until the pressure was 300 kPa. In the final regime, only the vessel contained LH_2, and the thermal radiation into the vessel alone was 7 watts.

Startup Tests:

The reactor was first operated with the Unit 2 CNS on March 6, 2002. Since the NBSR was never operated with Unit 1 warm, it was decided to skip the measurement of the moderator chamber temperature vs. reactor power with the refrigerator shutdown and the vacuum backfilled. Instead, there was a routine reactor startup, progressing through steps to 20 MW. The tests included verification of stable operation, measurement of routine operating parameters, and determination of limits governing reactor restart following a refrigerator failure. Since we have not yet tested our ability to operate the reactor with the refrigerator shutdown, the reactor must never be operated at a power greater than 200 kW with the cold source shutdown.

Routine Reactor Startup:

The first test of the cold source was to verify its stable operation as heat deposited in the moderator chamber and liquid hydrogen increased from its thermal radiation 'background' to as much as 1360 watts, as predicted by the MCNP results. We had successfully demonstrated the operation of the thermosiphon with no heat load, and our ability to restart the thermosiphon after a refrigerator trip, during two weeks of tests before the reactor startup.

To assure that the moderator chamber remained filled with liquid hydrogen, and to report initial estimates of the gain over Unit 1, we were assisted by instrument scientists at NG-0, NG-4 and NG-7. At least one of those instrument monitors was recording the flux each time the reactor power was increased.

As was the case with Unit 1, the surest indication that the thermosiphon was operating properly was the decrease in the output of the return gas heater in the refrigerator as the heat deposited in the cold source increased. The refrigerator is programmed to adjust the flow of cold helium to the condenser as needed to maintain a nearly constant hydrogen pressure AND to maintain the helium return gas temperature at 18 K. As the rate of evaporation of LH_2 increases with reactor power, more hydrogen vapor must be condensed to maintain a constant pressure, so the helium refrigerant is increasingly warmed flowing through the condenser and less heat is required from the heater. The difference between the heater power with the reactor shutdown and heater power with the reactor at 20 MW is an indirect measurement of the heat deposited in the source (also see Section 7.4).

Figure 7.2 is a plot of the heater output and reactor power during the March 6, 2002 startup. The reactor power has been renormalized and multiplied by 100

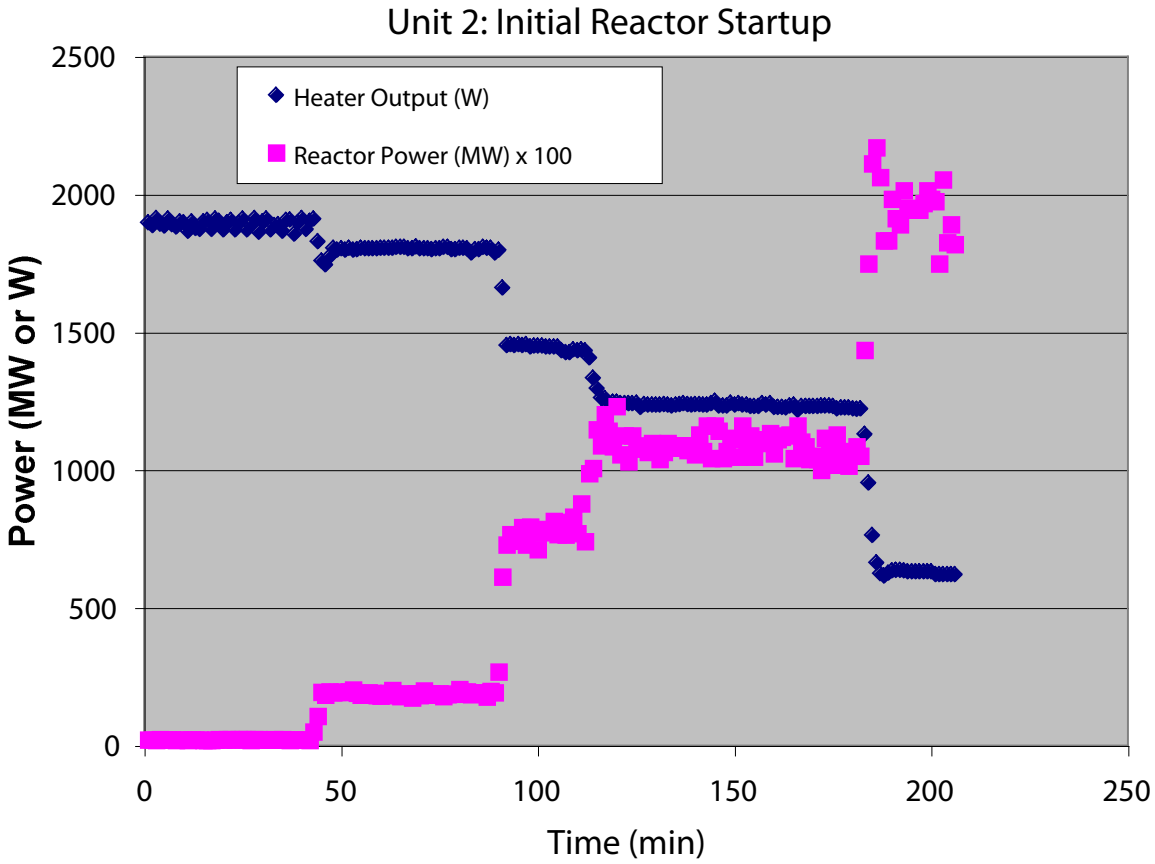

Figure 7.2. Response of the refrigerator return gas heater as reactor power is increased from 0 to 20 MW. As the heat load from the cold source is met by the hydrogen condenser, the heater power needed to keep the return gas at 18 K decreases. The difference in the heater output provides an indirect measure of the CNS heat load.

for display purposes. During the startup, the reactor power was increased in steps to 100 kW, 1 MW, 5 MW, 10 MW (for at least one hour), and finally 20 MW. The actual power somewhat exceeded the 'nominal' power for the steps prior to 10 MW, at which time the reactor thermal power could be determined. With every increase in reactor power there was a proportional decrease in heater power, an indirect measure of the nuclear heat load. (The average of dozens of these indirect measurements of the heat deposited in the cold source at 20 MW is 1220 ± 60 watts, about 10 % less than the 1360 watt estimate using MCNP.)

Refrigerator Trip and Recovery:

From our operating experience with Unit 1, we know we can expect several interruptions of AC power each year that will trip the compressor and may or may not cause a reactor scram. If there is a refrigerator trip without a reactor scram, there must be an automatic reactor rundown to protect the moderator chamber from over heating. The rundown is generated by one of two hydrogen differential pressure transducers, comparing the H_2 pressure with the helium pressure in the ballast tank containment. To verify that the thermosiphon will restart, and continue to refill the vessel even with the reactor at 2 MW, we deliberately stopped the compressor and restarted the Auto-Cool sequence 55 seconds later, simulating an AC power interruption. Since this test caused a rundown and required a quick return to power, we first obtained approval from the Chief of Operations, and then established close coordination with the reactor operators. The above-mentioned flux monitors were ready to verify that the vessel remained filled with liquid hydrogen.

At the start of the test, the reactor had been at 20 MW for nearly an hour, so the heat load in the LH_2

vessel was at equilibrium (^{28}Al, with a half-life of 2.25 minutes, reaches saturation and contributes over 20 % of the heat load). The hydrogen pressure was 134 kPa, and reactor rundown had been set at 200 kPa. A brief chronology of events, as recorded every 5 seconds by the data logger, is as follows:

- 17:46:37 STOP Compressor 1.
- 17:47:12 Reactor rundown.
- 17:47:32 Start the Auto-Cool sequence, successfully restarting the compressor.
- 17:49 Rundown bypassed (by reactor operators) at approximately 200 kW.
- 17:50:12 Refrigerator turbine starts OK.
- 17:52:32 Maximum H_2 pressure recorded, P-3 = 355 kPa.
- 17:53 Start increasing reactor power to 2 MW.
- 17:55 Reactor at 2 MW; P-3 = 195 kPa and CNS alarms clear.
- 17:59 Increasing reactor power.
- 18:05 20 MW.

Figure 7.3 shows the hydrogen pressure and reactor power during the test. After the refrigerator has cooled the condenser below about 25 K, the H_2 pressure dropped rapidly. The thermosiphon restarts immediately, supplying the vessel with more LH_2. The vessel remained filled based on the behavior of the flux monitor at NG-7; the monitor count rate had exactly the same time-dependence as the reactor power curve in Figure 7.3. Increasing the reactor power to 2 MW slows only slightly the rate of the H_2 pressure decrease. Thus it is safe to raise the reactor power from 200 kW to 2 MW, holding at 2 MW as long as the pressure continues to drop. After all alarms have cleared, the power can be raised to 20 MW. The increase to 2 MW is at the discretion of the reactor supervisor, of course, but from the data, it could speed the recovery by about 3 minutes.

The ultimate confirmation of the proper operation of the thermosiphon, in the absence of a flux monitor, is the feedback through the return gas heater, as discussed in the reactor startup monitoring above. Figure 7.3 also shows reactor power and the heater output during the trip test. The heater output is slow to return to its initial value because the refrigerator must return to equilibrium after the trip. After

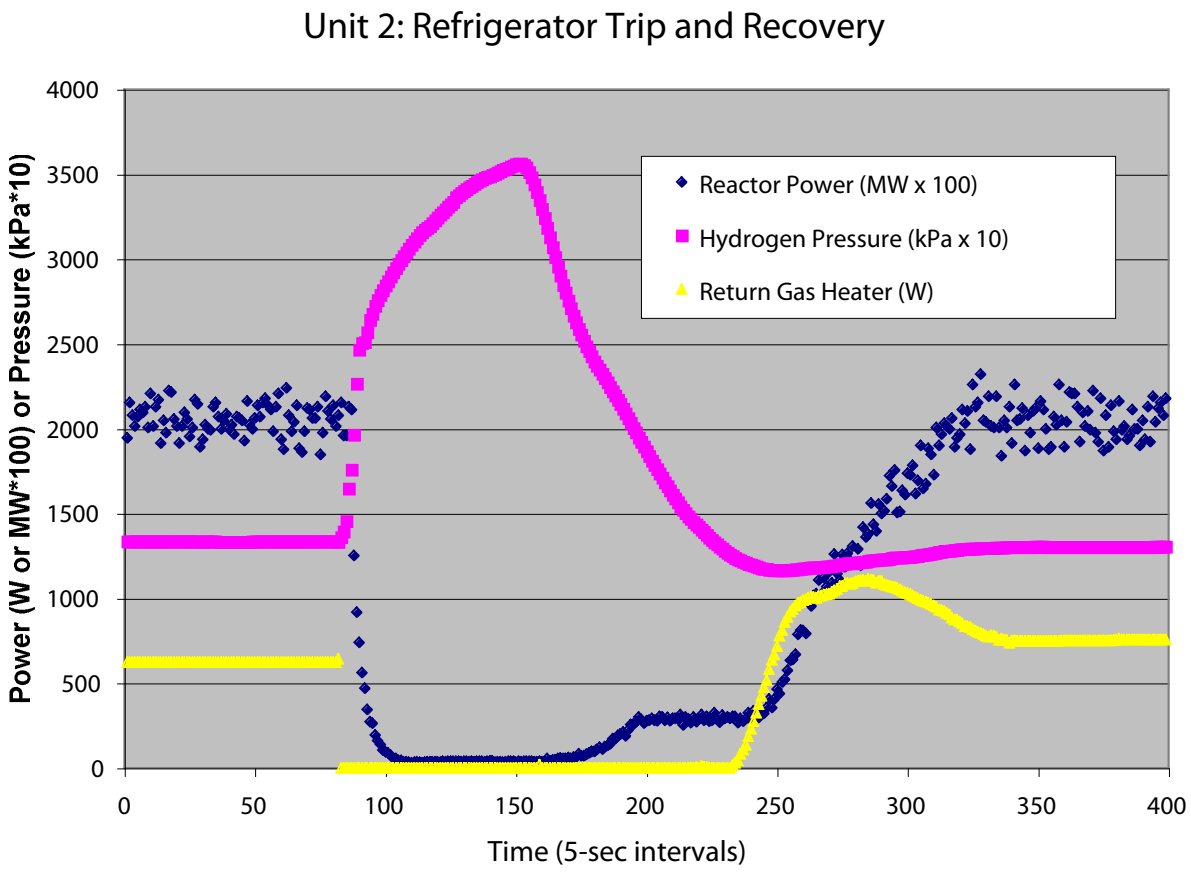

Figure 7.3. Unit 2 startup test of the ability to recover from a refrigerator trip.

passing 10 MW, however, the heater power was decreasing while the reactor power was increasing, proof that the thermosiphon had restarted. In this case, the heater power was about 620 watts before the trip, and returned to a new equilibrium of about 750 watts, as the reactor returned to 20 MW. When the reactor was shutdown, the heater supplied about 1900 watts in the absence of a load on the condenser. It is this roughly 1300 watt difference that proves the thermosiphon is supplying LH_2 to the vessel.

Typical values of operating parameters for Unit 2 and the refrigerator as of November 2005 are listed in Table 7.2.

Reliability:

Since the installation of Unit 2, the CNS reliability has been 100 %. "Lost" time due to the cold source is measured in minutes because it has not caused a single ^{135}Xe poison shutdown in 22 reactor cycles. The improvement is not the result of any design change of Unit 2. The restart routine in the PLC was modified and refined several times since the SMCs were first used in 1999, reflecting our experience with them. In addition, the large capacitors installed to balance the three phases of the 480 Volt supply in each motor control center were disconnected in February 2002 as we prepared to resume operation. Since that time, the compressors have been less likely to trip because of a brief AC power interruption. There have been only six compressor trips, and only one required changing compressors to recover.

7.4 Heat Load Measurements

Every shutdown and startup of the reactor provides an opportunity to record the change in the return gas heater power and make an indirect estimate of the nuclear heat load. Figure 7.4 shows the results of about forty such measurements on Unit 1 (top graph) and over sixty values for Unit 2. Unfortunately, the very nature of the measurements introduces a large uncertainty in the results, because the refrigerator parameters vary somewhat as the load-line valve, CV-424, opens or closes. As the valve opens, for example, from a few percent with the reactor shut down, to 40-50 % at 20 MW, the turbine exhaust pressure drops a few psia, increasing the turbine speed, efficiency and the refrigerator cooling capacity. An additional part

Table 7.2 Typical operating parameters for Unit 2 and refrigerator.

Parameter	Value	Units
Hydrogen Volume	2048	liters
Ballast Tank	2009	liters
LH_2 Vessel	5.0	liters
Condenser (H_2 side)	6.4	liters
Piping, etc.	27.6	liters
Pressure (warm)	420	kPa
Density (warm, 300 K)	0.339	kg/m^3
Inventory	695	g
Pressure (cold)	97	kPa
Temperature (saturation)	20.2	K
LH_2 Density	70.8	kg/m^3
GH_2 Density (20 K)	1.34	kg/m^3
Heat of Vaporization	446	J/g
LH_2 - Mass (total)	530	g
LH_2 - Volume (total)	7.6	liters
Moderator Chamber		
LH_2 Mass	325	g
Al Mass	2840	g
Insulating Vacuums	10^{-5}	Pa
He Containments	110-130	kPa
Refrigerator Power	2500	W
Motor Power	280	kW
Helium Flow *	125	g/s
Temperatures:		
Turbine Inlet	20.6	K
Turbine Exhaust	14.6	K
Condenser Inlet	14.9	K
Condenser Outlet	20.2	K
Heater Inlet	17.0	K
Heater Outlet (controlled)	18.0	K
CNS Heat Load **	1200	W
Heater Output **	700	W
Losses **	600	W
* 50 - 60% bypasses the load		
** ± 100 watts		

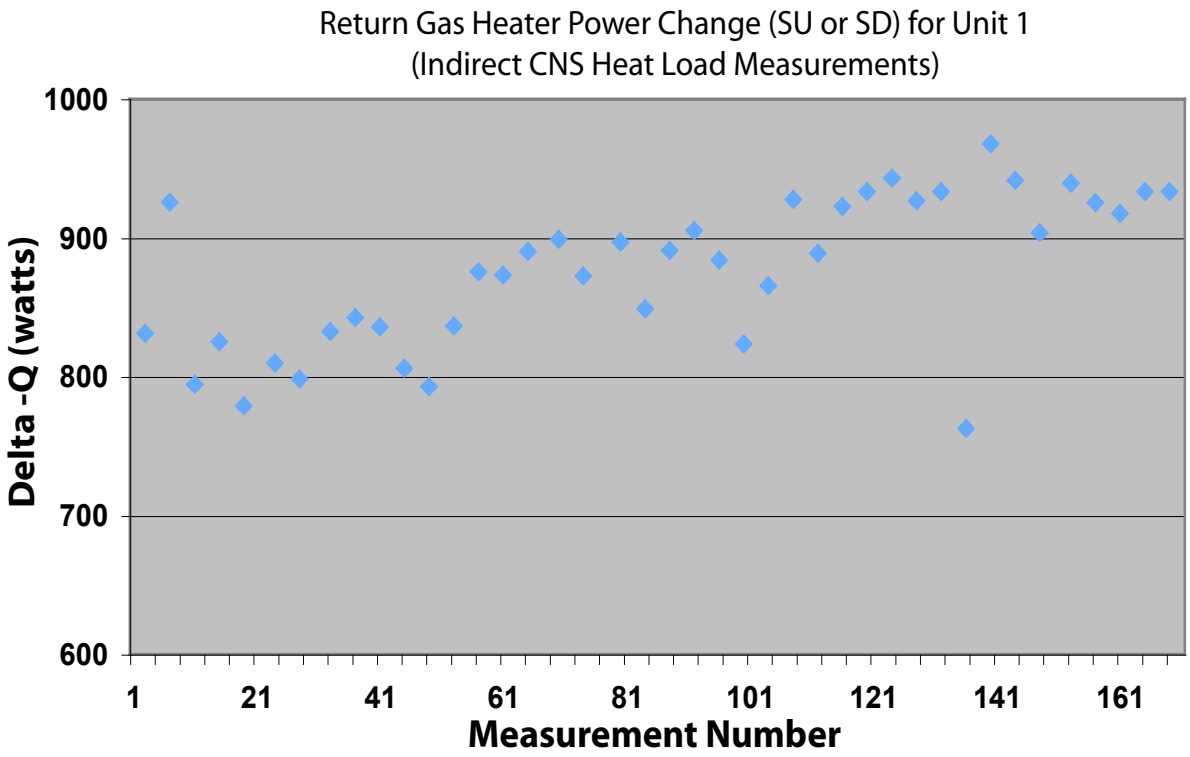

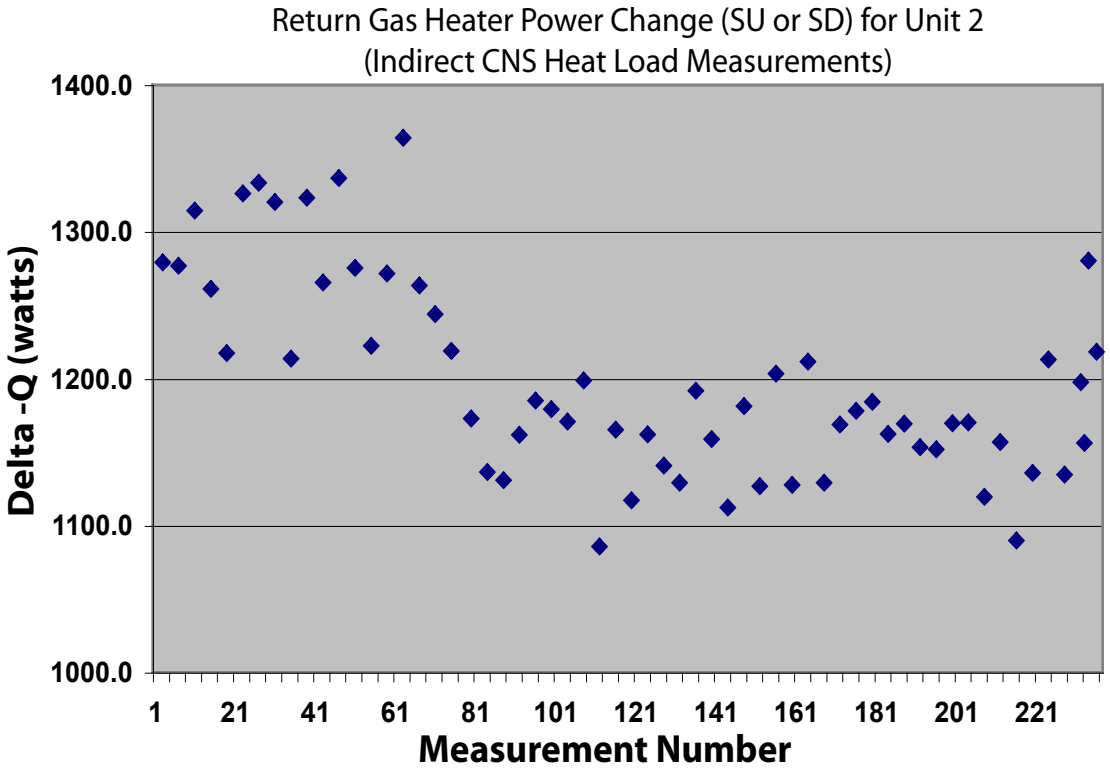

Figure 7.4. . Indirect Heat Load Measurements on Units 1 and 2. The ΔQ values are the changes in the return gas heater output before and after a reactor startup or shutdown. It is usually impossible to control all of the refrigerator parameters, which results in the large variation in the values of ΔQ.

of the uncertainty arises from the fact that the heater power may vary 30-50 W for no apparent reason.

The results for both units seem to divide into two groups. Compressor 2 was integrated into the system at measurement index number 70, for Unit 1, and the average of the results before and after that event are 830 W and 900 W, respectively. (The slide-valve loading of Compressor 1 was increased at that point to match the somewhat higher performance of Compressor 2.) There is an even more distinct divide for the Unit 2 results when the load bypass valve, CV-421, was closed from 75 % to 70 %, at index number 79; the average was 1280 W before the change, and 1160 W thereafter. It is not clear, in either case, which of the two groups has the lower systematic error. Giving equal weight to the groups of measurements we arrive at the following values for the nuclear heat loads:

- Unit 1 865 ± 40 W.
- Unit 2 1220 ± 60 W.

Since there is so much excess cooling capacity, it would seem that precise knowledge of the heat load is not so important. A future replacement or additional source, however, could tax the capacity of the refrigerator. It would also be nice to know the origin and magnitude of the losses in the load and the transfer lines. Finally, the heat load measurements are benchmarks for the MCNP computational method. The calculated values for Units 1 and 2 are 915 W and 1360 W, overestimates of 6 % and 11 %, respectively.

8.0 Accident Analysis

The cold neutron sources have operated very reliably for more than ten years. This section presents analysis of likely abnormal situations and highly unlikely accidents. The first five parts of this section describe the CNS response to abnormal incidents that have occurred or that are likely to occur over its lifetime. Parts 6 through 10 are analyses of unlikely or beyond unlikely accidents that could damage the cold source but would not pose any unreviewed safety question regarding the NBSR. These hypothetical events bound any credible accident scenarios.

8.1 Reactor Power Change

The refrigerator and hydrogen system control systems have been designed to automatically adapt to changes of heat load on the moderator chamber and cryostat. This implementation has been extensively tested, and it operates completely predictably even under the most difficult perturbation of a reactor scram. There are no consequences of an increase or decrease in reactor power.

Conversely, a change in the quantity of LH_2 in the moderator chamber has a very small effect on the reactivity of the core. Lengthy MCNP calculations show that emptying the vessel of LH_2 adds 0.1€ (+0.13$) or (+0.1 %Δk/k). This reactivity insertion is just one-fifth of the limit on "moveable experiments" in the core, and is easily offset by a 4-5 inch insertion of the regulating control rod.

Flooding of the cryostat assembly vacuum region with D_2O would represent a larger reactivity insertion, nearly 0.5 %Δk/k, which is the limit for a single moveable experiment. It is still a much smaller and slower reactivity insertion than the maximum reactivity insertion accident, +1.3 %Δk/k in 0.5 sec, that was shown not to damage the core in NBSR-14[10].

8.2 Refrigerator Failure

If the refrigerator fails, there will be no cold helium to re-condense the hydrogen vapor, and eventually the pressure in the moderator/ballast tank assembly will start to rise. In this case, the reactor will receive a rundown signal when the pressure reaches 135 kPa, upon which all shim control arms are inserted continuously into the reactor until the condition is removed. This will reduce reactor power immediately, and reduce the heat load on the moderator chamber. If the refrigerator function is not restored, all of the liquid will evaporate, and the system will be in a safe condition, as the reactor will not be restarted until cooling is restored and the pressure is reduced below the setpoint. The rundown can be bypassed when the reactor power is reduced to 200 kW, at which power level the heat load is reduced to an insignificant amount. There are no negative consequences to reactor safety from such an incident.

8.3 Sudden Loss of Electrical Power

When electrical power fails, the refrigerator will cease operation, and will come to a safe condition without operator intervention of any kind, even in the complete absence of power, as all automatic valves fail safe. The liquid in the moderator chamber will boil away slowly, and the hydrogen pressure will slowly rise to normal shutdown pressure as the vapor fills the ballast tank. Again, no operator intervention of any kind is required to reach a safe condition. If the power failure outage is site-wide, the reactor will also scram, so that heating will quickly decay to nominal values; if the reactor continues to operate, a rundown signal will be generated when the hydrogen pressure exceeds 135 kPa, and reactor power, and therefore nuclear heating, will be reduced to a level safe for the cold source. If the power outage is prolonged, the system will remain in a safe condition indefinitely, and will require no operator intervention. All valves in the refrigerator are fail safe, and the hydrogen system is entirely passive. No damage to any reactor system would occur from such an incident.

8.4 Loss of Cooling Water Flow to Cryostat and Plug Assembly

The non-cryogenic components of the cryostat assembly are cooled by circulating D_2O. The flow is monitored by two (for redundancy) flow sensors. If the cooling drops below 18.9 lpm, a value providing ample cooling at full reactor power, a rundown signal

will be generated and the reactor power will be reduced to a safe level until the problem is corrected. There are two rundown channels, and the rundown logic is one-of-two, so that failure to run down would require two failures, and is highly improbable. If both circuits were to fail, there are additional alarms generated by the PLC that would alert the reactor operators before there is any danger to the structural integrity of the cryostat assembly. If the reactor continued to operate for an extended period in spite of this signal, the cryostat assembly could be damaged, but there would be no damage to the reactor or its systems.

8.5 Loss of Cryogenic Insulating Vacuum

The only reasonable scenarios leading to a total loss of insulating vacuum are: failure of a vacuum pump and of the protective circuit which would isolate the system; a sudden leak in the helium containment surrounding the vacuum space; or a failure of the moderator chamber itself. The last of these is analyzed in Section 8.6 for the worst case of a sudden leak, and presents no hazard. For either of the other two possible scenarios, helium would leak into the vacuum, spoiling the cryogenic insulation. The heat load would exceed the capacity of the refrigerator, and the liquid would all vaporize (relatively slowly). The reactor would then be reduced in power by the rundown signal generated by high hydrogen pressure, and the incident would be over. No damage to any reactor component or system would occur.

8.6 Sudden Release of Liquid Hydrogen to Vacuum Space

Although the normal operating condition of the cold source with liquid in the moderator chamber is at approximately 100 kPa, and the moderator chamber is therefore at low stress (design working stress 500 kPa), a sudden large leak that releases all of the liquid to the vacuum space has been analyzed. The liquid hydrogen in the moderator chamber during operation is under its saturated vapor pressure, and is approximately 5 liters at 20.27 K and 101.3 kPa (1 bar), which corresponds to 354 g (see table 8.1[18]). The volume contained by the helium jacket, which is the pressure containing barrier, is 47 liters, neglecting all connecting tubing.

In the event of a sudden leak in the moderator, the 354 g of liquid would first cool down as a result of the expansion into a larger volume, but would then increase rapidly as a result of vaporization. Some of the excess pressure would be vented to the ballast tank and other components outside the cryostat. For a conservative bounding estimate, however, this venting is neglected, and it is assumed that all is converted instantaneously to vapor at 28 K (lowest temperature at which entire inventory will be vapor). From Table 8.1, the vapor density at 28 K is 7.53 g/liter, so that the 354 g will fill the available volume of 47 liters at just over 600 kPa (87 psi). This is well below the design working pressure, let alone the rupture pressure (>8270 kPa) of the helium jacket. Therefore, there would be no damage to any reactor component, nor would there be any release of hydrogen to the confinement building. Note that venting will occur, and the actual pressures would be much less than 600 kPa in an actual incident.

Table 8.1 Selected cryogenic properties of hydrogen.

Temperature	Form	Pressure (kPa)	Density (kg/m^3)	Enthalpy (kJ/kg)
20.27	Liquid	101.3	70.786	-256.2
20.27	Vapor	101.3	1.3380	189.3
28	Vapor	600.	7.53	189.3.

8.7 Slow leak of Air into Vacuum Vessel

The design of the NIST liquid hydrogen cold neutron source is focused on prevention of mixing of hydrogen and air. To this end, all hydrogen containing structures are completely surrounded by inert gas (usually helium) contained in an additional containment vessel. These containments are filled to a pressure of approximately 125 kPa with helium that is analyzed for oxygen impurities immediately before filling, so that there is no possibility of air leaking into the space immediately surrounding the hydrogen moderator chamber. The pressure in each containment volume is continuously monitored, and an alarm is annunciated when the pressure reaches 100 kPa. In spite of these precautions, the consequences of a slow leak from the

containment into the vacuum surrounding the cold moderator chamber is calculated, *assuming that the containment is filled with 100 % air.* For this to happen, a helium supply bottle would have to be filled with air, and not have been analyzed, in direct contradiction of all procedures. It is further assumed that the leak is not noted until the pressure drops to the alarm point of 100 kPa. The volume of the containment surrounding the cold zone of the moderator chamber is approximately 14 liters; therefore, this would imply a total volume of 14x25/125 = 2.8 STP liters (3.3 g) of air that would be cryo-trapped on the moderator chamber. The oxygen in this air would be converted to ozone by the radiation field, which can spontaneously recombine with reasonably large energy release. Assuming that this energy both ruptures the vessel and ignites a detonation, the magnitude of the peak pressure can be estimated. Measurements have been made for the more challenging conditions of 300 cc of solid air (528 g) combining with liquid hydrogen in a closed vessel[19] of total volume 32.6 liters. In this case, the peak pressure reached only 1050 psi, a value that would be greatly reduced for the actual conditions of a 47 liters volume and 3.3 g of air. These values imply a pressure less than 883 kPa, which is much less than the allowed working pressure for the helium jacket. Therefore, there would be no safety consequences, either from damage to the reactor thimble or from any release to the confinement building from such a hypothetical accident.

8.8 Hydrogen Release to Confinement Building

The cold source system is designed to prevent such an occurrence during normal operation, both by passive features and by procedures. All hydrogen containing systems are protected from accidental breakage by being buried in shielding, in the floor, or being surrounded by steel protective structures. The 133 kN (15 ton) annular crane is prevented from entering the zone where hydrogen system components are contained by electrical interlocks, that can only be bypassed by reactor management (reactor supervisor or above). During reactor operation, additional personnel would be detailed to observe and control any crane use in this area, to ensure that no shields that protect hydrogen lines were removed. During maintenance procedures, the ballast tank is isolated from the moderator, so that only the hydrogen present in the moderator chamber, heat exchanger and piping could be released. The volume of the moderator, heat exchanger and piping were measured for the first source, and determined to be a total of 47 liters; the volume of the moderator chamber alone was 17 liters. For the second generation source, the moderator chamber is just 5 liters, so that 37 liters could be available for release when the ballast tank is isolated. Maintenance procedures require emptying this volume by use of a hydrogen absorbing system, and backfilling with helium to obtain a non-flammable mixture before opening or working on the hydrogen system.

Although any release would require multiple system and procedural failures, the consequences of a release have been analyzed. The design allows a warm pressure of 500 kPa, which would allow release of approximately 13 g (the mass release required to reduce the Unit 2 (17 g for Unit 1) pressure to barospheric). It is extremely difficult to predict actual gas behavior during any accidental release, but it is useful to look at some limit cases. The volume of the first floor of the confinement building, which is the area to which hydrogen would be released, is approximately 4000 m^3, and a complete release as described would add 0.15 m^3 of hydrogen. When completely mixed, this is considerably below the flammable limit of 4 % by volume. Thus, the possibility of deflagration or detonation exists only during that period when the gas is being released, and is mixing with the air. The ventilation system supplies conditioned air from a supply duct on the wall behind the area of hydrogen containing equipment at a measured rate of approximately 240 m^3 per minute, divided between three equal registers, one of which discharges directly into the area containing hydrogen. For estimation purposes, the local volume for hydrogen release and mixing can be specified as the area above the guide shielding, a volume of approximately 200 m^3, which connects directly with no obstructions to the rest of C-100. Further progress in estimating consequences requires specification of the nature of the release. For a "slow" release of less than 1 l/s for 140 s or more, there is little or no danger of a large energy release. The quantity of hydrogen-air mixture within flammable limits at any time will be small. (A recent simulation for a garage of dimensions similar

to the hydrogen release volume as part of a study of hydrogen use for transportation with a much faster release rate indicates little risk. This simulation did not incorporate active ventilation.) [20]. The hydrogen will rise into the local volume and rapidly be mixed to well below flammable limits by the action of convection and the forced ventilation. Any reaction would be a slow deflagration, which could generate hot flames, but no destructive shock waves.

A rapid release, however, that might occur if a guillotine break occurred as a result of misuse of a crane, tearing the heat exchanger from the wall, would have more serious effects. In this case, the release would proceed at sonic velocities, so that the entire 13 g was released in less than 1-2 s. Such a release would create a well mixed volume as part of the release – less than the full 13 g, but certainly a substantial fraction of 13 g. In order to estimate the consequences of such a release, the equivalent weight of TNT must be determined. This is not as straightforward as simply converting at the usual rate of 24 g TNT per g hydrogen, since allowance must be made for the details of mixing (not all of the gas will be at stoichiometric conditions), and for reflections of the blast from adjacent walls, ceilings, shields, and reactor shielding. Given the arrangement at the assumed point of release (near the reactor face over the guide shields), a reasonable assumption is that we should double the charge to account for reflection from the ceiling, while halving the charge to account for the actual mixture conditions. The net result is that the effective TNT weight, W, is taken as 0.3 kg for use in the scaling for hydrogen blast effects. Although a detonation is highly unlikely (no detonations are known for unconfined spills of less than 100 kg of hydrogen, and this assumed spill is only weakly confined), that is what is assumed by the use of TNT equivalent, and so the assumption is highly conservative. The distance, Z, of the release and detonation from the confinement building walls is approximately 10 m, so that the scaled distance ($Z/W^{1/3}$) is 15 $m/kg^{1/3}$. Using standard blast data[21], this gives rise to a peak reflected overpressure of 6000 Pa (0.7 psi) and a peak reflected impulse of 25.4 Pa-s at the wall. These values are well below any possibility of serious structural damage, and will result in no harm to the reactor or confinement. However, the consequences for equipment and personnel closer to such a blast would be very serious. Once again, all of the design and procedures established for the maintenance and operation of the source are explicitly for the purpose of preventing such an event, and two or more independent failures are required to even make it possible.

8.9 Stoichiometric Mixture of Hydrogen and Air in Moderator Chamber

Although the entire design philosophy is to prevent air from mixing with the hydrogen in the moderator, and despite the absence of any scenario to accomplish the hypothetical accident, it is assumed that a stoichiometric mixture of hydrogen and air is present in the moderator chamber at a pressure of 100 kPa. If a normal deflagration occurs, the peak pressure would be 827 kPa (120 psi), which is much less than the calculated 2.6 MPa (375 psi) or measured breaking pressure 3.3 MPa (475 psi) for the moderator chamber. The temperature of the gas produced after the event would be approximately 3000 K, which would be given up to the aluminum vessel. Since the relative mass of the hot gas to aluminum is of order 0.4 %, the temperature of the vessel will not increase by more than 8 K, which will not affect the properties of the vessel. Since everything will be contained within the moderator, there will be no effect on the reactor or the confinement building.

8.10 Maximum Hypothetical Accident

The maximum hypothetical accident (MHA) for the NBSR liquid hydrogen source begins as a sudden rupture of the vacuum line to the cryostat simultaneously with its helium jacket. This in itself has no serious consequences, but the MHA goes on to postulate that this rupture is followed by a rupture in the moderator shell, followed by complete mixing of the solid air cryo-pumped on the moderator chamber shell, followed by a strong ignition source. This scenario is not credible, so that the consequences of this analysis bound all possible accidents of this type. At each stage of the analysis, the extraordinarily conservative nature of the assumptions will be elucidated.

The first stage of the scenario, a rupture of the vacuum line and its helium shield line, is improbable, but not incredible. The only identified scenario assumes that the 133 kN (15 ton) crane (or a load on it) snags the module containing the vacuum pumps, pulling it over, and ripping the vacuum line. However, the crane is interlocked to prevent operation in the area of the vacuum module, so that this assumes a failure of the interlock. Further, it is unlikely that simply tipping the module over would rupture both lines – either no damage to the vacuum line or a slow leak of helium is more probable. However, the assumption is that there is a "guillotine" break in the vacuum line, which admits air into the vacuum space around the moderator chamber. The source is assumed to be full of liquid hydrogen (a volume of 5 liters), with the refrigerator operating. Under these conditions, air will rush into the vacuum space, and will be cryo-pumped onto the surface of the moderator, which will be at 21 K, well below the solidification temperature of both nitrogen and oxygen. At this point, the gross vacuum alarm on the hydrogen system will cause an interruption in the flow of cold helium into the condenser, and the liquid hydrogen will begin to boil away. It is conservative to assume that the reactor is shut down, as this will reduce the heat load, leaving more hydrogen to be boiled off by removing the heat evolved in the condensation and solidification of air.

As the room temperature air enters the moderator chamber vacuum space, part of it will be cooled down by contact with the moderator chamber surface, and solidified. The heat evolved in each of these steps is computed from the data in Table 8.2[22,23].

This heat must be removed from the system by boiling of liquid hydrogen, which requires an average heat input between 100 and 400 kPa of approximately 419 J/g. Thus, for every gram of air that is cryopumped onto the moderator chamber surface, there will be 555/419 = 1.32 g of hydrogen boiled off from the moderator. The limiting case of hydrogen available comes with the reactor off, so that very little vapor is being generated as a result of nuclear heating. This condition also maximizes the amount of air cryopumped, again because the heat load is minimal. The volume of the moderator chamber is 5 liters, and at 100 kPa pressure, this corresponds to 354 g of liquid hydrogen. This liquid will all be boiled off by condensation of 354/1.32 = 268 g of air, or approximately 240 cm^3. As soon as the vacuum ruptures, the refrigerator will automatically stop providing cooling to the condenser, and the liquid hydrogen will decrease in volume in the moderator chamber until it is all gone. Note that the vacuum line surrounds the supply and return lines for hydrogen between condenser and moderator chamber, so that no new hydrogen will flow into the chamber after the rupture. In fact, it is probable that most of the liquid would be immediately blown from the moderator chamber by the sudden increase in heat load; however, this possibility is ignored for conservatism. Clearly, the amount of hydrogen is considerably above stoichiometry at the beginning of the incident, and the amount of oxygen available for a reaction will be maximum when all of the liquid is gone, at which point there will be 25 g of cold hydrogen vapor available. The amount of oxygen available at this time

Table 8.2 Selected properties of nitrogen and oxygen.

Property	N_2	O_2	Air(J/g)
Volume Fraction Used	0.79	0.21	1.0
Mass fractions	.77	.23	1.0
Enthalpy (300 K, 100 kPa)	272.71 (J/g)	311.20 (J/g)	282.6 (J/g)
Enthalpy (MP[1], 100kPa)	-193.53	-150.78	-183.7
Heat of Fusion	26.0	13.9	23.2
Solid cooling to 25 K (including phase transitions)	67.5	60.1	65.8
Total Heat Evolved J/g	559.7	536.0	555.3

• [1] MP=Melting Point; Air 59.8 K (liquidus), N_2 63.16 K, O_2 54.37 K

(from above estimate) will be 268*0.23 = 62 g, which can react with 7.8 g of hydrogen.

The MHA now *assumes* that the moderator vessel now ruptures (with no reasonable scenario), *and* that a large energy ignition source then fires (again with no credible scenario). The results of Ward[19] *et al* showed that reaction of 300 cm^3 of solid oxygen with 21 g of hydrogen in a closed vessel of 33 liters resulted in a maximum pressure of 6.8 MPa. The present vacuum

vessel has a volume of 47 l, and Ward *et al* showed that yield was inversely proportional to volume, implying a maximum pressure of 4.8 MPa, which is significantly below the calculate breaking pressure of > 8270 kPa (the test vessel did not break at 8960 kPa). Therefore, the MHA will be entirely contained within the vacuum vessel, and will cause no damage to the reactor or confinement building.

9.0 Acknowledgements

The authors acknowledge the help and assistance of many different people at the NCNR over the past 10-15 years, in the design, fabrication, installation, operation and maintenance of the hydrogen sources. In particular, we thank Jim Moyer and Lew Robeson for their engineering design and drafting; Don Pierce for leading the installation of Unit 2; George Baltic and his technical team for their work on installation; Bob Williams (Big Bob) for his removal and installation work on the first source; George Baltic and Scott Slifer for their exceptional welding work; the reactor electronics staff for their work on the interface with reactor systems; Don Fravel, Tom Green and Dennis Nester for their operation and maintenance of the source; Jeremy Cook for the TOF analysis; the reactor operations staff for their help in many areas, and the Health Physics group, especially Les Slaback for helping us to do it safely. Thanks also to Jim Siewarth and Doug Olson for creating the mockup and conducting the thermal hydraulic tests in Boulder. We have also benefited from many discussions with almost everyone in the organization.

9.1 References

1. S. J. Cocking and F. J. Webb, Section 4 in *Thermal Neutron Scattering*, edited by P. A. Egelstaff, Academic Press, London and New York (1965); F. J. Webb, Reactor Science and Technology (Journal of Nuclear Energy Parts A/B), 187-215 (1963).

2. National Bureau of Standards, *FSAR on the National Bureau of Standards Reactor, NBSR-9*, U. S. Department of Commerce, (1966).

3. Robert S. Carter, *Safety Analysis Report on the D_2O Cold Neutron Source for the National Bureau of Standards, NBSR-13*, National Bureau of Standards, U. S. Department of Commerce, (1984).

4. H. Hoffman, "Experimental Investigations of Heat Transfer Behavior of a Horizontally Arranged Cylindrical Cold Neutron Source in a Vaporizing Deuterium Flow," Proc. Cryo. Eng. Conf., 390-303, Helsinki (1984); H. Hoffman and J. M. Astruc, "Experimental Investigations of the Fluid Dynamics of a Thermal Siphon with Vaporizing Deuterium for a Horizontally Arranged Cylindrical Cold Source," 462-465, *ibid*; "Natural Convection Cooling of a Cold neutron Source with Vaporizing Deuterium at Temperatures of 25 K", in *Natural Convection: Fundamentals and Applications*, S. Kakac, W. Aung, R. Viskanta editors, Hemisphere Publishing Corp., New York, 1140-51 (1985).

5. J. D. Siegwarth, D. A. Olson, M. A. Lewis, J. M. Rowe, R. E. Williams and P. Kopetka, "Thermal Hydraulics Tests of a Liquid Hydrogen Cold Neutron Source," National Institute of Standards and Technology, NISTIR 5026 (1994).

6. Paul Ageron, "Cold Neutron Sources at ILL," Nuc. Inst. Meth., **A284**, 197-199 (1989); P. Ageron, "Neutronic Design of the ILL Cold Sources – An Historical Perspective" in Proceedings of the International Workshop on Cold Neutron Sources, March 5-8, 1990, Los Alamos, N. M., LA-12146-C, 1-19 (1991).

7. T. E. Fessler and J. W. Blue, "Radiation-Induced Conversion of Liquid Hydrogen," Phys. Rev. Let. **14**, 811 (1965).

8. Nelms, L. W. and Carter, H. G., "NERVA Irradiation Program: GTR Test 21, vol. 2, Nuclear Radiation-Induced Conversion of Para Hydrogen to Ortho Hydrogen," U. S. Atomic Energy Commission, FZK-351-2 (1968).

9. J. F. Briesmeister, ed., *MCNP – A General Monte Carlo N-Particle Transport Code, Version 4B*, Los Alamos National Laboratory, LA-12625-M, Los Alamos, New Mexico (March 1997).

10. *NBSR-14: Safety Analysis Report (SAR) for License Renewal of the National Institute of Standards and Technology Reactor – NBSR*, NIST Internal Report NISTIR 7102 (2004).

11. Croff, A. G., "A User Manual for the ORIGEN2 Computer Code," ORNL/TM-7175, Oak Ridge National Laboratory (July 1980).

12. Trellue, H.R., "Development of MONTEBURNS: A Code that Links MCNP and ORIGEN in an Automated Fashion for Burnup Calculations," LA-13514-T, Los Alamos National Laboratory (December 1998).

13. Douglas E. Peplow, "A Computational Model of the High Flux Isotope Reactor for the Calculation of Cold Source, Beam Tube, and Guide Hall Nuclear Parameters," Oak Ridge National Laboratory, ORNLTM-2004/237 (2004).

14. B. Farnoux and P. Breant, "Upgrade of the Experimental Facilities of the Orphee Reactor," Proceedings of the Third Meeting of the International Group on Research Reactors (IGORR-III), September 30-October 1, 1993, Naka, Japan.

15. A.E. Dukler, Moye Wicks III and R. G. Cleveland, "Frictional Pressure Drop in Two-Phase Flow: A. A Comparison of Existing Correlations for Pressure Loss and Holdup and B. An Approach through Similarity Analysis," AIChE J **10**, 38-51 (1964).

16. L. S. Tong and Y. S. Tang, *Boiling Heat Transfer and Two-Phase Flow*, 2nd Edition, Taylor and Francis, Washington, DC, 188 (1997); A. E. Dukler and A. Taitel, *Two-Phase Gas-Liquid Flow: A Short Course on Principles of Modeling Gas-Liquid Flow and on Modern Measuring Methods*, Univ. of Houston, Houston, Texas (1991).

17. J. P. Iman, *Heat Transfer*, McGraw-Hill Inc. (1981).

18. R. D. McCarty, J. Hord and H. M. Roder, *Selected Properties of Hydrogen*, NBS Monograph 168, (1981).

19. D. L. Ward, D. G. Pearce and D. J. Merrett, "Liquid Hydrogen Explosions in Closed Vessels," Adv. Cryo. Engineering, **9**, 390-400 (1964).

20. W. Breitung, G. Necker, B. Kaup and A. Vesser, "Numerical Simulation of Hydrogen Release in a Private Garage", Proceedings of Hypothesis IV, Strahlsund, Germany, 268 (2001).

21. W. E. Baker, P. A. Cox, P. S. Westine, J. J. Kulesz and R. A. Strehlow, *Explosion Hazards and Evaluation, Vol. 5 of Fundamental Studies in Engineering*, Elsevier Scientific Publishing Company, New York (1983).

22. R. T. Jacobsen, S. G. Penoncello, and E. W. Lemmon, *Thermodynamic Properties of Cryogenic Fluids*, Plenum Press, New York and London, (1997).

23. R. B. Scott, *Cryogenic Engineering*, D. van Nostrand Co., Inc., Princeton, NJ (1959).

9.2 Appendix

```
unit2:  advanced LH2 cold source for mcnp5, As built 24x32-cm
c
c     with vapor in exit hole  3.0 cm LH2
c     Inner ellipsoid at 76.5, outer centered at 76 cm
c     .09 in walls
c
c     LH2 cold source ad00 (11/00):
701  4  -.063   201 -202  -210 vol=726    imp:n,p=54  $lh2
702  4  -.063   201 -202  -227 210  imp:n,p=54  $lh2
703  4  -.063   201 -202  -225 227  imp:n,p=54  $lh2
704  4  -.063   201  -202 225  203  imp:n,p=54  $lh2
705  6  -.035  -211  207            imp:n,p=27  $ lh2 separator
706  0          -208                imp:n,p=27
707  6  -.0013 -209 201 225 -202 vol=600  imp:n,p=27  $ vapor @ 1.1 bar
709  0          -218  207 #(-212)    imp:n,p=27
710  0          -215  212 218        imp:n,p=27
711  2  -2.7  -201  208  203  227    imp:n,p=27  $ Al wall, inner sphere
712  2  -2.7  -201  208 -227         imp:n,p=27  $   "         "     "
713  2  -2.7  -212  211  207         imp:n,p=27  $ Dome
714  2  -2.7  -203  209 -207 208 227 imp:n,p=27          $ Al support ring
715  2  -2.7  -207 202 -227          imp:n,p=27  $Al: Chamber
716  2  -2.7  -207 202 227 #760 203  imp:n,p=27 $Al:    "
717  2  -2.7  -201 208 -209 225      imp:n,p=27 $ Al - exit hole
718  2  -2.7  -207 202 -209 225      imp:n,p=27 $ Al      "
c
720  2  -2.7  -217 218 -225  #(-216)    imp:n,p=27    $Al: He jacket
721  2  -2.7  -217 218  225  #(-216) #761 #763
                #751 #752      imp:n,p=27   $Al:      "
722  2  -2.7  -216 215  218 #760      imp:n,p=27 $ remove He jackt section
723  3  -1.1  -205 204 -273 232 #(-242) #(-244)  imp:n,p=9
724  3  -1.1  -227 -270 217 #(-216) #(-229)      imp:n,p=9   $d2o: cryostat
725  3  -1.1 227  217 -273 -225  216  229        imp:n,p=9   $d2o:  cryostat
726  3 -1.1  -273 -204 225  217 #751 #752   #(-229)
          #(-242) #(-244) #756 #757   #(-216) imp:n,p=9
727  3 -1.1  205 -273 -127 #741 #742 #743 #(-242) #(-244)
          #744 #745 #746 #747 imp:n,p=9  $source reflector,coolant
728  2  -2.7  227 273 -219 -127 #746 #747   imp:n,p=3   $Al:  d2o jacket
729  2  -2.7  -227 -220  270         imp:n,p=3   $Al:      "
730  2  -2.7  -205 204 -232 231      imp:n,p=9   $ 'Al collar'
c
740  0       -205 204  -231          imp:n,p=27
741  0       205 -292  -295 -127 imp:n,p=27 $  void through D2O
742  0       205 -293   296 -127 imp:n,p=27
743  0       205 -298   297 -296 295 -127 imp:n,p=27
744  2  -2.7 -297 287 -127 205 -296 295   imp:n,p=9
745  2  -2.7 -288 298 -127 205 -296 295   imp:n,p=9
746  2  -2.7 -284 292 -127 205 -295       imp:n,p=9
747  2  -2.7 -285 293 -127 205  296       imp:n,p=9
748  3  -1.1 -228 217                     imp:n,p=9
749  2  -2.7 -229 228 217                imp:n,p=9
c
751  0       -293  -204  218  299              213 imp:n,p=9
752  0       -292  -204  218 -299              213 imp:n,p=9
756  2  -2.7 -284  292 -204  217 -299          213 imp:n,p=9
757  2  -2.7 -285  293 -204  217  299          213 imp:n,p=9
c
760  0        -241 -127 225 215      imp:n,p=3
761  2  -2.7  -242 241 -127 225 216  imp:n,p=3
762  3  -1.1  -243 -127 225 229      imp:n,p=3
763  2  -2.7  -244 243 -127 225 229  imp:n,p=3
c
731  2  -2.7  -283 219 -127  227 #746 #747    imp:n,p=3   $Al: reactor vessel
732  2  -2.7  -227 -280 220  223     imp:n,p=3   $Al:     "
733  3  -1.1 -222 280 -221 223 -224  imp:n=1  imp:p=1   $d2o:  reflector
734  3  -1.1  283 227 -224 -127      imp:n=1  imp:p=1  $d2o:      "
735  3  -1.1 -224 -227 280 222       imp:n=1  imp:p=1  $d2o:      "
736  3  -1.1  223  221 -224 -222       imp:n=1  imp:p=1  $d2o
c
737  3  -1.1  -223 -224 8              imp:n=1  imp:p=1  $(ec=737)
738  3  -1.1  -127 8 -9 224            imp:n=1  imp:p=1  $(sc=738)
c
200    0         -1   2   -3        imp:n=27  imp:p=1  $ beam to DXTRAN
201    0      8  -2  -3   127      imp:n=27   imp:p=1
202    0      8  127  -10  3   -1       imp:n,p=27
998    0         -127 8    9  -10      imp:n,p 0
999    0          1:  10:  -8          imp:n=0   imp:p=0  $ outside
c     SURFACES:

1     1  py  200.
2     1  py  199.5
3     1  cy    3.
8     1  py   55.5
9     1  cy   30.
10    1  cy   40.
127   1  cz  150.
c     these are the CNS surfaces for Unit 2:
  201 1 sq  2.0194 1 1 0 2r  -182.25 0 76.5  0
  202 1 sq  1.7778 1 1 0 2r  -256    0 76 0
  204 1 py  96.0
  203 1 sq  1.7331 0 1 0 2r  -108.16  0 0 0   $ .2 cm thick support ring
  205 1 py  97.0
  207 1 sq  1.7657 1 1 0 2r  -261.3072  0 76 0    $ .065-in outer wall
```

```
  208 1 sq  2.0519 1 1 0 2r  -175.5625  0 76.5 0  $ .090-in inner wall
  209 1 sq  1.7778 0 1 0 2r  -100    0  0 0            $ exit hole
  210 1 py  65.0
  211 1  s   0 76 16   5.0
  212 1  s   0 76 16   5.25
  213 1 py  82.
  215 1  s   0 76 16    6.5
  216 1  s   0 76 16    7.5
  217 1 sq  1.6402 1 1 0 2r  -333.0625  0 76 0
  218 1 sq  1.7101 1 1 0 2r  -289.0000  0 76 0
  219 1 cy  28.0
  220 1 sq  1.000  4.500  1.000 0.0 0.0 0.0 -784.00  0.  69.7  0.
  221 1 sq  1.     5.3389  1.   0.  0.  0.  -930.25  0.  67.2  0.
  222 1 py 67.2
  223 1 py 55.52
  224 1 cy 29.98
  227 1 py 69.7
  225 1 py 76.
  228 1  s   0 76 -16  6.2
  229 1  s   0 76 -16  7.2
  231 1 cy  11.5
  232 1 cy  13.
  241 1 c/y 0 19.7  2.8
  242 1 c/y 0 19.7  3.3
  243 1 c/y 0 -19.7 2.8
  244 1 c/y 0 -19.7 3.3
  270 1 sq  1. 4.7452 1. 0. 0. 0.  -748.5696  0. 69.7 0.
  273 1 cy  27.36
  280 1 sq  1. 4.08 1.  0. 0. 0.  -858.49  0. 69.7 0.
  283 1 cy  29.3
  284 5 cy  13.
  285 6 cy  13.
  287 1 pz  -13.
  288 1 pz   13.
  292 5 cy   11.
  293 6 cy   11.
  295 5 px    0.
  296 6 px    0.
  297 1 pz  -11.
  298 1 pz   11.
  299 1 px    0.

m2    13027.62c  1 $Al
m3    1002.66c .66334  1001.62c .00333  8016.62c .33333 $99.5% pure d2o
mt3   hwtr.60t  lwtr.60t
c
c     MODIFIED ORTHO-PARA MIXING --- ORIGINAL METHOD:
c     1004.62c and h4para.61t are copies of 1001.62c and hpara.61t
c        with ZAID = 1004, needed for mixing ortho and para LH2.
c
m4   1001.62c .5    1004.62c .5
mt4  hortho.61t      h4para.61t  $ from sab2002
m6   1001.62c .5    1004.62c .5
mt6  hortho.61t      h4para.61t  $ from sab2002
c
c     Change angles to 16.5 degrees for CTE,CTW:
*tr5   -18.83 94.66 0  27.75 62.25 90    117.75 27.75 90   90 90 0
*tr6   -18.83 94.66 0  -5.25 95.25 90     84.75 -5.25 90   90 90 0
*tr1     0     0    0  11.25 78.75 90    101.25 11.25 90   90 90 0
c
c      Current Tallies:
fq0    e c
c
c      tallies from the kcode calc:
f14:n  701 707
fm14   1.528e18
e14    5-9
fc14   Cold neutron flux in LH2 and exit hole.
c
f61:n  204
fs61   -231
e61    5e-9
c61    .99  1.0
sd161  415.5 1
fm61   1.525e18
c
f161:n  205
fs161   -209
sd161   235.62  1 $ area
e161    5e-9
c161    .99  1.0
fm161   1.525e18
c       tallies inside dxtran sphere:
f11:n   2
fs11    -3
sd11    28.27 1
fm11    1.525e18
e11     1e-9  18i  2e-8
c11     .9992 .9996 1.0 t
tf11    3j 1 j 3 1 j
c
f21:n   2
fs21    -3
sd21    28.27 1
fm21    1.525e18
```

```
e21     5e-9  18i  1e-7 1e-6 1-5 1-4 1-3 1-2 .1 1 20 t
c21     .9992 .9996 1.0 t
c
f31:n   2
fs31    -3
sd31    28.27 1
fm31    1.525e18
e31     1e-9  18i  2e-8
c31     .9996 .9998 1.0 t
c
f41:n   2
fs41    -3
sd41    28.27 1
fm41    1.525e18
e41     5e-9  18i 1-7 3-7 1-6 3-6 1-5 3-5 1-4 3-4
                  1-3 3-3 1-2 3-2  .1  .3 1 3 10 20 t
c41     .9996 .9998 1.0 t
c
c
f151:n   2
fs151    -3
sd151    28.27 1
fm151    1.525e18
fc151   energy bins for wavelengths 20.5,19.5,18.5, .. 1.5, and 0.5 A
e151   .1933e-9 .2136-9 .2373-9 .2652-9 .2984-9
      .3381-9 .3863-9 .4457-9 .5199-9 .6142-9
       .7368-9 .9001-9 1.1243-9 1.4441-9 1.9226-9 2.6853-9
        4.0114-9 6.631-9 12.997-9 36.102-9 324.92-9
c151    .9996 .9998 1.0  t
c
c     PROB
mode  n
prdmp 2j 1 1
tmp    1.7235e-9 16r 2.77e-8 41r
c
c     ssw 8 (737) -9 (739) $ write surf source card from kcode prob
c
ssr    old 8 9   new 8 9  wgt 1.  psc 1.
dxt:n  -39.02  196.16 0   3.1 3.1
c
```